

ALTERATIONS IN CEREBELLAR PROTEIN
SYNTHESIS IN PROPYLTHIOURACIL-INDUCED
HYPOTHYROID RATS

A DISSERTATION
SUBMITTED IN PARTIAL FULFILLMENT OF THE REQUIREMENTS
FOR THE DEGREE OF DOCTOR OF PHILOSOPHY
IN THE GRADUATE SCHOOL OF
TEXAS WOMAN'S UNIVERSITY
COLLEGE OF ARTS AND SCIENCE
DEPARTMENT OF BIOLOGY

BY

DIANE M. JAWORSKI, B.S., M.S.

DENTON, TEXAS

May, 1991

TEXAS WOMAN'S UNIVERSITY
DENTON, TEXAS

May, 1991

To the Dean for Graduate Studies and Research:

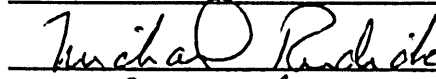
I am submitting herewith a dissertation written by Diane M. Jaworski entitled "Alterations in Cerebellar Protein Synthesis in Propylthiouracil-Induced Hypothyroid Rats". I have examined the final copy of this dissertation for form and content and recommend that it be accepted in partial fulfillment of the requirements for the degree of Doctor of Philosophy, with a major in Molecular Biology.

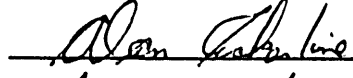


Dr. Mills, Major Professor

We have read this dissertation
and recommend its acceptance:







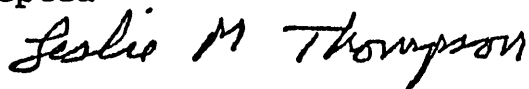




Department Chairperson

Dean of College

Accepted



Dean for Graduate Studies and Research

Copyright c Diane M. Jaworski, 1991

All rights reserved

Dedicated to the loving memory of
my maternal grandparents,
Joseph and Isabel Czyzewski

ACKNOWLEDGEMENTS

I would like to thank the members of my graduate research committee for their guidance and assistance through this project. Each member in their own way has provided a unique input into my graduate career. Dr. Mills, as the major professor, provided the technical training. Financial support was made available through a teaching assistant position from Dr. Schwalm. Drs. Uphouse and Rudick challenged my academic potential and nurtured the ability to synthesize and critically evaluate data. In addition, Dr. Uphouse served as a role-model and confidant through difficult times. Finally, Dr. Cockerline provided training in photomicroscopy. Although not on my committee, Dr. Droge deserves recognition for his contribution of training in the use of the Zeiss-Video Plan.

On a personal note, I would like to thank those individuals who provided moral support and encouragement. First, and foremost, my achievements would not have been possible without the loving devotion of my beloved parents, Witold and Jane Jaworski, they have stood by me and supported me through all phases of my education. In addition, my friends Jill Wallace, Melika Davis and Connie Kilday were always there when I needed them. The camaraderie of fellow graduate students Leslie Sinclair-Worley, Sharmin Maswood and Sylvia Montanez was also appreciated.

The expeditious completion of this project was made possible by the assistance and support provided by Dr. Cheryl M. Craft, Director of the Laboratory of Molecular Neurogenetics, Department of Psychiatry, The University of Texas Southwestern Medical Center. In addition to the training she provided in the polymerase chain reaction technology, Dr. Craft supplied the financial and technical support for the northern hybridization experiments of this project. As importantly, Dr. Craft provided a research environment to which I might not otherwise have been exposed. Training with Dr. Craft and her postdoctoral fellow, Valerie Simonneaux, proved to be an enlightening experience, both professionally, as well as personally. Words cannot express the gratitude I owe to Cheryl and Valerie for their support and encouragement.

ALTERATIONS IN CEREBELLAR PROTEIN
SYNTHESIS IN PROPYLTHIOURACIL-INDUCED
HYPOTHYROID RATS

Diane M. Jaworski

May, 1991

Thyroid hormones play an important role in the regulation of gene expression and cerebellar development in the rat. The drug propylthiouracil was used to disrupt thyroid hormone synthesis. This permitted investigation of gene expression under three different states of hormonal deprivation: early in development (PTU 1), late in development (PTU 2), and continual deprivation (PTU 3). The effects of these deprivations on some aspects of the synthesis of two proteins known to be affected by T_3 , apolipoprotein E (apo E) and transferrin (T_f), were investigated.

Thyroid hormone's permissive role on growth and development, morphological features as well as body and organ weights were analyzed and found to be significantly reduced in the hypothyroid state. The development of cerebellar cortical strata and cellular morphology was altered by prenatal, as well as postnatal PTU administration.

To establish cerebellar synthesis of apo E and T_f , total RNA was extracted, poly A⁺ RNA isolated and translated in an *in vitro* reticulocyte lysate system. The specific proteins were immunoprecipitated and analyzed by SDS-PAGE.

To correlate these results with the amounts of mRNA's for apo E and T_f , northern hybridization was performed.

Both apo E and T_f levels synthesized *in vitro* with RNA from control animals increased as development proceeded, with apo E produced in greater quantity. While hepatic apo E synthesis increases in the hypothyroid state (presumably as a result of regulation at the transcriptional level), cerebellar apo E translatable mRNA levels were not affected by PTU treatment. Like hepatic T_f , cerebellar T_f levels were substantially reduced in the hypothyroid state, as compared to control values. Developmentally, apo E mRNA levels declined, while T_f mRNA levels and T_f synthesized *in vitro* were parallel in control animals. PTU 1 treated animals, in which free T_3 in the circulation increased after PN day 20, demonstrated increases in both apo E and T_f mRNA levels at the same time point.

It appears that the regulation of apo E and T_f mRNA levels differ from each other within the cerebellum and may be regulated differently from those of the liver. The increase in *in vitro* protein synthesis and mRNA levels in PTU 1 treated animals may be a result of developmental recovery, rather than specific T_3 mediated gene regulation.

TABLE OF CONTENTS	Page
ACKNOWLEDGEMENTS.....	iv
ABSTRACT.....	vi
LIST OF FIGURES.....	x
LIST OF TABLES.....	xiii
LIST OF ABBREVIATIONS.....	xiv
I. INTRODUCTION.....	1
Cerebellar Anatomy and Circuitry in Rats....	3
Cerebellar Development in Rats.....	18
Thyroid Hormone Synthesis, Action and Metabolism.....	22
Regulation of Thyroid Hormone Function.....	26
Propylthiouracil Effects.....	29
Effect of PTU on Cerebellar Development.....	31
Effects of Hypothyroidism on Protein Synthesis.....	34
Transferrin Structure, Function and Synthesis.....	35
Apolipoprotein E Structure, Function and Synthesis.....	38
II. MATERIALS AND METHODS.....	43
Animal Care and Treatment.....	43
Histology.....	46
PTU / T ₃ Assay.....	48
Statistics.....	49
RNA Extraction.....	50

Poly A ⁺ RNA (mRNA) Isolation.....	52
<i>In vitro</i> Translation.....	53
Immunoprecipitation of Translated Products..	54
Electrophoretic Protein Analysis.....	55
Preparation of Competent Bacterial Cells....	56
Large Scale Preparation of Plasmid DNA.....	57
Electrophoresis of Plasmid DNA and cDNA Isolation.....	59
Polymerase Chain Reaction Amplification....	60
Preparation of Labelled Probes.....	62
RNA Separation by Electrophoresis on Denaturing Gels.....	66
Northern Hybridization.....	67
III. RESULTS.....	69
Routes of PTU Administration.....	70
PTU Induces Gross Morphological Alterations.	73
Analysis of Body and Organ Weight.....	77
Altered Histogenesis Produces Unique Cerebellar Histology.....	92
Serum PTU and Free T ₃ Analysis.....	126
Cerebellar <i>In Vitro</i> Translation Profile....	131
Polymerase Chain Reaction Amplification....	144
Northern Hybridization.....	145
IV. DISCUSSION.....	150
REFERENCES.....	180
APPENDICES.....	191

LIST OF FIGURES

Figure	Page
1. Brain, dorsal view, rat.....	4
2. Cerebellum, dorsal view, rat.....	6
3. Transverse section of cerebellum.....	7
4. Neuronal elements of the mammalian cerebellum.....	8
5. Diagram of the afferent fibers of the cerebellum...	9
6. Basic circuit diagram for the mammalian cerebellum.	11
7. Diagram of the efferent fibers of the cerebellum...	13
8. Cerebellar cortex.....	15
9. Types of glial elements.....	17
10. Thyroid hormone synthesis and metabolism.....	23
11. Thyroid hormone metabolism via deiodination.....	25
12. Structures of commonly used hyperthyroid therapeutic agents.....	28
13. Restriction endonuclease map of the pSP65 vector...	63
14. Restriction endonuclease map of the apo E cDNA.....	65
15. Morphological alterations at postnatal day 1.....	74
16. Morphological alterations at postnatal day 10.....	75
17. Morphological alterations at postnatal day 20.....	76
18. Morphological alterations at postnatal day 30.....	78
19. Morphological alterations at postnatal day 60.....	79
20. Effect of hypothyroidism on body weight.....	82
21. Effect of hypothyroidism on brain weight.....	84
22. Effect of hypothyroidism on cerebellum weight.....	86

23.	Effect of hypothyroidism on brain:body weight ratio.....	88
24.	Effect of hypothyroidism on cerebellum:brain weight ratio.....	91
25.	Postnatal Brain Development.....	93
26.	Histological Alterations at Postnatal Day 1.....	94
27.	Histological Alterations at Postnatal Day 10.....	96
28.	Cortical Stratification at Postnatal Day 10.....	97
29.	Histological Alterations at Postnatal Day 20.....	98
30.	Granule cell Migration and Synapsis.....	100
31.	Purkinje cell Morphology at Postnatal Day 20.....	102
32.	Histological Alterations at Postnatal Day 30.....	104
33.	Purkinje cell Morphology at Postnatal Day 30.....	107
34.	Purkinje cell Soma Displaced by PTU 1 Treatment...109	
35.	Histological Alterations at Postnatal Day 60.....	110
36.	Purkinje cell Morphology at Postnatal Day 60.....	113
37.	Purkinje cell Dendritic Arborization.....	114
38.	Developmental alterations in total cerebellar cortical depth.....	115
39.	Developmental alterations in the cerebellar external granule layer (Egl).....	117
40.	Developmental alterations in the cerebellar molecular layer.....	119
41.	Developmental alterations in the cerebellar internal granule layer (Igl).....	121
42.	Developmental alterations in Purkinje cell somal area.....	124
43.	Developmental alterations in Purkinje cell Form PE.....	125

44.	Vehicle treated cerebellar protein profile.....	133
45.	PTU 1 treated cerebellar protein profile.....	134
46.	PTU 2 and PTU 3 treated cerebellar protein profile.	136
47.	Comparison of total profile with immunoprecipitated protein profile.....	138
48.	Apolipoprotein E protein profile.....	140
49.	Transferrin protein profile.....	142
50.	Electrophoresis of PCR amplified products.....	146
51.	Northern hybridization of apo E mRNA.....	147
52.	Northern hybridization of transferrin mRNA.....	149

LIST OF TABLES

Table	Page
1. Serum PTU Concentration.....	122
2. Free T ₃ Concentrations.....	124

T ₄	3,5,3',5'-tetraiodothyronine
T _f	transferrin
TBG	thyroxine-binding protein
TBPA	thyroxine-binding prealbumin
TEMED	N,N,N',N'-teteramethylethylenediamine
TRH	thyrotropin-releasing hormone
Tris-HCl	Tris (hydroxymethylaminomethane)
TSH	thyroid-stimulating hormone/thyrotropin

CHAPTER I

INTRODUCTION

Developmental neurobiology investigates how molecular and cellular interactions generate the anatomical complexity of the mammalian central nervous system (CNS). This complexity has restricted the analysis of genetic expression and regulation to limited regions. The cerebellar cortex provides a relatively simple model to examine developmental expression, since it contains five major classes of neurons whose anatomical and physiological interrelationships and developmental profile have been described in detail.

Developmental patterns in rats may be altered during critical periods by various means. Thyroid hormones are known to regulate the establishment of the cerebellar cortical strata. Hypothyroidism results in delayed differentiation and migration of granule cells, thus producing anomalous neural circuits. Thyroxine is also known to play a permissive role in the expression and regulation of a number of genes. Thus, within the cerebellum, thyroxine status regulates both morphology and gene expression. Since most cerebellar neurogenesis occurs postnatally, the timing of hormone manipulation may be used to delineate thyroid hormone action on development and gene regulation.

The investigation of gene regulation is complicated by the myriad of proteins and neurotransmitters localized within the CNS. In recent years, several substances typically not regarded as neural in origin have been isolated within the CNS (e.g. substance P, vasoactive intestinal peptide, angiotensin). Two serum proteins, apolipoprotein E (apo E) and transferrin (T_f), have been detected within the cerebellar cortex by immunohistochemical means. Hepatically synthesized apo E is responsible for cholesterol transport, while T_f is responsible for iron transport. Whether these serve unique roles within the CNS is yet to be determined.

Most studies of apo E and T_f regulation have focused on hepatic synthesis in mature animals. This study investigates the effects of thyroid hormone deprivation early, late, and throughout development to: (1) determine the permissive role thyroxine plays in growth and development; (2) determine whether postnatal thyroxine depletion affects the establishment of normal cortical strata; (3) produce a developmental profile for cerebellar apo E and T_f mRNA's using *in vitro* translation; and (4) determine the effect of thyroid hormones on the cerebellar expression of both proteins.

Cerebellar Anatomy and Circuitry in Rats

The cerebellum, which represents one-eighth of the total brain mass (Figure 1), is an organ of sensori-motor coordination whose organization, like the retina, consists of a laminated structure in which the basic internal structure is similar throughout. The cerebellum has long been used as a model to investigate the patterns of neuronal development, since it possesses only a few morphologically distinct cell types and its cytoarchitecture is well characterized (Ramón y Cajal, 1911; Palay and Chan-Palay, 1974).

The cerebellum lies within the inferior occipital fossae, beneath the occipital lobes of the cerebrum from which it is separated by the transverse fissure and the tentorium cerebelli, an extension of the cranial dura mater. The cerebellum is connected to the cerebrum, pons and medulla by three pairs of peduncles. The superior peduncles connect the cerebellum with the midbrain and form the upper lateral boundaries of the floor of the fourth ventricle. The middle peduncles, the largest of the three pairs, connect the cerebellum and pons. The inferior peduncles connect the cerebellum and the medulla oblongata and form part of the lateral wall of the fourth ventricle. The cerebellum consists of two hemispheres connected by a narrow lobe, the vermis. The anterior and posterior lobes regulate subconscious skeletal muscle movement, while the flocculonodular

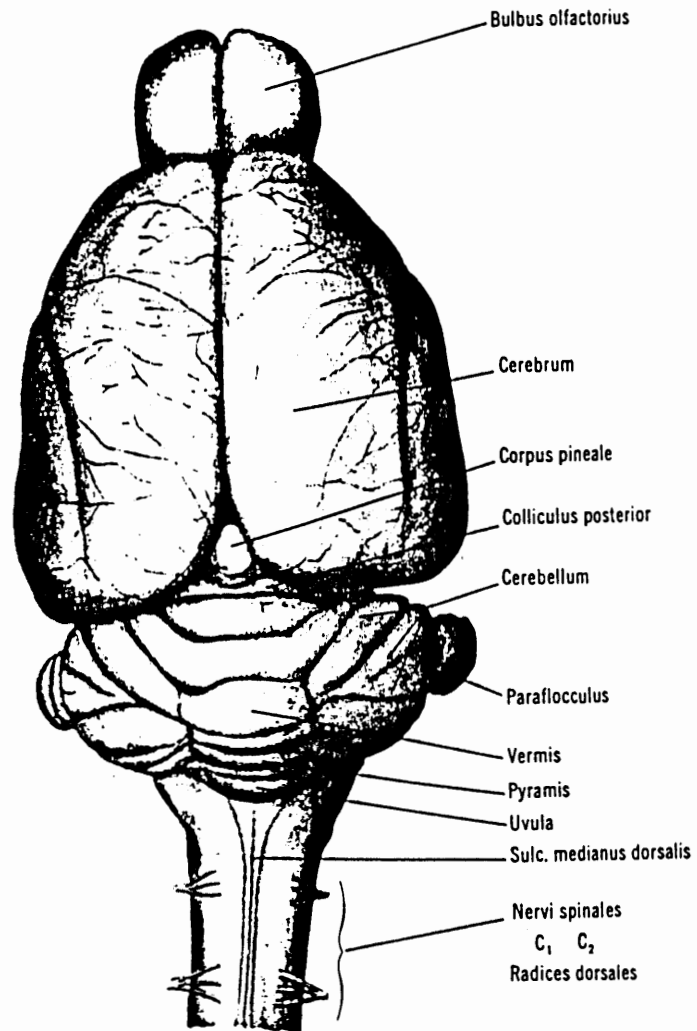


Figure 1. Brain, dorsal view, rat. Approximately 5X magnification. (Zeman and Innes, 1963)

lobe is involved in equilibrium (Figure 2). The cerebellar surface is not as convoluted as that of the cerebrum since the gyri and sulci are arranged into folia which are narrower, more numerous, and somewhat straighter than those of the cerebrum and are oriented transversely to the longitudinal axis of the animal. Like the cerebrum, the cerebellum consists of both gray and white matter (arbor vitae). The gray matter is found both externally within the cortex, and internally within the white matter as aggregations, called the cerebellar nuclei (Gray, 1977).

The cerebellum consists of three cortical layers (Figure 3): (1) the molecular layer, containing stellate and basket cells, as well as Purkinje cell dendrites and parallel fibers; (2) the Purkinje cell layer, consisting of isoplanar Purkinje cell somata and Bergmann glial cells; and (3) the granule cell layer, which contains granule and Golgi type II cells along with the afferent climbing and mossy fibers (Figure 4).

There exist five primary afferent pathways of the cerebellum (Figure 5). These include the corticoponto-cerebellar tracts from the motor regions of the cerebral cortex. Included in this tract are fibers from the pyramidal cells of the motor areas within the frontal lobe which project to the

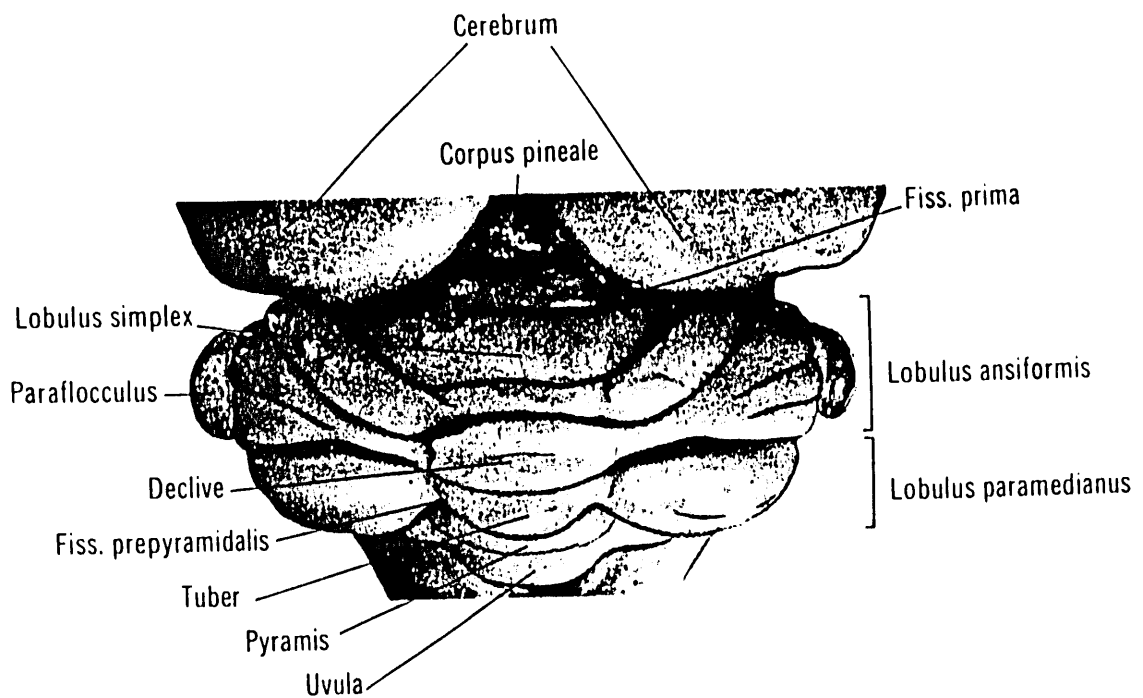


Figure 2. Cerebellum, dorsal view, rat. Approximately 6X magnification. (Zeman and Innes, 1963)

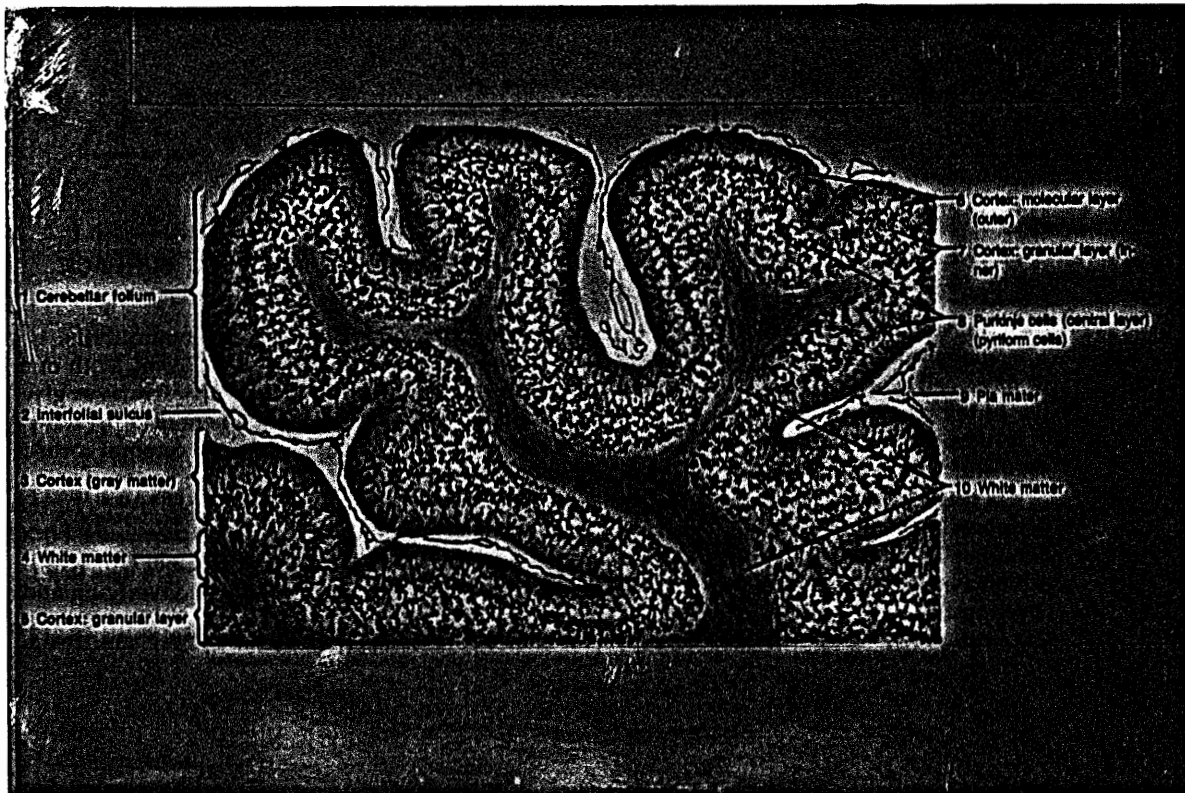


Figure 3. Transverse section of cerebellum. Silver impregnation by Cajal's method, 45 X magnification. (diFiore , 1989) Reprinted with permission of Lea & Febiger Publishing Company.

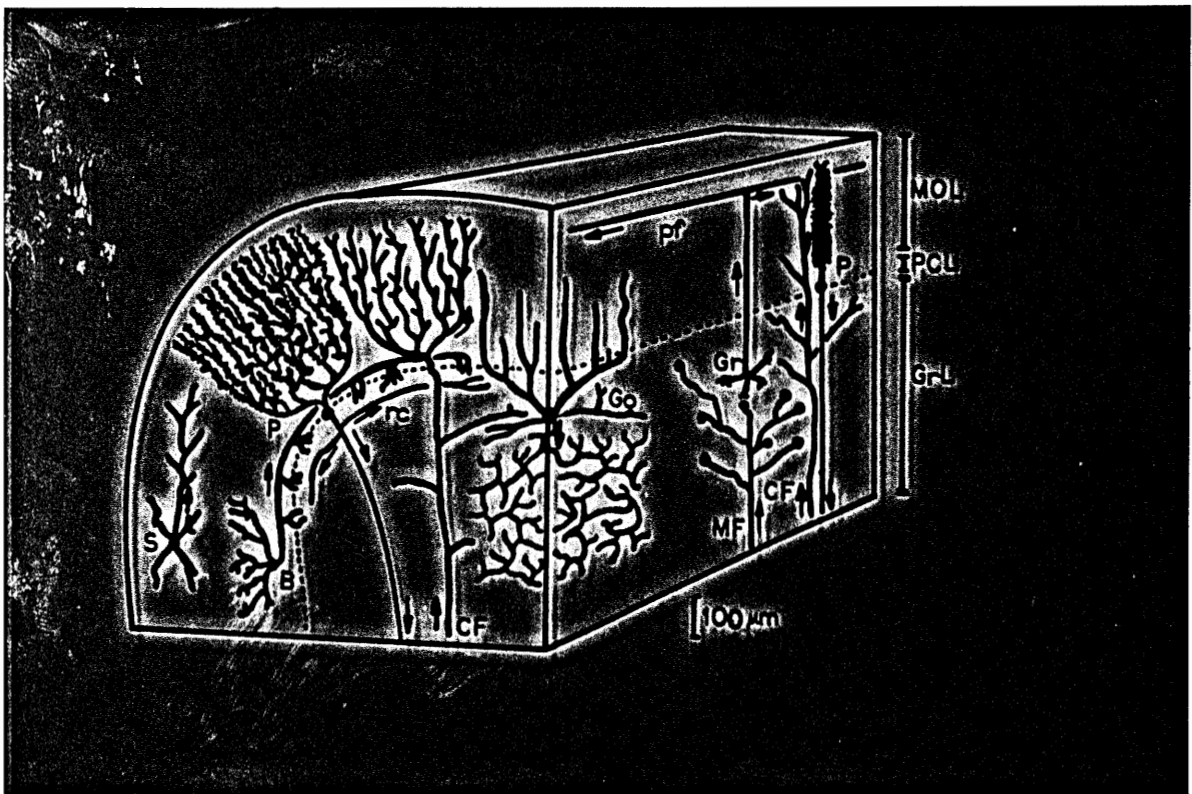


Figure 4. Neuronal elements of the mammalian cerebellum.
 Inputs: mossy fibers (MF) & climbing fibers (CF)
 Principal Neurons: Purkinje cell (P) with re-
 current collateral (rc)
 Intrinsic Neurons: granule (Gr), stellate (S),
 basket (B) and Golgi (Go) cells
 Histological layers are shown at the right:
 molecular layer (MOL), Purkinje cell
 layer (PCL), granule cell layer (GrL)
 (adapted from Shepherd, 1979)

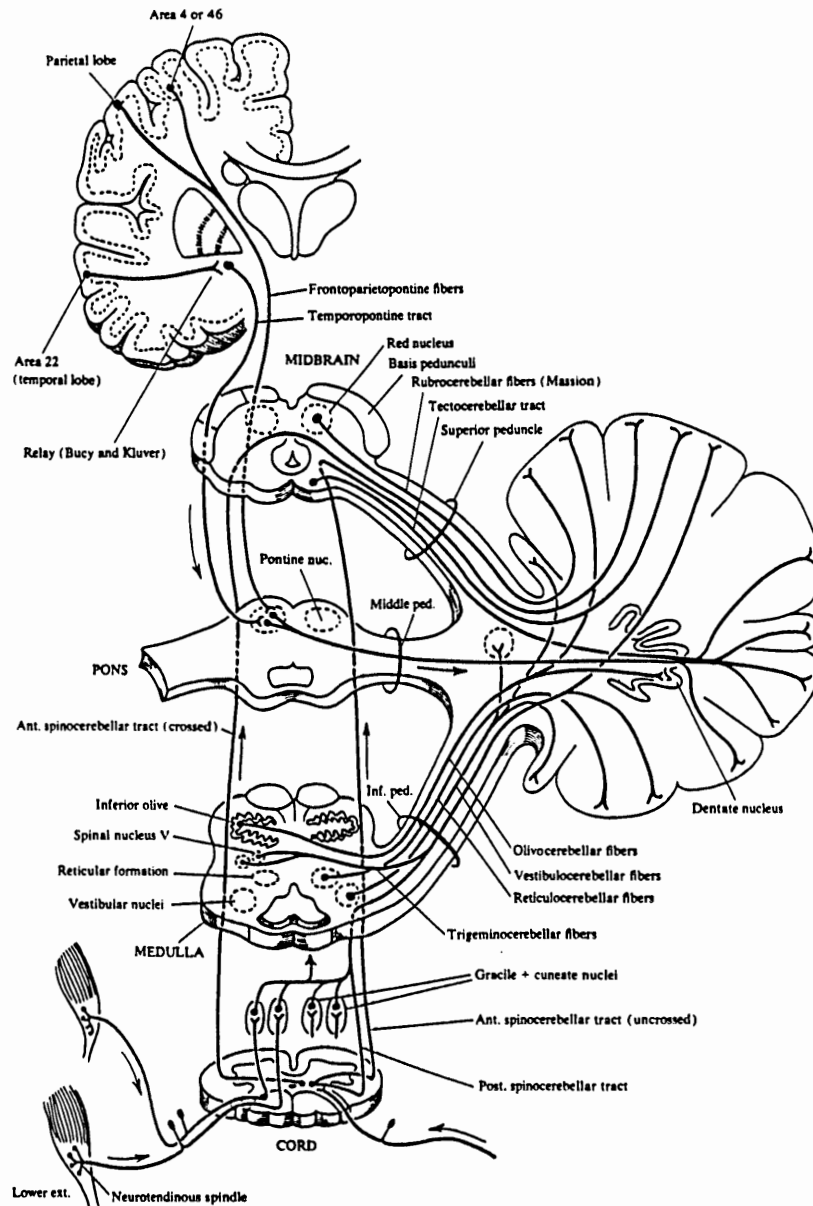


Figure 5. Diagram of the afferent fibers of the cerebellum. The five primary pathways include the cortico-pontocerebellar, vestibulocerebellar, spino-cerebellar, reticulocerebellar and olivocerebellar fibers. From Pansky B., Budd G. C., Allen D. J.: REVIEW OF NEUROSCIENCE, Second Edition, Copyright (c) 1988 Macmillan Publishing Company, a Division of Macmillan, Inc. Reprinted with permission of Macmillan Publishing Company.

enter the cerebellum directly from the vestibular nerve. At least two separate spinocerebellar tracts exist - those serving the lower and upper portions of the body. Several of the nuclei of the reticular formation provide reticulocerebellar connections. Finally, the olivocerebellar tract includes fibers from the inferior olivary nucleus and its associated accessory olivary nuclei which cross the medulla oblongata and enter via the cerebellar peduncle (Willis and Grossman, 1973). These pathways enter the cerebellar cortex via two fiber types - climbing and mossy (Figure 6). Climbing fibers originate primarily from the inferior olivary nucleus, with additional monoaminergic input from the reticular formation (Szentágothai and Rajkovits, 1959), including noradrenergic input from the locus ceruleus and serotonergic input from the raphe nuclei. Mossy fibers, which are larger and more numerous than climbing fibers, represent the terminals of spinocerebellar and pontocerebellar fibers. Climbing fibers terminate on the thorns of the Purkinje cell branchlets, while mossy fibers terminate in structures known as glomeruli. The cerebellar glomerulus is situated in the granule cell layer and consists of: (1) a mossy fiber rosette; (2) the dendrites of many granule cells; (3) proximal aspects of Golgi cell dendrites; and (4) the terminals of Golgi cell axons (House et al., 1979).

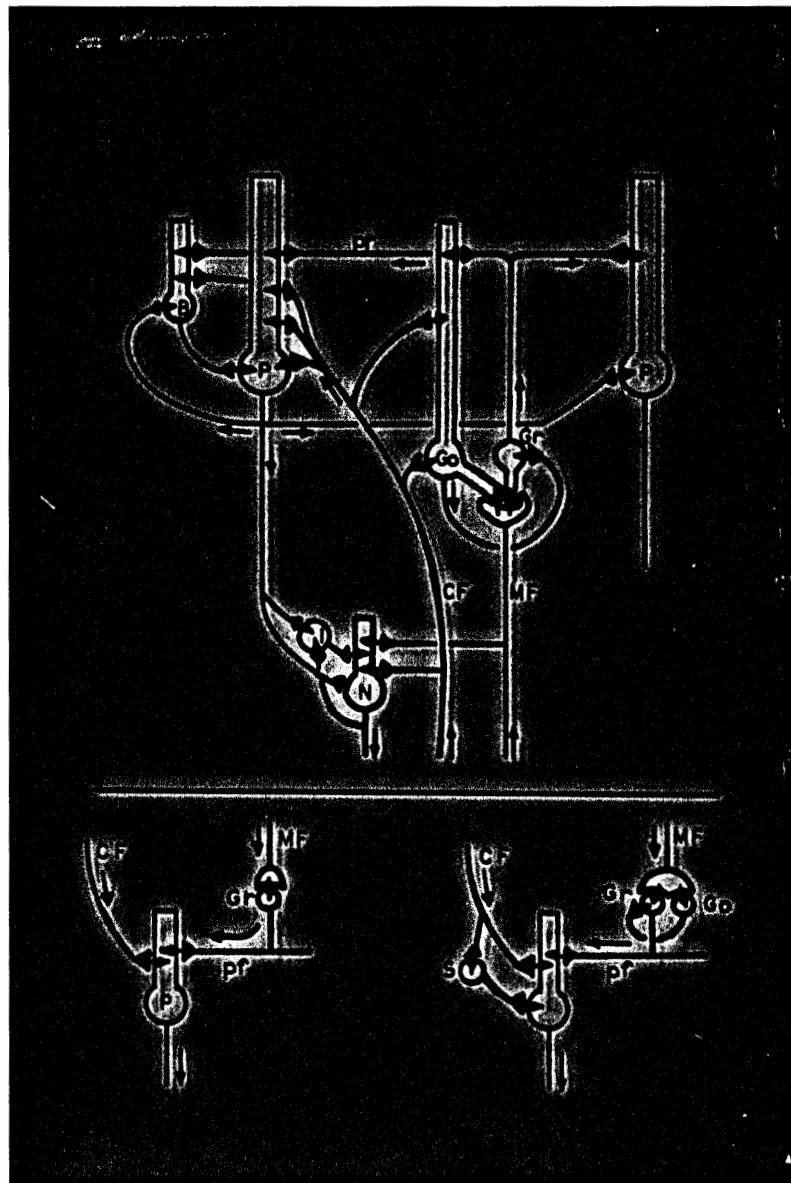


Figure 6. Basic circuit diagram for the mammalian cerebellum.
 Inputs: mossy fibers (MF) & climbing fibers (CF)
 Principal Neurons: Purkinje cell (P)
 Intrinsic Neurons: granule (Gr), stellate (S),
 basket (B) and Golgi (Go) cells
 Deep Cerebellar Nuclear Cells: principal nuclear
 cell (N) and intrinsic neuron (I)
 (adapted from Shepherd, 1979)

Climbing and mossy fibers also send collateral branches to the cerebellar nuclei. All of the cerebellar output is by way of the Purkinje cell, the principal cortical neuron. Purkinje cells possess large cell bodies (20 - 40 μm) with a 10 μm dendritic tree that gives rise to primary, secondary and tertiary branches with approximately 100,000 spines per Purkinje cell (Shepherd, 1979). These dendritic spines not only increase the surface area of the dendritic membrane, but also act as specific anatomical sites required for proper synaptic structure and function. The Purkinje cell bodies are aligned at the junction of the molecular and granule cell layers approximately 400 μm below the cortical surface. This arrangement allows for maximum convergence whereby the Purkinje cell is apposed by the greatest possible number of parallel fibers within the expanse of its dendritic tree. Although Purkinje cells are the only route out of the cerebellar cortex, few of them leave directly. Rather, they project to the cerebellar nuclei, which in turn give rise to cerebellar output. The Purkinje cells of the cerebellar hemispheres project to the dentate nuclei; those of the intermediate cortex project to the globose and emboliform nuclei; and those of the vermis to fastigial nuclei (Figure 7).

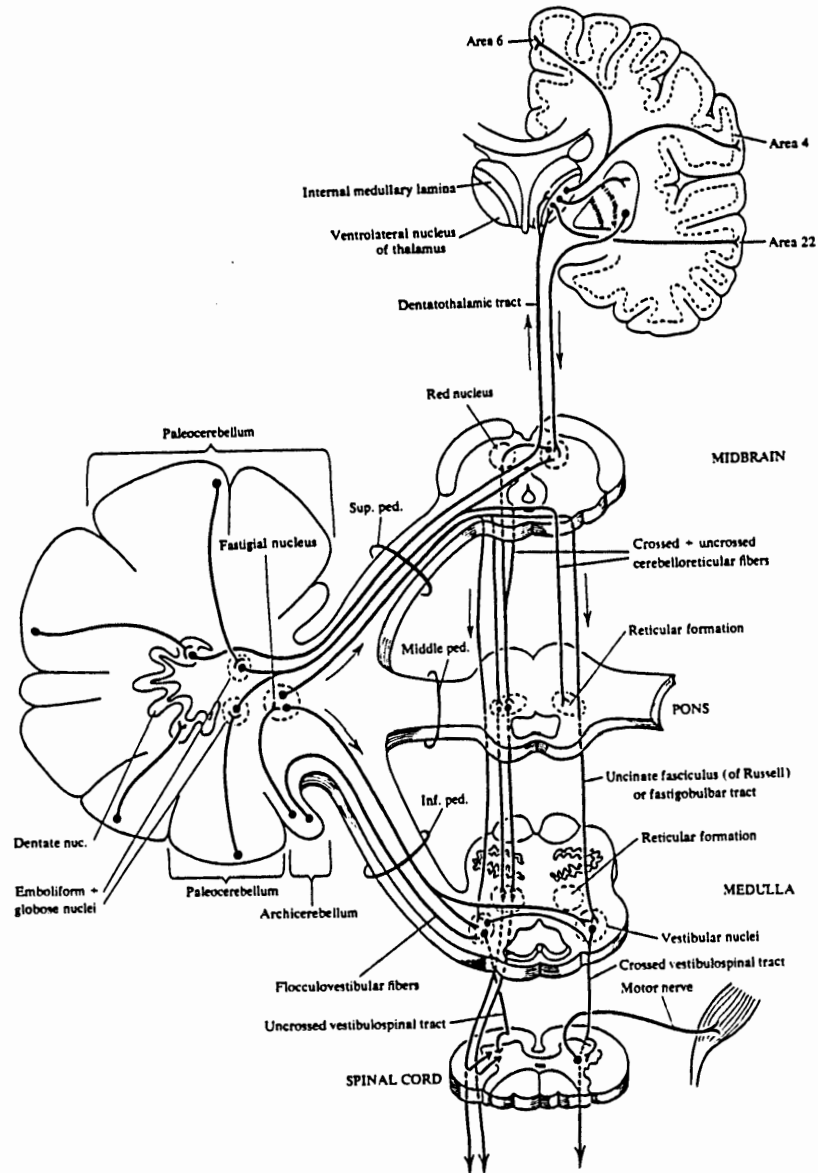


Figure 7. Diagram of the efferent fibers of the cerebellum. Cerebellar outflow indicating route via cerebellar nuclei and brain stem, and ultimate destination on spinal motor neurons and skeletal muscles is depicted. From Pansky B., Budd G. C., Allen D. J.: REVIEW OF NEUROSCIENCE, Second Edition, Copyright (c) 1988 Macmillan Publishing Company, a Division of Macmillan, Inc. Reprinted with permission of Macmillan Publishing Company.

There exist three primary efferent pathways of the cerebellum. In the dentatothalamic pathway the axons from the dentate nucleus terminate in the thalamic ventral lateral nucleus, which in turn projects to the motor areas of the cerebral cortex. Neurons of the intermediate nucleus and the globose and emboliform nuclei terminate on neurons within the red nucleus. Most of the cells of the red nucleus then project to the spinal cord. Terminals from the vermis are directed to the fastigial nucleus, which in turn projects to the lateral vestibular nucleus and the reticular formation. Those Purkinje cells that leave the cortex directly project primarily to vestibular nuclei. The cerebellar hemispheres and the dentate nucleus largely modulate limb muscle movement, while the vermal cortex and fastigial nuclei modulate trunk muscle movement and posture (Willis and Grossman, 1973). Since the deep nuclei receive stimulatory inputs from both mossy and climbing fibers, the function of the Purkinje cell is to provide inhibitory modulation of deep nuclear function.

The cerebellum also consists of three types of intrinsic neurons, so called because their connections lie entirely within the cortex itself (Figure 8). Golgi cells, large neurons with cell bodies about the size of Purkinje cells, are inhibitory to granule cells. Stellate cells, so called due to the star-shaped appearance of their dendritic trees,

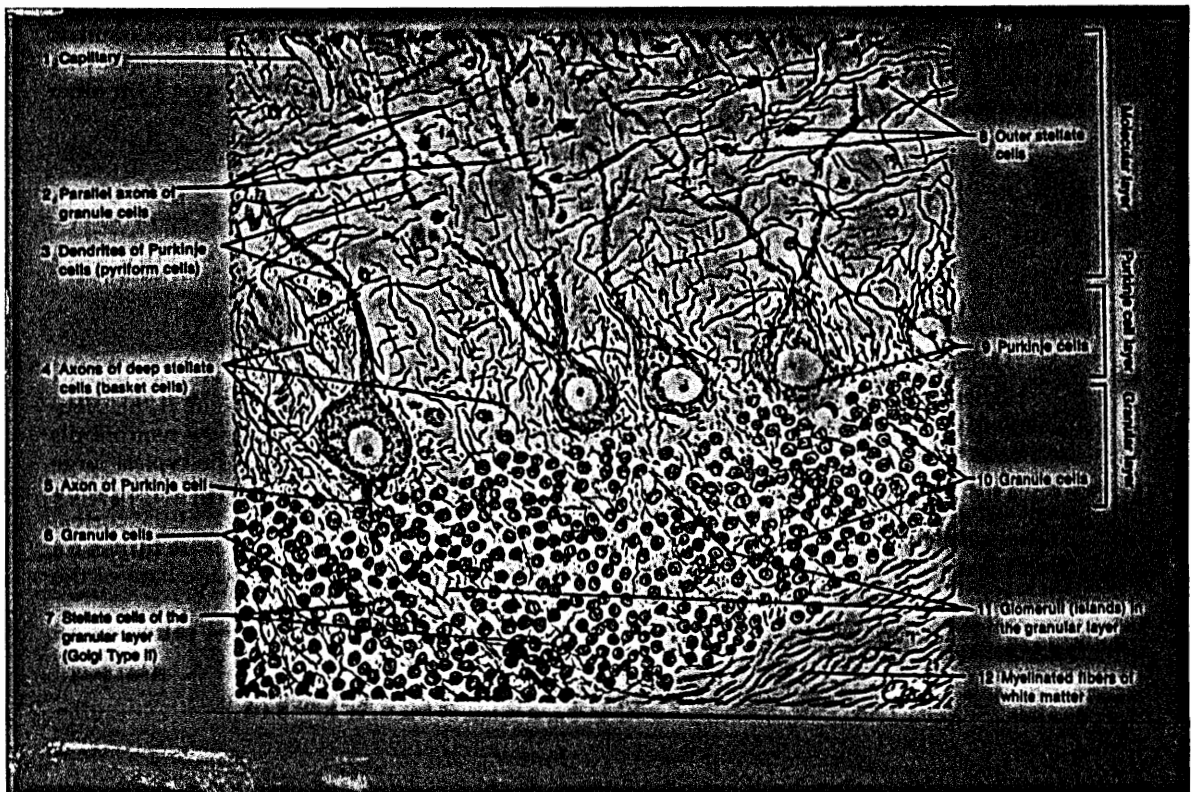


Figure 8. Cerebellar cortex.
 Silver impregnation by Cajal's method, 300 X magnification. (diFiore , 1989) Reprinted with permission of Lea & Febiger Publishing Company.

and basket cells (the most highly differentiated type of stellate cell) are inhibitory to Purkinje cells. Granule cells possess small cell bodies (6 - 9 μm) that give rise to three to five dendrites (1 μm x 30 μm); and are among the smallest in the brain (Shepherd, 1979). Granule cell axons bifurcate within the molecular layer to give rise to parallel fibers which synapse with the dendrites of Golgi, stellate and basket cells.

The neuronal elements of the cerebellar cortex are bounded by typical glial neuropile, which includes the phagocytic microglia and macroglia (Figure 9). Astrocytes and oligodendrocytes are the two primary types of macroglia. The star-shaped astrocytes are subdivided into fibrous astrocytes, which are associated with the myelinated axons of the white matter, and protoplasmic astrocytes, which are associated with the cell bodies, dendrites and synapses of the gray matter. Astrocytes contain end-feet that contact blood capillaries and thus serve an important role in the establishment and maintenance of the blood brain barrier. Oligodendrocytes are smaller glial cells whose function is to produce myelination within the central nervous system.

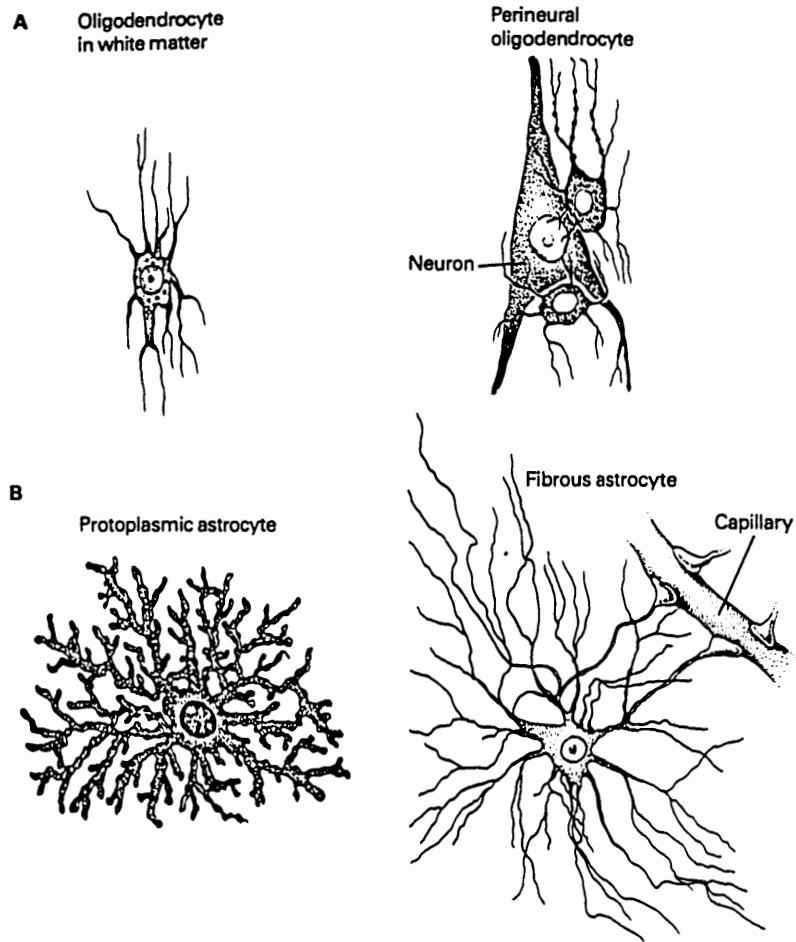


Figure 9. Types of glial elements.

Two types of macroglia exist within the nervous system, oligodendrocytes (A) and astrocytes (B). Note that the end-feet of the fibrous astrocytes establish contact between the capillaries and neurons. Reprinted by permission of the publisher from Chapter 2 by Kandel & Schwartz, *Principles of Neural Science*, pg. 18. Copyright 1985 by Elsevier Science Publishing Co., Inc.

Cerebellar Development in Rats

In the development of the central nervous system, the early rapid increase in brain size is due to the growth of the forebrain, as a result of an increase in nerve cell body size. As development proceeds the proportion of water decreases. This early high fluid content undoubtedly allows for plasticity and facilitates growth. An inverse relationship exists between the amount of myelin and the percentage of water within the brain (Himwich, 1973). The protein content in the rat brain shows the most rapid increase from postnatal (PN) days nine to twelve, followed by a reduced rate of accumulation to adult values at thirty days of age (Pitts and Quick, 1967). This increase in protein content appears to be concomitant to the inversely proportional decrease in water content. There exists a correlation between the total weight of the body and that of the brain. Although after maturing the male brain weighs more than the female brain, there appears to be no difference between the sexes in regard to the proportion of the brain parts in relation to the whole brain. Neuronal development, including that of the cerebellum, also appears to proceed equally in both sexes. The process of neuronal development includes three primary events: histogenesis, migration and synaptogenesis.

Histogenesis involves the generation of neurons and glial cells within the proliferative zones. The histogenesis of cerebellar cortical neurons originates from two germinal zones. Purkinje and Golgi cells originate from the roof of the fourth ventricle. Purkinje cells only develop processes after becoming associated one-to-one with climbing fibers. This association is possible, because both cell types are generated at the same stage (Kornguth and Scott, 1972). Purkinje cells begin to differentiate between post-natal (PN) days 7 and 12. The second germinal zone, known as the external granule layer, gives rise to basket cells which differentiate between PN days 6 and 7, stellate cells which differentiate between PN days 8 and 11 and granule cells that begin differentiation at PN day 10, and some glial cells which continuously differentiate (Nicholson and Altman, 1972a). Although basket and stellate cells are produced within the external granule layer, their numbers are relatively insignificant in comparison to the enormous production of granule cells, the most numerous neurons in the cerebellum.

Migration involves the displacement of post-mitotic neurons from their place of origin to their final destination. During this migratory process, neurons must establish appropriate structural and functional synapses. The most extensively studied aspect of neuronal development within

the cerebellum involves the migration of granule cells and their subsequent frequent synapses with Purkinje cell dendritic trees. Purkinje and granule cells have very different developmental histories. While Purkinje cells arise early in development and are not affected by postnatal applications of antimitotic agents, most granule cells are generated postnatally. In addition, Purkinje cells remain quiescent until the proliferation of the external granule layer and only begin to rapidly differentiate after being activated by granule cells migration past them. This creates two developmental questions. First, how do granule cells recognize the dendritic spines of Purkinje cells in order to make synaptic contact? This problem is solved by the juxtaposition of simultaneously growing granule cell axons and Purkinje cell dendrites, even before the granule cell soma becomes translocated inward past the Purkinje cell dendrites and soma (Sidman, 1975). The progenitors of the granule cells lying within the external granule layer become post-mitotic and emit tangentially directed axons known as parallel fibers, while still close to their positions of generation. The cell body then migrates inward, trailing a perpendicular axon, and eventually comes to rest below the Purkinje cell layer, at which point it develops dendrites (Lund, 1978). Second, since granule cells arise late in development, how do they migrate through paths blocked by

ontogenetically mature cells? Rakic (1971) proposed that the constant apposition of the Bergmann glia to granule cells during this migratory process may be indicative of a guidance mechanism. Although universal agreement has not been reached as to the exact role of the Bergmann fiber in cell migration, it appears that the later post-mitotic granule cells are guided to the deeper layers by these glia, and the remaining neurons are generated in an inside-out order (Angevine and Sidman, 1961). Some of the cells generated by the external granule layer migrate only as far as the molecular layer and then differentiate. According to Altman (1972) the basket and stellate cells differentiate at this location because their processes are oriented at right angles to the parallel fibers, impeding them from penetrating through the bed of parallel fibers.

Synaptogenesis and the establishment of adult connectivity are the result of a cascade of complex molecular events, rather than a single-step process. At first, a transient redundancy exists, due to recognition of pre- and post-synaptic components. This is followed by the regression of non-stabilized synapses to produce the mature neuronal network.

Thyroid Hormone Synthesis, Action and Metabolism

The biogenesis of thyroid hormone involves a three stage process (Figure 10). The initial event involves the active transport and concentration within the thyroid follicle (at least 25 times its concentration in plasma) of inorganic iodide absorbed from the small intestine. Next, iodine is oxidized by the hydrogen peroxide-dependent enzyme thyroid peroxidase, an amphiphilic membrane protein tightly bound to the endoplasmic reticulum of follicular cells. Once activated, the iodine combines with tyrosyl moieties of the glycoprotein thyroglobulin to form mostly 3-monoiodo- and 3,5-diiiodotyrosines. Finally, the iodotyrosines undergo coupling via ether linkages to form thyroxine (3,5,3',5' - tetraiodothyronine, T_4) and 3,5,3'-triiodothyronine (T_3). Selective iodination of specific tyrosine residues produces ten times as much T_4 as T_3 . Peptide bond cleavage by lysosomal proteases within follicular cells results in the release of the hormone from thyroglobulin and subsequent secretion by exocytosis, mostly in the form of T_4 . Once in circulation, the iodothyronines are transported bound to specific binding proteins. Approximately ten times more T_3 than T_4 is transported free in serum (0.3% free T_3 , compared to 0.03% free T_4). The three thyroid hormone binding proteins, albumin, thyroxine-binding prealbumin (TBPA) and

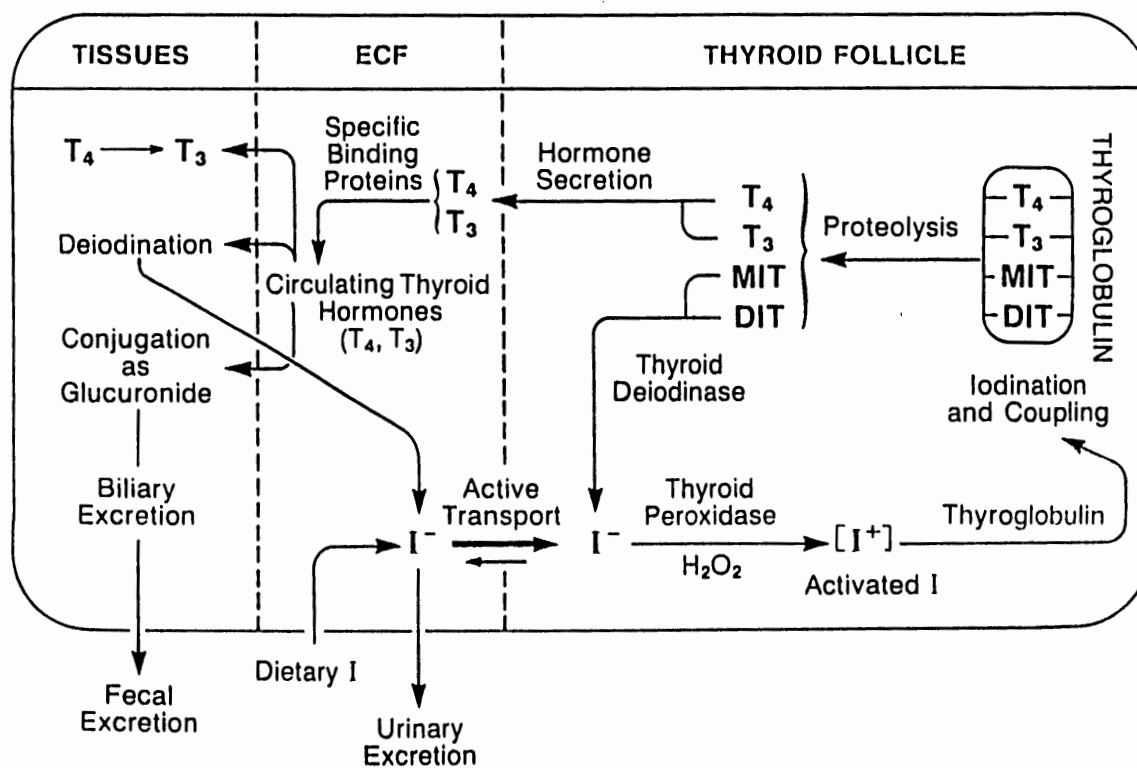


Figure 10. Thyroid hormone synthesis and metabolism. MIT, monoiodotyrosine; DIT, diiodotyrosine; T_4 , thyroxine; T_3 , 3,5,3' - triiodothyronine; I^+ , activated iodide; ECF, extracellular fluid (Griffin and Ojeda, 1988)

thyroxine-binding globulin (TBG), all bind T_4 more tightly than T_3 . Peripheral deiodination of T_4 produces the active hormone T_3 and the noncalorigenic reverse T_3 (rT_3) (Figure 11). While the liver is the major site of deiodination, deiodinase activity has been localized in both cerebral and cerebellar cortexes as well as in the pituitary (Nunez, 1984). Triiodothyronine receptors are widely distributed throughout the body, with the anterior pituitary demonstrating the highest concentration within the central nervous system. These receptors are associated with acidic nonhistone nuclear proteins and bind T_3 ($K_d=10^{-10}$ M) with greater affinity than T_4 ($K_d=10^{-9}$ M). Neuronal nuclei possess a far greater number of T_3 binding sites than glial nuclei (Gullo et al., 1987). Once bound, thyroid hormone exerts its action on basal metabolism by altering protein synthesis and stimulating the Na^+ , K^+ ATPase, thus increasing oxygen consumption and oxidative metabolism.

The iodothyronines may be inactivated by deiodination, with the release of urinary free iodide and the production of noncalorigenic forms, or via enterohepatic metabolism. In the latter case, liver thyroxine is conjugated with glucuronic acid and, to a lesser extent, sulfate on its phenolic hydroxyl group. These conjugates are excreted in bile, transported to the small intestine, and hydrolyzed by

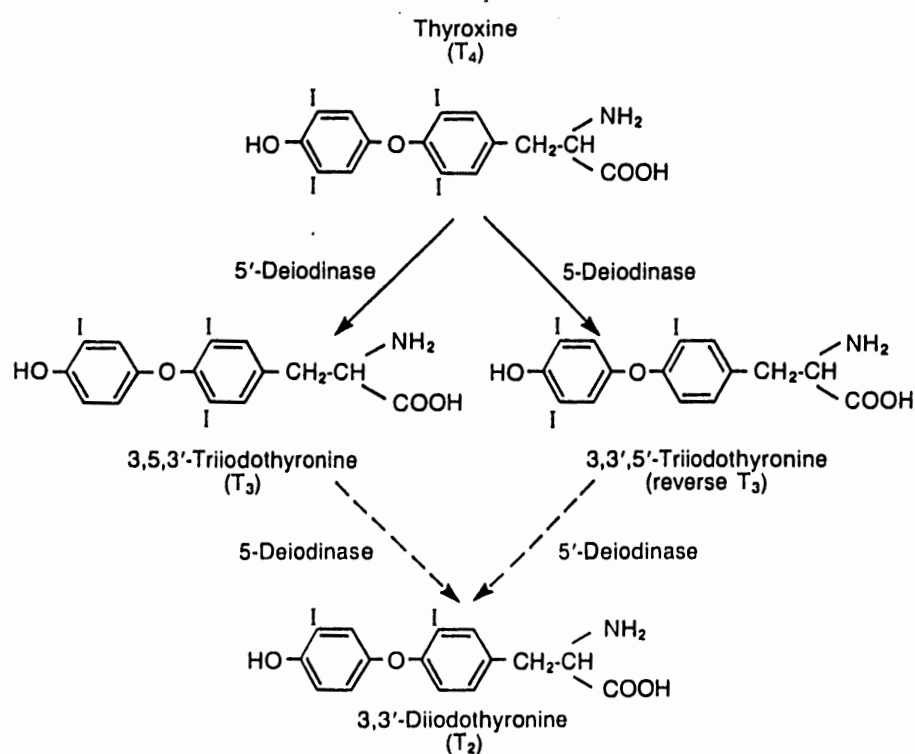


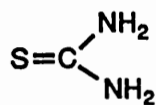
Figure 11. Thyroid hormone metabolism via deiodination. Two types of deiodinases are involved in thyroid hormone metabolism. The 5'-deiodinase produces the metabolically active hormone T₃ while the 5-deiodinase produces the noncalorigenic reverse T₃. Further deiodination produces the inactive metabolite T₂. (Griffin and Ojeda, 1988)

intestinal bacterial enzymes liberating free hormone for re-absorption or fecal loss due to bacterial decarboxylation.

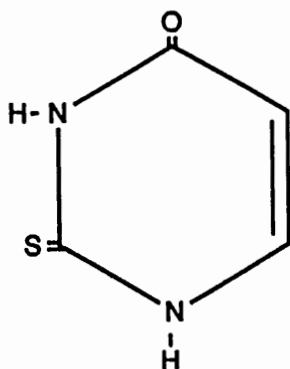
Regulation of Thyroid Hormone Function

Thyroid hormone function is regulated along the hypothalamic-pituitary-thyroid axis. The tripeptide thyrotropin-releasing hormone (TRH) is secreted via the hypothalamic-hypophyseal portal circulation. At the anterior pituitary, TRH interacts with both thyrotrophs and mammotrophs. Activation of thyrotrophs to release thyroid-stimulating hormone (TSH) is achieved by the generation of the second messengers inositol triphosphate and diacylglycerol. TSH is a 28 kD glycoprotein consisting of two noncovalently bound subunits (α & β). The α subunit is common to follicle stimulating hormone, luteinizing hormone and human chorionic hormone, while the β subunit conveys the hormonal specificity. TSH stimulates follicular iodothyronine secretion by interaction with specific thyroid cell surface receptors, activating adenylate cyclase and ultimately enhancing cAMP production. Either T_4 or T_3 can inhibit TSH secretion via negative feedback, but since T_3 is formed in the anterior pituitary by type II deiodination it appears to serve a more important regulatory role.

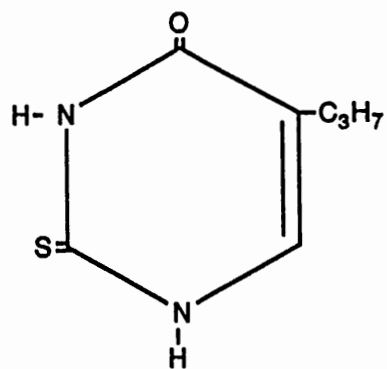
An antithyroid agent is designated as any substance which inhibits thyroid hormone function. This may be accomplished by inhibiting utilization of the hormone by acting as a structural analog, altering the feedback system whereby T_3 inhibits hypophyseal thyrotropin release, or via inhibition of thyroid peroxidase-catalyzed iodination or peripheral deiodination. There exists a variety of means whereby hypothyroidism may be induced. Surgical and radiothyroidectomy are effective, but pharmacological agents are preferred because they avoid the associated trauma, while maintaining parathyroid function. Natural goitrogens are found in cabbage, cauliflower, kale and mustard greens, and animals maintained on diets containing large quantities of these vegetables have a tendency to develop goiters. The most commonly used therapeutic agents are the thioureyline drugs. Thiouracil (TU), which incorporates thiourea into a six-membered heterocyclic ring to form the thioureyline class of compounds, was abandoned due to excessive side effects. The propyl derivative of TU, known as 4-hydroxy-2-mercapto-6-propylpyrimidine (PTU), maintained the antithyroid potency and serendipitously diminished the toxicity. A more potent compound methimazole, and the substituted form carbimazole, were introduced later (Cooper, 1984) (Figure 12).



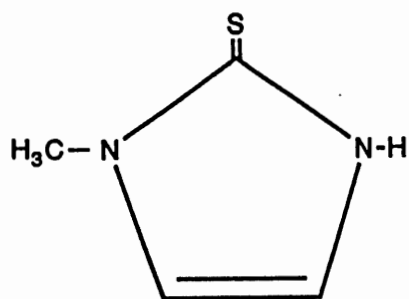
Thiourea



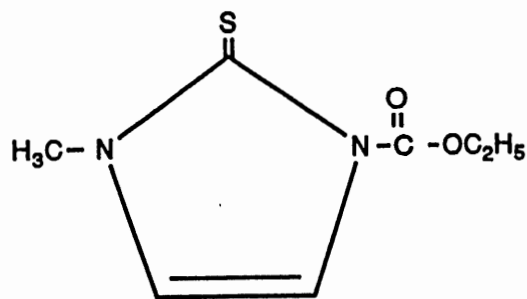
Thiouracil



6-Propyl-2-Thiouracil



Methimazole



Carbimazole

Figure 12. Structures of commonly used hyper thyroid therapeutic agents.
 Thioureylene drugs are substituted forms of thiourea. The most widely used goitrogen is 6-propyl-2-thiouracil (PTU).

Propylthiouracil Effects

PTU exerts both intra- and extrathyroidal effects. Within the thyroid gland PTU inhibits iodotyrosine coupling and iodide organification. Contrary to previous reports that PTU might also inhibit thyroglobulin synthesis, Moura and coworkers (1990) demonstrated that PTU (1 $\mu\text{mol}/100\text{ g}$ body weight) had no effect on thyroglobulin synthesis and that inhibition of thyroglobulin iodination was the primary mechanism of PTU action. Extrathyroidal effects included alterations in RNA and protein synthesis within target tissue, and inhibition of thyroxine deiodination, serum transport of thyroxine, and the biliary and fecal paths of metabolism. Thyroid deficiency decreased the rate of protein synthesis, while the rate of RNA synthesis and the overall DNA content were hardly affected. Since the amount of protein and RNA relative to DNA declined, it may be inferred that hypothyroidism results in alterations in cell size rather than total number. These data suggest that in the developing brain thyroxine is involved primarily in the regulation of translation of the genetic message into protein (Balázs et al., 1968). The thioureylene drugs inhibit iodination by competing with tyrosine or tyrosyl residues of thyroglobulin for the activated iodine, which is reduced by the sulfhydryl group of these compounds, resulting in the formation of a disulfide (Nagasaka and Hikada, 1976; Taurog,

1976). PTU appears to preferentially inhibit 5-deiodination of T_4 to T_3 rather than 5'-deiodination of T_4 to rT_3 , since serum rT_3 levels increase and T_3 levels decrease in a hypothyroid state (Cavalieri and Pitt-Rivers, 1981). Thyrotrophs detect the decrease in T_3 concentration and hypersecrete thyrotropin. Follicular hypertrophy results due to the absence of iodothyronine synthesis. Since PTU administered to hypophysectomized rats produces similar results, it is clear that goiter production is the direct result of increased pituitary TSH secretion (Morreale de Escobar and Escobar del Rey, 1967). Goiter production is not due to the toxic effects of PTU, because thyroxine treatment is successful in correcting many of the associated developmental abnormalities in PTU-treated animals. If thyroxine is administered in conjunction with PTU, thyrotrophs take up T_4 , convert it to T_3 via the PTU-insensitive type II deiodinase, and this causes a decrease in thyrotropin secretion. Meanwhile, peripheral cells dependent on intracellular deiodination remain affected by hormonal deprivation. Serum-binding interactions with iodothyronines increase in the hypothyroid state. TBG concentrations exhibit a transient postnatal surge and are enhanced in PTU-treated animals, while TBPA concentrations show little developmental alteration and do not respond to thyroid hormone depletion.

Since TBG is affected by thyroid deficiency it appears to be the primary thyroid hormone binding protein in the rat (Savu et al., 1989). PTU treatment also alters clearance of thyroxine and its metabolites, except for that of glucuronidate conjugates of T_4 . However, inhibition of the type I deiodinase results in enhanced biliary excretion of sulfonated conjugates of T_4 and accumulation of T_3 sulfonates (Rutgers et al., 1989; Rutgers et al., 1990). PTU treated animals also excrete increased amounts of calorogenic material. Therefore, PTU affects intracellular iodothyronine concentrations as well as extracellular availability.

Effect of PTU on Cerebellar Development

It is generally accepted that hormones can alter the developmental expression of a number of genes. The classical work of Gudernatsch (1914) demonstrated that thyroid hormones could induce metamorphosis in anuran tadpoles. Ever since the discovery that hypothyroidism produces mental retardation, and that androgens modulate sexual behavior in males, hormones have been considered to exert environmental influences on neural development (McEwen, 1981; Toran-Allerand, 1984). Critical developmental processes that shape the immature brain, such as the extent of neurite outgrowth, the establishment and maintenance of synaptic

contacts, and levels of neurotransmitter synthesizing enzymes, have been shown to be affected by thyroid hormones (Aizenman and de Vellis, 1987). Immunoreactive thyroglobulin has been detected on the 15th day of gestation in the fetal rat, with detectable T_4 and T_3 present two days later (Kawaoui and Tsuneda, 1986). It also has been demonstrated that the thyroid gland becomes responsive to TSH on the 18th embryonic day and that extensive numbers of thyroid hormone receptors already exist on the 19th embryonic day, at which time the brain becomes responsive to thyroid hormone (Aizenman and de Vellis, 1987). Therefore, in order to investigate the effect of thyroid deprivation on development, antithyroid agents must be administered *in utero* prior to the 18th embryonic day. D'Angilo (1967) demonstrated that goitrogens could cross the placenta to block fetal thyroid hormone function, while Legrand (1967) showed that the goitrogen PTU is transported in the mother's milk. Since the rat is an altricial animal at birth and most cerebellar neurogenesis occurs postnatally, the effects of an altered thyroid state on cerebellar development may be studied.

The literature contains extensive treatises evaluating the effects of PTU on cerebellar development, with perhaps the most noteworthy being the work of Legrand. The effects of PTU treatment are evident even at the initial event of

neural development, neurogenesis. PTU-treated animals exhibit a decreased rate of cell proliferation; however, this appears not to be due to a change in the length of the cell cycle or the duration of individual phases (Nicholson and Altman, 1972a; Jacobson, 1978). While granule and Purkinje cell numbers appear to be unaffected, the number of basket cells is reduced, but the number of stellate cells and astrocytic glia, particularly Bergmann glia, is enhanced (Nicholson and Altman, 1972a; Clos and Legrand, 1973; Lauder, 1977; Legrand, 1979). Even though the Purkinje cell numbers are unaltered by PTU treatment, they exhibit altered morphology, including abnormal somal shape, decreased number of Nissl bodies, increased numbers of mitochondria, and delayed and decreased dendritic arborization (Legrand, 1967). It appears as though the total number of cells within the cerebellum remains constant, since the glia to neuron ratio is increased. However, a decrease in cell size leads to an increased packing density, particularly within the molecular layer (Nicholson and Altman, 1972a; Lauder, 1977).

Cell migration is also affected by hypothyroidism. Granule cell migration across the molecular layer is retarded by one week and the external granule layer persists beyond 21 days, the normal period of disappearance (Legrand, 1967; Hamburg, 1968). The delay in migration results in

altered synaptogenesis since cellular differentiation and synaptic competence must occur within a narrow critical period. In addition to an overall reduction in the number of synapses, there is an increase in inappropriate heterologous synapses (e.g. a greater than one-to-one relationship of climbing fibers to Purkinje cells) (Nicholson and Altman, 1972b; Legrand, 1986). Synapsis with appropriate targets is required for differentiation and continued cell viability. Due to the delay in granule cell migration the glomeruli differentiate into smaller, less homogeneous structures (Legrand, 1967; Legrand, 1979). Because the differentiation of basket cells requires the formation of synapses with Purkinje cells, there will be a reduction in the number of cells capable of differentiating into basket cells if the Purkinje cell loses its synaptic capability. Thus, the number of basket cells declines while the number of stellate cells is augmented. Hypoplastic neuropil, decreased length of parallel fibers and increased cell death within the granule layer results in decreased synaptic density (Nicholson and Altman, 1972b; Lauder, 1977).

Effects of Hypothyroidism on Protein Synthesis

It is obvious that the absence of thyroid hormone during critical periods of neural development creates altered cellular morphology and synaptogenesis within the

cerebellum. These alterations result in the cerebellum's inability to regulate motor coordination properly, and leads one to question whether the genetic expression of these abnormal cells is modified. While Bass and Young (1973) showed that hypothyroidism results in a reduction in the number of oligodendrocytes, Legrand (1986) observed a retarded formation and maturation of oligodendrocytes without an effect on their final number. This delay in maturation causes a significant delay in and reduction of myelin deposition (Balázs et al., 1969; Walters and Morell, 1981). Almazan and coworkers (1985) demonstrated that the expression of the myelin components 2',3'-cyclic nucleotide 3'-phosphodiesterase and myelin basic protein are affected by the thyroid state. The hypothyroid state has also been linked to altered expression of other cerebellar components. Dziegielewska (1985) showed that alterations in the developmental expression of plasma proteins purportedly synthesized within the cerebellum, such as transferrin and low density lipoprotein is influenced by hormonal status.

Transferrin Structure, Function and Synthesis

Serum transferrin (T_f), the second most abundant plasma protein, is a non-heme iron binding protein related to lactotransferrin, ovotransferrin and melanotransferrin

(Review, deJong et al., 1990). It is composed of a single polypeptide chain containing 679 amino acids with two N-linked oligosaccharide chains. Rat T_f has a calculated molecular weight of 76.5 kDa or 74 kDa for the unglycosylated *in vitro* synthesized form (Huggenvick et al., 1987). Each T_f molecule contains two iron binding sites which bind one ferric (Fe³⁺) iron and one carbonate or bicarbonate anion (HCO³⁻ or CO₃²⁻). In the absence of these anions, other anions may be substituted, including pyruvate, lactate, malate, oxalate and ethylenediamine-tetraacetate. Transferrin may also bind other metal ions instead of iron, including Cu²⁺, Co²⁺, Mn²⁺, Cd²⁺ and Ni²⁺ (Morgan, 1981); however, binding to iron is preferred. Saturation of transferrin rarely occurs since there exist more T_f binding sites than total plasma iron (Fletcher and Huehns, 1968). Protonation of the anion results in anion release, destabilization of the complex and release of iron to form apotransferrin, the protein without associated iron. As opposed to the other iron transport proteins haptoglobin, ferritin and vitellogenin, transferrin is not denatured or catabolized during transport and therefore can be considered the only true iron carrier.

Transferrin's primary function is iron binding and transport from the intestine, reticuloendothelial system and

liver parenchymal cells to other cells. Utilizing *in vitro* cell culture experiments, T_r has been shown to be required as a growth factor for the differentiation of cells maintained in serum-free medium (Goubin et al., 1983; Morgan, 1983; Aizemann and de Vellis, 1987; Schaeffer et al., 1989) and as a neurotrophic factor (Beach et al., 1983; Bloch et al., 1985). This may be substantiated by the fact that T_r is widely distributed throughout the central nervous system and that T_r receptors are found in high density on rapidly proliferating cells (Kahn et al., 1987).

Although T_r is synthesized primarily in the liver, extrahepatic gene expression has been detected in fetal muscle, lymph nodes, activated T lymphocytes, macrophages, marrow, spleen, thymus, salivary glands, ovary, testes and mammary gland (Morgan, 1983; Schaeffer et al., 1989). In the brain, the concentration of transferrin mRNA is approximately one-tenth of that in the liver (Levin et al., 1984; Kahn et al., 1987). Bloch (1985) detected the synthesis and storage of T_r within oligodendrocytes and found that stained cells were arranged either singly or in small clusters associated with capillaries. Within the cerebellum, the white matter was heavily labelled, the gray matter was free of detectable label and few, if any, cells were labelled within the molecular layer (Bloch et al., 1985, Connor and

Fine, 1986). Transferrin receptors were demonstrated on developing, but not adult neurons (Oh et al., 1986). Within the cerebellum, Purkinje cells were weakly stained and no immunoreactivity was detected within the granular or molecular layers (Giometto et al., 1990).

Transferrin concentrations are low at birth and gradually increase, during the time of myelination, to plateau at adult levels by 60 days of age (Connor and Fine, 1987; Kahn et al., 1987). Radioactive amino acid incorporation into hepatic transferrin is known to be affected by fasting and PTU treatment (Morgan, 1969; Kahn et al., 1987).

Apolipoprotein E Structure, Function and Synthesis

Plasma lipoproteins are water soluble complexes responsible for the transport of lipids and are generally divided into categories based on density. These include chylomicrons, very low density lipoproteins (VLDL), low density lipoproteins (LDL) and high density lipoproteins (HDL). Each lipoprotein complex contains a protein component known as an apolipoprotein. For example, apolipoprotein B (apo B) is the major protein of LDL, and apolipoprotein E (apo E) was first detected in VLDL, but has also been detected in LDL, HDL and chylomicrons. Apo E is an arginine rich glycoprotein that exists in three isoforms which result from differences in glycosylation (particularly post-translation-

al sialylation) and in amino acid sequence. It is synthesized with an 18 amino acid signal sequence, but does not have a propeptide form, and the mature protein consists of 293 amino acids with a calculated mass of 34 kDa (McLean et al., 1983). Two types of apo E receptors are known to exist. One type, found in both hepatic and extrahepatic tissues, is utilized by both apo B and apo E. A second, unique hepatic receptor interacts with apo E alone (Mahley et al., 1984).

The function of all apolipoproteins is transport and receptor-mediated uptake of lipids; however, their wide distribution suggests other possible roles such as the regulation of local hormonal homeostasis by acting as a neurotransmitter or neurohormone precursor. Apo E containing lipoproteins bind lymphocytes and suppress their response to mitogens. Therefore, apo E may participate in the regulation of the immune system (Boyles et al., 1985).

Apo E is synthesized in the liver, but is also synthesized and secreted, to a lesser extent, by extrahepatic tissues including brain, adrenal, spleen, kidney and muscle. It has been estimated that extrahepatic synthesis could account for as much as 20% of the total apo E produced and that the concentration of apo E mRNA in the brain is one-third of that in the liver (Mahley et al., 1984). Within the central nervous system, apo E has been localized exclu-

sively to astrocytic glia, both fibrous and protoplasmic, and specialized astrocytes including Bergmann glia (Mahley et al., 1984; Boyles et al., 1985; Elshourbagy et al., 1985). Immunologically detectable apo E was homogeneously distributed in cell bodies, within the Golgi apparatus, and along glial processes (Boyles et al., 1985; Lin et al., 1986).

Fetal liver contains low levels of apo E; however, just prior to parturition there is a rapid induction of synthesis. In contrast, brain apo E levels are low even after birth and only gradually increase (Elshourbagy et al., 1985) and become stabilized (Panduro et al., 1987) as development proceeds. PTU treatment results in decreased activities of hepatic lipase, lipoprotein lipase, and lecithin:cholesterol acyltransferase, three enzymes responsible for plasma lipoprotein metabolism (Valdermarsson, 1983). This accounts for the hyperlipidemia and hypercholesterolemia associated with hypothyroidism. Dory and Roheim (1981) observed 100% increases in plasma apo E concentrations in PTU-treated animals, while Davidson and coworkers (1988) detected a twofold increase in hepatic apo E synthesis rates. Increased hepatic synthesis and plasma levels of apo E might be the result of alterations in apo E mRNA content. Apostolopoulos and coworkers (1987) observed a slight decrease in hepatic mRNA levels, but others have found apo E mRNA levels to be compa-

rable in hypothyroid and euthyroid animals (Davidson et al., 1988; Staels et al., 1990). If the thyroid state does not influence apo E mRNA levels, altered gene expression cannot be invoked to explain the alterations in plasma apo E levels. Therefore, it would appear that apo E gene regulation by thyroid hormone is exerted at a translational or post-translational level (Panduro et al., 1990). Apo E levels within the brain would appear to be restricted to the brain by the blood brain barrier. Since astrocytes act as a metabolic interface in the blood brain barrier and are responsible for regulating the interstitial fluid composition, astrocytic apo E synthesis may play a critical role in the regulation of cholesterol metabolism within the central nervous system. As with transferrin, since apo E is abundant in serum, its rate of synthesis rather than tissue concentrations must be used in order to investigate the regulation of developmental gene expression.

The morphological alterations in central nervous development induced by hypothyroidism are well documented. Only recently has attention been focused on the expression of endogenous proteins. While the initial work was performed on primary cell culture, immunohistochemical studies in adult animals followed. With the advent of improved molecular techniques it is possible to investigate the synthesis of proteins both *in vitro* and *in situ*. This is particularly

important for those proteins whose concentrations might be misinterpreted from synthesis outside the central nervous system (e.g. angiotensin, substance P, plasma proteins, etc.). The following study will utilize modern molecular techniques to examine the postnatal developmental expression of transferrin and apolipoprotein E genes within the cerebellum of propylthiouracil-induced hypothyroid rats.

The aims of the study are to:

- 1) Establish a developmental pattern of transferrin and apolipoprotein E protein synthesis.
- 2) Establish a developmental pattern of transferrin and apolipoprotein E mRNA expression.
- 3) Determine the effects of altered cerebellar morphology induced by hypothyroidism upon transferrin and apolipoprotein E mRNA expression and protein synthesis.

CHAPTER II
MATERIALS AND METHODS

Animal Care and Treatment

Animals (F-344, Fisher rats) were housed in the university vivarium and were maintained on a 14:10 light/dark cycle, with water and Purina Rat Chow given *ad libitum*. Vaginal smears were used for timing pregnancies, and animals which were "sperm positive" were considered to be at day 0 of gestation. To minimize nutritional influences on development, litter size was maintained at 8 pups or less. Male rats were sacrificed on postnatal (PN) days 1, 10, 20, 30, and 60; where day 0 was considered to be the day of birth and weaning occurred on PN day 21. For tissue preparation, the animals were decapitated, the brains quickly removed, and rinsed twice in ice-cold phosphate-buffered saline solution (PBS = 150 mM NaCl, 10 mM Na₂HPO₄, 2 mM NaH₂PO₄). Seasonal and circadian variations were eliminated by sacrificing all animals within a 2 month period and at the same time of day. The cerebella were dissected free of other brain tissue and then frozen in liquid nitrogen. Pools of tissue were stored frozen at -80 °C until used.

In order to use the propylthiouracil (PTU) model of the hypothyroid state, it was necessary to establish an appropriate treatment regimen. Various routes of PTU administration were attempted with limited success. First, intubation of 50 mg PTU in water per day according to Legrand (1967) was attempted. Intubation of 50 mg PTU in a sesame seed oil emulsion was also attempted. Next, various solvent systems were tried and dimethylsulfoxide (DMSO) selected, since only small volumes were required for neonatal intubation. PTU solubility in water was assayed and was found to be soluble only in strong alkali (0.5 N NaOH, pH \geq 12). This pH is intolerable for physiological administration, but it was found that the solution could be titrated to pH 10 with concentrated hydrochloric acid, while allowing the PTU to remain in solution. Having exhausted all attempts at intubation, other routes of PTU administration were sought.

The most commonly used route for PTU administration is as a 0.1% solution in drinking water. Not only is PTU not soluble at that concentration, but it also adheres to the water bottle resulting in inconsistent doses. In addition, PTU is a bitter tasting compound and drug delivery is diminished as water consumption decreases. To overcome the solubility difficulties, the PTU was first dissolved in

NaOH, then added to the drinking water. However, the bitterness of this solution was only accentuated. In order to mask the bitter taste, dextrose was added to the basic PTU solution to 5%. Within a matter of hours the sodium hydroxide oxidized the dextrose and the solution turned brown.

Finally, subcutaneous administration of the alkaline PTU solution appeared to be the most viable means of PTU administration. To prepare the hypothyroid model 6-propyl-2-thiouracil (Sigma Chemical Co., St. Louis, MO) was administered according to Lau and Slotkin (1982). Three treatment regimens were utilized. Briefly, dams were given daily PTU injections (20 mg/kg body weight subcutaneously, s.c.) or equivalent volumes (1.0 ml/kg) of vehicle (0.5 N NaOH, pH 10.0) for 15 days, from day 16 of gestation. Neonates were given PTU (20 mg/kg at 1.0 ml/kg s.c.) or vehicle beginning on PN day 1 and every day thereafter for 9 days (PTU 1). As a parallel control, another treatment group was not subjected to *in utero* PTU administration and 0.1% PTU was only supplied in the drinking water from PN day 10 until sacrificed (PTU 2). In an attempt to determine the effects of prolonged PTU treatment, following PTU injections as before, animals were maintained on 0.1% PTU until sacrificed (PTU 3). Due to the delayed developmental state, hypothy-

roid pups were not weaned until PN 30. Since no data are available on solution stability and the maintenance of therapeutic potency, fresh PTU was prepared for each treatment regimen.

The effects of hypothyroidism was assessed histologically (Legrand, 1967) and the extent of hypothyroidism with assays, indirectly by measuring serum PTU and directly by assay of serum free T_3 , as described below. In addition, comparisons were made of body, brain, and cerebellum weights; weight ratios of brain:body and cerebellum:brain were compared under control and hypothyroid conditions.

Histology

To evaluate histological alterations in the cerebellum, control and hypothyroid animals were anesthetized with Nembutal (40 mg/kg, intraperitoneal) and perfused transcardially with PBS, until venous return was clear, followed by buffered formalin (10% formalin, 29 mM Na_2HPO_4 , 54 mM NaH_2PO_4 , pH 7.4) at room temperature for 5 min for 10 day old animals to as long as 1 hr for 60 day old animals. Brains were removed, cerebella were blocked to minimum size, and were fixed by immersion overnight in 10% buffered formalin at 4 °C. Tissue blocks were rinsed in phosphate buffer

(20 mM Na_2HPO_4 , 80 mM NaH_2PO_4 , pH 7.4) and then cryoprotected by diffusion exchange in 10% sucrose-phosphate buffer for 1 hr. Once equilibrated, the tissue was quickly frozen in isopentane at -80°C , mounted onto a brass chuck, and blocked with OCT embedding medium (Polysciences Inc., Warrington, PA). Ten micrometer frozen sections were collected by thaw-mounting onto gelatin coated slides (0.1% gelatin with 0.01% chromic potassium sulfate) and allowed to dry overnight. Sections were stained in cresyl violet followed by dehydration in an ethanol series (30%, 50%, 70%, 95%, 100% twice, xylene twice) and Permount preparation, according to standard histological techniques.

The effect of hypothyroidism on Purkinje cell dendritic arborization was determined by the rapid Golgi method of staining (Millhouse, 1981). Immediately following decapitation of the animals, the cerebellum was removed and blocked to minimum size. The tissue was then fixed by immersion in 2.5% potassium dichromate with 0.33% osmium tetroxide at room temperature for 2-8 days for brains from 30 and 60 day old animals, and for 10-12 days for brains from animals up to 3 weeks of age. After decanting the fixative, an equal volume of 0.75% silver nitrate solution was added. The silver nitrate solution was gently swirled, decanted and refilled with fresh silver nitrate solution. The tissue was

stained with silver nitrate solution for 24-36 hr at room temperature in the dark. To clear the silver nitrate precipitate on the tissue, it was rinsed in 80% ethanol. In order to follow dendritic processes, 100 μm sections were cut on a Lancer Series 1000 vibratome. Sections were mounted onto gelatin coated slides (see above), sections dehydrated with three 15 min changes of absolute ethanol, and then cleared with three 15 min changes of methyl salicylate (oil of wintergreen), where the first bath was a 1:1 mix of alcohol and oil. Sections were placed in one 15 min bath of xylene for final clearing, air dried, and mounted immediately, as described above. To quantitate histological alterations, images were digitized from camera lucida drawings using the Zeiss video plan image analysis system.

PTU / T₃ Assay

The concentration of PTU in serum was determined according to the method of Ratliff et al. (1972). Two milliliters of serum were mixed with 4.0 ml of buffer-chloride solution (50 mM boric acid, 50 mM KCl, 1.7 M NaCl, pH 8.0) and 1% 2,6-dichloroquinone-4-chloroimide (Sigma Chemical Co., St. Louis, MO). After exactly 10 min, 4.0 ml of chloroform were added and thoroughly mixed by vortexing for one min. Following centrifugation at 1000 rpm for 10 min, the

dark-colored aqueous phase was aspirated and the remaining organic phase was filtered. The absorbance of the filtrates was determined at 435 nm and results (in $\mu\text{g/ml}$) were interpolated from a previously prepared standard calibration curve over a range of 0 - 12.5 $\mu\text{g/ml}$.

To verify directly the hypothyroid state and to correlate the findings of the PTU assay a free T_3 radioimmunoassay (Diagnostic Products, Los Angeles, CA) was used (Larsen, 1976). One milliliter of [I^{125}] free T_3 and 100 μl of rat serum was added to a free T_3 antibody-coated tube and vortexed briefly. After a 3 hr incubation at 37 °C, the solution was aspirated and binding determined by counting for 1 min in a gamma counter. Free T_3 concentrations in pmol/l were determined from a standard calibration curve over a range of 0 - 44 pg/ml. Since this is a competition assay, the counts are inversely proportional to free T_3 concentrations.

Statistics

Results are presented as the mean \pm standard error of the mean (sem). In order to determine the effect of age and PTU treatment on the parameters measured, a two-way analysis of variance (ANOVA) was performed. The data presented for

PTU 3 at PN day 30 represent an N = 1. No data are available for PTU 3 at PN day 60, due to 100% mortality. In order to perform statistical analysis it was necessary to block the data so that PN day 60 PTU 3 data was not required. The first analysis of variance omitted data at PN day 60 and had a critical treatment value of $F_{3,237} = 2.65$ for body and organ weight and $F_{3,\infty} = 2.61$ for histology. The second analysis of variance omitted data for PTU 3 and had a critical treatment value of $F_{2,353} = 3.03$ for body and organ weight and $F_{2,\infty} = 3.00$ for histology, at the $p \leq 0.05$ level. The significance of these differences was then determined post-hoc by the Tukey test (Zar, 1984).

RNA Extraction

Total RNA was isolated by phenol/chloroform extraction according to the method of Paul & Gilmour (1968). The frozen cerebellar tissue was homogenized in five volumes 1X SET buffer (25 mM Tris-HCl pH 7.4, 2 mM EDTA, 1% SDS) and then one volume of 10% Triton X-100/10% sodium deoxycholate and one volume 10X SET buffer were added and vigorously mixed. Phase extraction of nucleic acids was accomplished by adding to the homogenate an equal volume of buffer saturated (1X SET) phenol (16% aqueous):chloroform:isoamyl alcohol at a

ratio of 25:24:1. Phases were vigorously mixed for 10 min on a wrist action shaker and then separated by centrifugation for 15 min at 8,000 rpm (brake off). The nucleic acids in the aqueous phase were re-extracted three times with an equal volume of the organic phase and separated as before by centrifugation. Nucleic acids were precipitated from the aqueous phase by adding 0.1 volume of 2.0 M NaCl and 2 volumes of absolute ethanol at -20 °C for at least 8 hr.

Contaminating DNA and/or glycogen was removed from the RNA pellet by performing four sodium acetate washes (3.0 M $\text{CH}_3\text{COONa}\cdot 3\text{H}_2\text{O}$, 5 mM EDTA, pH 6.0) to dissolve the DNA and glycogen while keeping RNA out of solution. The resulting pellet was collected by centrifugation at 8,000 rpm. The RNA pellet was equilibrated in 70% ethanol containing 0.2 M NaCl and precipitated as above.

Since phenol is a relatively slow denaturant, precautions must be taken to avoid RNase digestion. Tissue must be kept frozen until homogenized, all solutions should be ice-cold and the procedure carried out on ice.

Since only one PTU 3 animal survived to PN day 30, it was necessary to utilize an RNA extraction procedure intended for small sample sizes (Chomczynski & Sacchi, 1987). The denaturing solution used in this method includes 4 M guanidinium thiocyanate, 25 mM sodium citrate, pH 7.0;

0.5% sarcosyl, and 0.1 M 2-mercaptoethanol (solution D). Extraction took place in solution D, 0.2 M sodium acetate, pH 4.0, water saturated phenol, chloroform (1 : 0.1 : 1 : 0.2), followed by precipitation with one volume isopropyl alcohol at -80 °C. After centrifugation, the pellet was washed with 75% ethanol and RNA solubilized in 1X TE Buffer (10 mM Tris, 1 mM EDTA, pH 7.6). The quality (absence of contaminating DNA) and yield of RNA was greater than all other extraction methods used.

Poly A⁺ RNA (mRNA) Isolation

Messenger RNA was isolated by oligo (dT) cellulose affinity chromatography (Aviv & Leder, 1972). Total RNA, after the 3.0 M sodium acetate washes and precipitation, was collected by centrifugation at 10,000 rpm for 20 min at 4 °C. The resulting pellet was dissolved in water (1 ml/g tissue) and an appropriate amount of 2X loading buffer (20 mM Tris-HCl pH 7.6, 2.0 mM EDTA, 0.4 M NaCl) to bring the RNA concentration between 10 and 20 A_{260nm}/ml. The sample was loaded onto an oligo (dT) cellulose column (Collaborative Research Inc. Bedford, MA) at 20 drops/min for three successive passes. The column was then washed with 20-30 volumes of loading buffer (10 mM Tris-HCl pH 7.6, 1.0 mM EDTA, 0.2 M NaCl) in 5 ml aliquots in order to remove non-

polyadenylated RNA (Poly A^(c) RNA is mostly rRNA, tRNA). Poly A⁺ RNA was eluted from the column by the addition of 1 ml aliquots (about 10-12 ml total) of elution buffer (10 mM Tris-HCl pH 7.6, 1.0 mM EDTA) at the rate of 10 drops/min. The eluate was collected in individual tubes and the absorbance at 260 nm determined. Fractions containing the majority of Poly A⁺ RNA were pooled and RNA precipitated by adding 0.1 volume of 3.0 M NaCl and 2 volumes of absolute ethanol and placing the solution at -20 °C overnight. Following centrifugation, the mRNA pellet was resuspended in elution buffer to 1 mg/ml and stored at -20 °C.

***In vitro* Translation**

In vitro translation of cerebellar mRNA was performed in a micrococcal nuclease-treated, reticulocyte lysate, translation system (Pelham & Jackson, 1976) (Promega, Madison, WI). The reaction mix consisted of 100 μ l reticulocyte lysate, 9 μ l amino acid mixture without methionine and 26 μ l L-[³⁵S]-methionine (800-1000 Ci/mM) (ICN, Cleveland, OH). The translation mixture (20 μ l of reaction mixture along with an appropriate amount of mRNA and water to a total volume of 25 μ l with approximately 0.5 μ g mRNA) was incubated at 30 °C. At 0, 10, 20, 40, and 60 min intervals 1 μ l aliquots of the translation mixture were streaked onto #540

Whatman paper and precipitated in ice-cold 10% trichloroacetic acid (TCA) containing 0.1% methionine. Filters were washed in 10% TCA, boiled 3-4 min in 5% TCA, dehydrated in 95% ethanol for 2-3 min, and allowed to air dry. The dried filters were placed into vials containing 4 ml of Ecolite scintillation liquid and the extent of protein synthesis was established by determining [³⁵S]-Methionine incorporation using a Beckman LS 9000 liquid scintillation beta counter.

Immunoprecipitation of Translated Products

Two x 10⁵ cpm of *in vitro* translated proteins were dissolved in 1.0 ml PBS containing 0.2% Triton X-100 and 0.2% sodium deoxycholate (PBS-TX/DOC). The solution was then pre-absorbed with 30 μl Pansorbin (Calbiochem, La Jolla CA) (Mills et al., 1985; Kessler, 1981). After centrifugation at 6,000 rpm for 10 min, 1 μl rabbit anti-rat apo E (kindly supplied by Dr. K. Weisgraber) or rabbit anti-rat T_f (Organon, Durham, NC) was added and incubated at 4 °C for 16-24 hr. Ten microliters Pansorbin was added and incubation continued for 1 hr. The immunoprecipitate was pelleted by centrifugation and washed twice in 1.0 ml PBS-TX/DOC. The washed pellet was suspended in 50 μl SDS sample buffer and heated for 5 min at 90 °C to release the antibody/

antigen complex. The bacteria were pelleted and the supernate removed for electrophoresis.

Electrophoretic Protein Analysis

A cerebellar protein synthesis profile was produced by polyacrylamide gel electrophoresis containing sodium dodecyl sulfate (SDS-PAGE) according to the method of Laemmli (1970). Equal amounts, approximately 200,000 cpm, of *in vitro* synthesized proteins in sample buffer (10% glycerol, 5% β -mercaptoethanol, 3% SDS and 0.5X Upper Tris) were heat denatured at 90 °C for 2-3 min. Samples were loaded onto a 5% stacking polyacrylamide gel (0.125 M Tris pH 6.8, 0.1% $(\text{NH}_4)_2\text{SO}_5$, 0.1% SDS and 0.5 $\mu\text{l}/\text{ml}$ TEMED) overlying a 10% resolving polyacrylamide gel (0.375 M Tris pH 8.8, 0.1% $(\text{NH}_4)_2\text{SO}_5$, 0.1% SDS and 0.67 $\mu\text{l}/\text{ml}$ TEMED). Electrophoresis was carried out at 80 V through the stacking gel and protein separation was achieved by electrophoresis at 120 V until the bromophenol blue tracking dye reached the bottom of the resolving gel. The buffer system consisted of Tris-glycine (22.75 mM Tris pH 8.8, 0.18 M glycine) containing 0.1% SDS.

To fix the proteins and to remove SDS from the gel, the gel was placed in 20% methanol/7% glacial acetic acid and agitated on a gyratory shaker overnight. After decanting the fixative, the gel was stained in 0.25% Coomassie Brill-

liant Blue G250 dissolved in 10% methanol/4% perchloric acid for 45 min, destained by three changes of fixative at 1 hr intervals, followed by two changes (1 hr each) of a 20% methanol/2% glycerol drying solution. The gel was placed on Whatman 3MM paper, and dried using a heated gel dryer, under vacuum, for 3 hr. The dried gel was exposed to Kodak X-AR x-ray film for various lengths of time and developed according to standard Kodak photographic techniques. Quantitative analysis of proteins synthesized was determined by densitometric scanning of the developed autoradiogram.

Preparation of Competent Bacterial Cells

Cells competent to take up DNA were prepared according to Mandel and Higa (1970). Two fresh colonies of *Escherichia coli* DH-5 α cells were grown overnight on NZY media. The overnight culture was inoculated into 60 ml NZY broth and incubated with shaking at 37 °C until the $A_{600\text{nm}} = 0.6$. After chilling the suspension in an ice bath, the cells were isolated by centrifugation at 3400 rpm at 0 °C for 5 min. The resultant pellet was resuspended in 50 ml ice-cold Buffer A (25 mM Tris-HCl, pH 7.5 and 10 mM NaCl) and centrifuged as before. This pellet was resuspended in 25 ml ice-cold Buffer B (25 mM Tris-HCl, pH 7.5, 10 mM NaCl,

50 mM CaCl₂) and incubated in an ice bath for 30 min. Competent cells were isolated by centrifugation at 1800 rpm at 0 °C for 5 min and resuspended in 5 ml ice-cold Buffer B. To 200 µl competent cells 50 ng pBR322 plasmid containing apo E cDNA was added and incubated for 30 min in an ice bath, followed by heat shock treatment in a 42 °C water bath for 1 min. After cooling on ice, 50 to 100 µl aliquots were spread onto antibiotic plates (NZY plates with 40 µg/ml tetracycline) in order to select resistant colonies.

Large Scale Preparation of Plasmid DNA

Plasmid DNA was amplified and isolated according to Sambrook et al. (1989). One fresh bacterial colony was inoculated into NZYM medium and incubated with shaking at 37 °C until the absorbance at A_{600nm} = 0.8-1.0. Transformed bacterial cells were treated overnight with 150 mg/l chloramphenicol in order to amplify plasmid copy number per cell. Cells were isolated by centrifugation at 5000 rpm at 5 °C for 15 min and resuspended in 20% sucrose/ 0.05 M Tris-HCl, pH 8.0.

Spheroplasts were prepared with lysozyme and 50 mM Tris-HCl, pH 8.0/ 20 mM EDTA, the resulting suspension was incubated at 56 °C for 1 hr along with proteinase K-celulose to digest proteins and 10% SDS to denature proteins.

Additional amounts of 50 mM Tris-HCl, pH 8.0/ 20 mM EDTA and 10% SDS were added along with 5 M NaCl and incubation continued at 37 °C overnight. The salt binds SDS to DNA in order to facilitate alcohol precipitation. Following cooling to -20 °C and centrifugation, the chromosomal DNA was pelleted, while the plasmid DNA remained in solution. The plasmid/SDS/salt complex was precipitated with absolute ethanol, centrifuged, and washed with 70% ethanol to remove any residual SDS and salt. Cellular RNA was removed by alkaline hydrolysis for 1 hr at 68 °C with 0.05 M sodium citrate, pH 8.0. Incubating the nucleic acid solution in sodium citrate at 68 °C raised the pH of the solution a sufficient amount to hydrolyze RNA without affecting the plasmid.

Plasmid purification by density centrifugation was accomplished by adding 9.43 g cesium chloride and 0.4 ml ethidium bromide (10 mg/ml) to exactly 10 ml solution. The solution was then sealed in a polyallomer tube and centrifuged in a Type 80 Ti rotor at 55,000 rpm for 17 hr in a Beckman L8-70 centrifuge. The plasmid band was collected and immediately extracted four times with equal volumes of isopropyl alcohol to remove the ethidium bromide. Desalting and removal of the cesium chloride from the plasmid DNA was accomplished by filtration through a G-25 Sephadex NAP-10

column (Pharmacia, Piscataway, NJ). The DNA concentration was measured at $A_{260\text{ nm}}$ and purity determined by calculating the $A_{260\text{ nm}}/A_{280\text{ nm}}$ ratio. Generally, a 260/280 ratio of 1.9 or greater is preferred. DNA concentration was determined as follows: $A_{260\text{ nm}} \times 10\text{X dilution} \times 50 = \mu\text{g DNA per ml}$.

Electrophoresis of Plasmid DNA and cDNA Isolation

The cDNA fragment of interest was separated from the remaining plasmid DNA by cutting with the appropriate restriction endonuclease (Pst I and Hinc II for pT₁₀, Bam HI and Hind III for apo E). The resultant fragment (10 μl DNA sample in 0.1% bromophenol blue/50% glycerol tracking dye) was then isolated by electrophoresis in a 1.0% agarose gel with 1X TBE buffer (89 mM Tris-borate, 2 mM EDTA, pH 8.0) at 60 V for 2 hr. In order to visualize the fragment, the gel was stained with 1 $\mu\text{g/ml}$ ethidium bromide in 1X TBE and observed on a short-wave (302 nm) UV transilluminator (Spectroline Model TR-302). The cDNA band was excised from the gel and soaked briefly in 0.5X TBE. The DNA was eluted from the gel slice in 0.5X TBE in an Elutrap apparatus (Scheicher and Schuell, Keene, NH) and purified in a Centricon micro-concentrator (Amicon, Danvers, MA).

Polymerase Chain Reaction Amplification

The following oligonucleotide primers were synthesized from the cDNA sequence for apo E (McLean et al., 1983) and transferrin (T_f) (Huggenvick et al., 1987) on a Milligen Biosearch model 8600 nucleic acid synthesizer:

apo E

5' sense 5' **AAGGATCCATGAAGGCTCTGTGGGCCCTG** 3'
 3' antisense 5' GGAAGCTTGATTTCTCCAGGGCAC 3'

T_f

5' sense 5' GGCCAGCAAAATGTGCTCCGAAC 3'
 3' antisense 5' ACTTGCTGTGAAAGTGCAGGCGTC 3'

For the purpose of subcloning, the apo E oligonucleotides were synthesized with unique restriction endonuclease extensions (underlined portion). Two nucleotides of the 3'antisense cDNA sequence were incorporated into the restriction sequence of Hind III (bold portion), while the 5' sense oligonucleotide includes the restriction sequence of Bam HI. To process, the oligonucleotides were cleaved from the

column in 5 ml of 30% ammonium hydroxide overnight at room temperature, followed by incubation at 55 °C for 3 hr. The solution and resin were aliquoted into 1.5 ml eppendorf tubes and dried in a Savant speed vac. The resulting pellet was washed with 1 ml of water and dried overnight as before. The samples were then pooled and dissolved in 100 μ l sterile Ultrapure water and the concentration determined ($A_{260\text{ nm}}$ of 250X dilution $\times 16.5 = \mu\text{g}/\mu\text{l}$).

Due to the extensive secondary structure created by the G/C tailing created for the initial cloning of the apo E cDNA and the high G/C content of the apo E cDNA insert, large scale preparation of plasmid DNA using traditional chloramphenicol amplification proved inefficient. Instead, amplification of the apo E cDNA was performed by the polymerase chain reaction (PCR) in an 100 μ l reaction volume containing 50 mM KCl, 10 mM Tris-HCl (pH 8.3), 1.5 mM MgCl₂, and 0.01 % gelatin plus each deoxynucleotide triphosphate at 200 μ M, 3' and 5' primers at 1 μ M and 10 μ l apo E-containing plasmid (1 ng) overlaid with 50 μ l mineral oil to prevent evaporation (Saiki et al., 1988). PCR was performed in an automated heating/cooling block (DNA Thermal Cycler, Perkin Elmer Cetus) using 2.5 units of *Thermus aquaticus* (Taq) DNA Polymerase. To sufficiently denature the apo E cDNA template for primer annealing, it was necessary to pre-heat the

template under oil at 95 °C for 15 min. The primers and reaction mix "cocktail", containing 4% dimethyl sulfoxide (DMSO), were added immediately and mixed thoroughly. Since primer annealing occurs as the tubes air-cool, the samples were not placed into the block until after the first denaturing cycle. The temperature-step cycle of 95 °C (1 min), 50 °C (2 min), and 72 °C (5 min) was repeated 30 times. This PCR product was then reamplified with a temperature-step cycle of 95 °C (1 min), 50 °C (2 min), and 72 °C (2 min) in the absence of DMSO for 30 cycles.

The amplification of the T_r cDNA did not require pre-heating or the inclusion of DMSO. The reaction conditions were identical to those for apo E with the exception that extension occurred for 2 min for both the initial amplification and subsequent reamplification.

Preparation of Labelled Probes

The rat transferrin (T_r) cDNA in pSP65 (kindly supplied by Dr. M. Griswold) is harbored within *E. coli* JM 105, and encompasses the carboxy terminal one-third of the transferrin protein. A 688 bp fragment of plasmid pTf10 (Huggenvik et al., 1987) was generated by Pst I and Hinc II digestion and subcloned into the pSP65 vector from Promega Biotech (Figure 13).

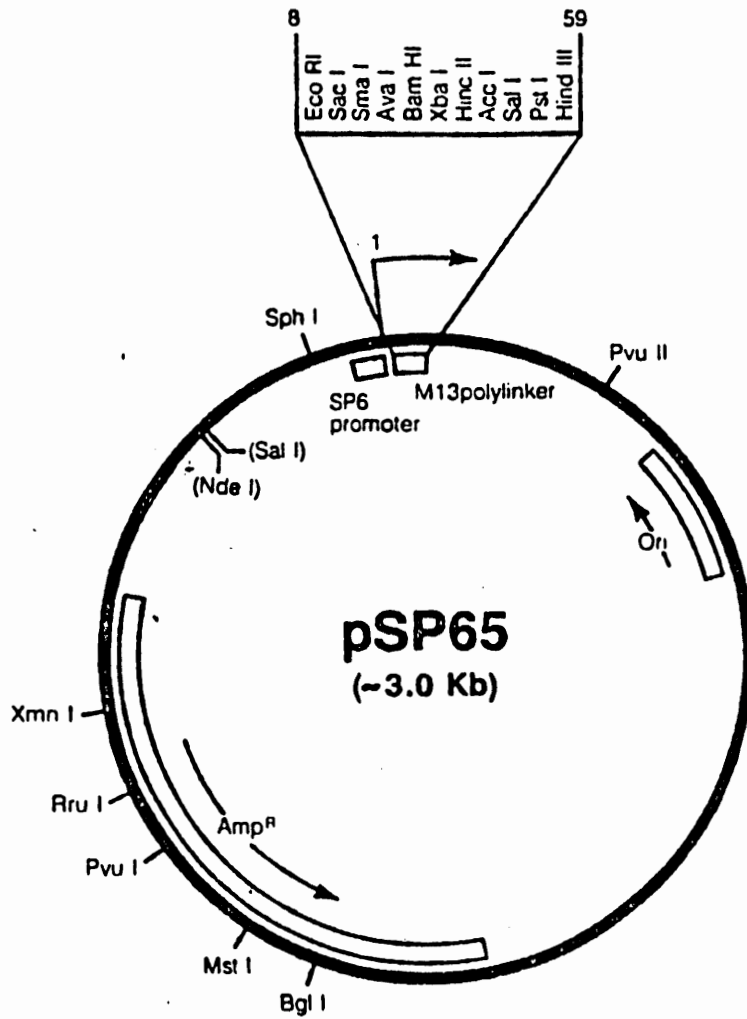


Figure 13. Restriction endonuclease map of the pSP65 vector.
(Promega Biotech)

The rat apolipoprotein E cDNA (kindly supplied by Dr. L. Chan) was placed within the *E. coli* pBR322 plasmid via G-C tailing. The double-stranded recombinant plasmid contains a ds-cDNA insert of 1 kb which represents the entire coding region of the corresponding mRNA (Figure 14).

For Northern hybridization, both double-stranded plasmids were labelled to specific activities of 1×10^8 cpm/ μ g DNA by random priming (Feinberg and Vogelstein, 1983). Fifty to one hundred nanograms of DNA template in 9 μ l of sterile Ultrapure water was denatured at 95 °C for 5 min and quick cooled on wet ice. To this 5 μ l α -[³²P] dCTP, 2 μ l 10X reaction buffer, 1 μ l each of dATP, dCTP and dGTP, and 1 μ l of Klenow enzyme (2 units/ μ l) were added (Boehringer Mannheim, Indianapolis, IN). After heating at 37 °C for 30 min, 80 μ l of sterile Ultrapure water were added and the incorporation of radioactive nucleotides determined in a Beckman Model 170M Radioisotope Detector. A 1 μ l aliquot of the probe was diluted 100 fold and 10 μ l aliquots spotted onto six Whatman DE81 ion exchange filters. After air drying, three of the filters were washed three times with 10% trichloroacetic acid and dried under vacuum. The percent incorporation was calculated by comparing the ratio of counts per minute (kcpm) of the washed to unwashed filters. Incorporations greater than 25% were considered acceptable.

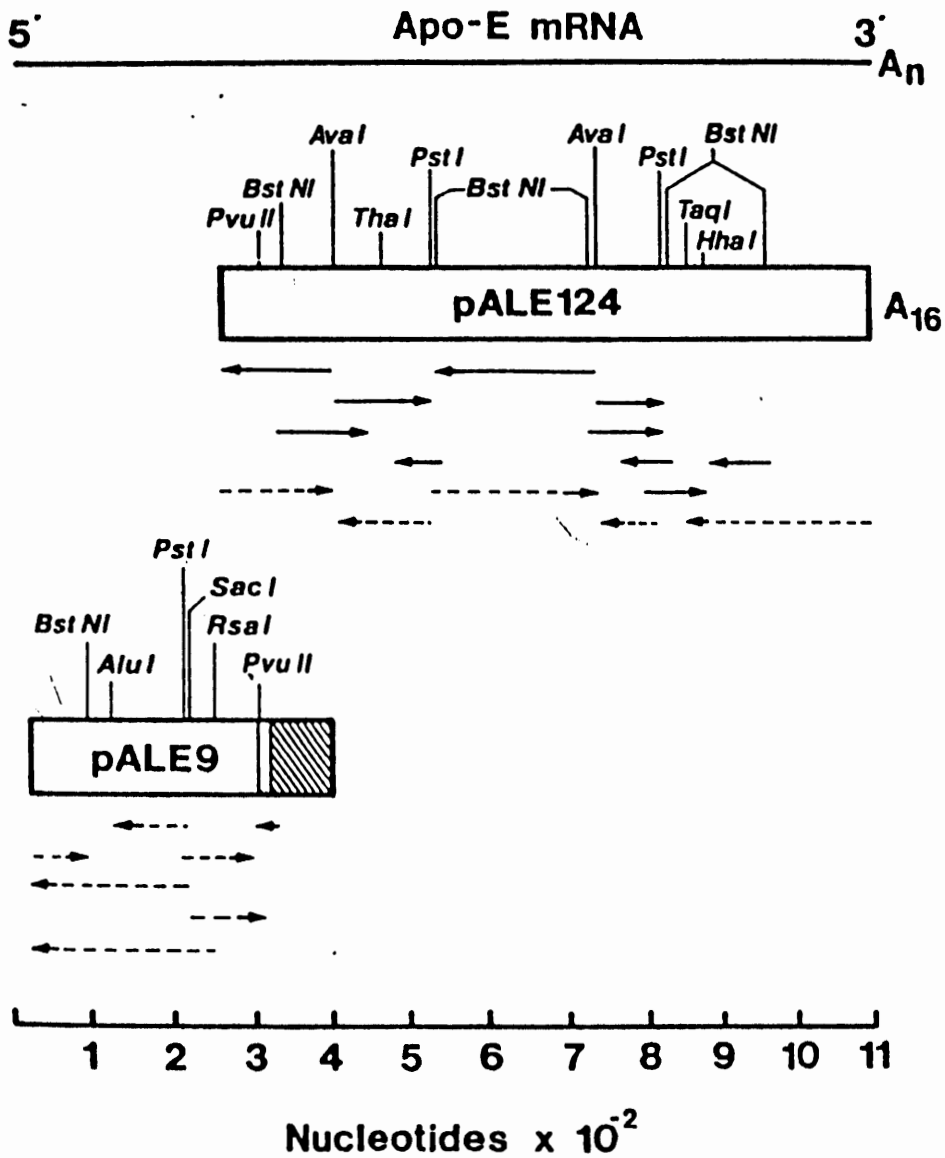


Figure 14. Restriction endonuclease map of apo E cDNA. The top horizontal line represents the length of apo E mRNA. The ds cDNA pALE124 contains only the carboxy terminal three-fourths of the corresponding mRNA. A second ds cDNA pALE9 contains the remaining portion of the apo E sequence, including a 48 bp region which overlaps that of pALE124 (shaded box). (McLean et al., 1983)

To precipitate the probe, 100 μ l phenol/chloroform/isoamyl alcohol (50/25/1) was added, vortexed for 30 sec and centrifuged briefly to allow phase separation. The upper aqueous phase was transferred to a fresh tube containing 36 μ l 10M ammonium acetate, 1 μ l *Torula* yeast RNA, and 288 μ l cold absolute ethanol and placed at -70 °C for at least 10 min. Following centrifugation at 20,000 rpm for 15 min at 4 °C, the ethanol was decanted, and the pellet dried under vacuum. The dried pellet was finally dissolved in 100 μ l sterile Ultrapure water.

RNA Separation by Electrophoresis on Denaturing Gels

RNA of varying sizes were resolved for Northern hybridization by electrophoresis on a 1.2% agarose gel (Lehrach et al., 1977) containing 6% formaldehyde, 40 mM MOPS pH 7.0, 10 mM sodium acetate, and 1 mM EDTA. The formaldehyde was deionized to neutrality by stirring with a mixed bed resin of Dowex and Chelex, followed by filtration through a sintered-glass filter. Samples placed in 50% formamide, 6% formaldehyde, 1X running buffer, and loading buffer (50% glycerol, 1 mM EDTA, 0.4% bromophenol blue, 0.4% xylene cyanol) were incubated at 60 °C for 10 min, and were then applied to wells. The gel was run in a circulating buffer reservoir at 80 V until the ion front

(first dye) reached the gel's edge. The gel was then stained with ethidium bromide, photographed, and destained on a gyratory shaker in Ultrapure water until fluorescence was no longer detected.

After destaining the gel, nucleic acids were transferred to a nylon membrane (e.g. Zeta-Probe) by electroblotting (Bittner, 1980). Nucleic acids were transferred in a Model TE 50 Transfor unit (Hoefer, San Francisco, CA) in 24 mM sodium phosphate pH 6.5 at 0.1 amps for 8 hr at 4 °C. The nucleic acids were crosslinked to the membrane while wet under ultraviolet light (302 nm) for one min. In addition, the membrane was baked two hr under vacuum at 80 °C, sealed in an air tight bag and stored at 4 °C until used for hybridization.

Northern Hybridization

Northern hybridization was performed according to the method of Craft et al. (1990). The membrane was prewashed 1.5-3 hr in 1 M NaCl, 0.1% SDS, 20 mM Tris-HCl, pH 8.0, and 1 mM EDTA at 65 °C. Samples were prehybridized in 40% formamide, 5X SSC, 1% SDS, 10X Denhardt's, 50 mM NaPO₄, 1% salmon sperm DNA, 20 µg/ml poly A, and 20 µg/ml *Torula* yeast RNA for 4-24 hr at 37 °C. Hybridization took place in 40% formamide, 5X SSC, 1% SDS, 1X Denhardt's, 20 mM NaPO₄,

1% salmon sperm DNA, 20 $\mu\text{g/ml}$ poly A, and 20 $\mu\text{g/ml}$ *Torula* yeast RNA and 1×10^6 cpm cDNA probe per ml of hybridization solution for 24-48 hr at 37 °C. To remove nonspecific binding, two post-hybridization washes were performed. Blots were washed three times in 2X SSC with 0.5% SDS for approximately 20 min at 37 °C followed by three 20 min washes at 37 °C in 0.5X SSC without SDS. Blots were sealed in an air tight bag and exposed to Kodak XAR-5 film at room temperature for varying lengths of time. If necessary, higher stringency washes were performed at 50 °C under the same salt conditions.

CHAPTER III

RESULTS

The primary experimental objective of this project was to establish a developmental profile for apolipoprotein E (apo E) and transferrin (T_f) within the cerebellum, and to determine what role thyroid hormones play in developmental regulation of transcription and expression of their genes. Various PTU treatment regimens were employed in order to delineate thyroid hormone effects on development and on gene regulation. In the following chapter, three distinct PTU treatments will be discussed. "PTU 1" represents the administration of PTU from embryonic day 16 (E 16) to postnatal (PN) day 10, in order to investigate thyroid hormone effects on development. "PTU 2" represents the administration of PTU from PN day 10 until sacrifice, in order to investigate thyroid hormone effects on gene regulation. "PTU 3" represents the administration of PTU from E 16 until sacrifice, in order to investigate long-term effects of PTU treatment.

While the principal objective was to investigate the role of thyroid hormone action at the molecular level, it was first necessary to verify that the PTU treatment had established a hypothyroid state. This was accomplished by four means: (1) monitoring the appearance of gross morpho-

logical signs of cretinism; (2) measuring alterations in body and organ weights; (3) observing histological alterations in the cerebellar cortex; (4) monitoring serum PTU and free T_3 levels.

Routes of PTU Administration

The establishment of a hypothyroid state via PTU administration is confounded by the unique solubility characteristics of this compound. PTU solubility at neutral pH is 1 part per 200 (personal communication, Sigma). When administered via intubation, variable amounts of PTU remained within the syringe, thereby preventing consistent delivery of the required dose. While DMSO proved to be an excellent solvent, it was discovered that DMSO had teratogenic effects and there was 100% mortality by postnatal (PN) day 2. While the literature lacks documentation of DMSO effects on development, Uphouse and coworkers (1982) found neural and endocrine changes when DMSO was used as a vehicle for chlordecone administration. Since PTU is absorbed via the gastrointestinal lining (Legrand, 1967), perhaps the use of DMSO as a vehicle allowed for too rapid an absorption of PTU, thus producing toxic effects. To obviate the teratogenic effects of DMSO, NaOH was used as a solvent.

Neonatal mortality after intubation of the resulting pH 10 solution was 100% by PN day 10. Upon autopsy, the gastrointestinal tract, particularly the stomach, was found to be filled with a white precipitate. Perhaps, the intubated solution was neutralized by gastric acid, precipitating the PTU and blocking absorption.

Once intubation was eliminated as a route of administration, the use of PTU in the drinking water was attempted. The combined use of NaOH to dissolve the PTU, and dextrose to overcome the bitter taste of the alkaline solution proved ineffective since the NaOH oxidized the dextrose, resulting in a brown solution. This apparently had no effect on the taste since animals consumed as much water as their control counterparts. However, urinary output and PTU clearance in animals consuming the dextrose solution was increased over animals consuming water only. Therefore, the ability to maintain a sufficient serum concentration of PTU was jeopardized.

As discussed earlier, it is imperative to begin PTU treatment prior to thyroid gland activation by thyrotropin at the sixteenth embryonic (E) day. Since most cerebellar neurogenesis in the rat is completed by the tenth postnatal day, PTU treatment of dams and pups ceased at PN day 10 (PTU 1). The overall mortality rate of PTU 1 treated animals was 14%. Using this treatment protocol PTU's effect on develop-

ment was ascertained. In order to determine the long-term effects of subcutaneous PTU administration on development, two litters of animals were maintained on PTU injections beyond PN day 10. Although all animals expired by PN day 20, the exact cause of death could not be determined. Serum PTU levels remained constant, and so it was hypothesized that either PTU exerted toxic effects or that other hormonal systems were being affected. In order to rule out the former, a dose response experiment was conducted. PTU was administered at 2, 4 and 10 mg/kg from E 16 to PN 10 as before. Even though serum PTU concentrations were linear over this dose range, body, brain and cerebellum weights and weight ratios of brain:body and cerebellum:brain were not significantly different. In addition, cerebellar development did not appear significantly different from controls at these PTU doses. Therefore, as determined from histological abnormalities, PTU doses of 20 mg/kg appeared necessary to maintain a hypothyroid state.

One final attempt at prolonging PTU treatment beyond PN day 10 was made. Following PTU injections as before, animals were maintained on 0.1% PTU in drinking water (PTU 3). In this case, 100% mortality occurred by PN day 60. Legrand (1967) maintained animals on 50 mg PTU per day from either E 16 or PN day 1 to the time of sacrifice, with the longest experiment continuing to PN day 35. No mention was made of

mortality rate. However, with the intubation of 50 mg PTU there is no way of determining the actual dose absorbed, since that amount of PTU is insoluble in the volume intubated. Perhaps this explains why treatment with 12.5 times as much PTU, administered via intubation as compared to subcutaneous injection, did not result in toxic levels.

PTU Induces Gross Morphological Alterations

As in humans, rats exhibit morphological signs of cretinism during states of thyroid hormone deprivation. While morphology may not be the most reliable means of gauging thyroid hormone status, it does provide invaluable information on developmental phenomena. Only control and PTU 1 treated animals were compared.

In PTU 1 treated animals, indications of retarded growth were apparent by the first postnatal day (Figure 15). However, the typical gross morphological characteristics of cretinism (e.g. delayed skeletal development, hair production, tooth eruption and eye opening) did not appear for several days. In addition to reduced growth, the first visible signs of cretinism were detectable by the 10th PN day (Figure 16). Treated animals had delayed nail and hair development with resultant eczema. Twenty day old animals exhibited the most extensive signs of cretinism (Figure 17).



Figure 15. Morphological Alterations at Postnatal Day 1.
The effects of PTU 1 treatment are evident even on PN day 1.
In addition to reduced body size, hypothyroid animals
exhibit a pallor skin coloration.

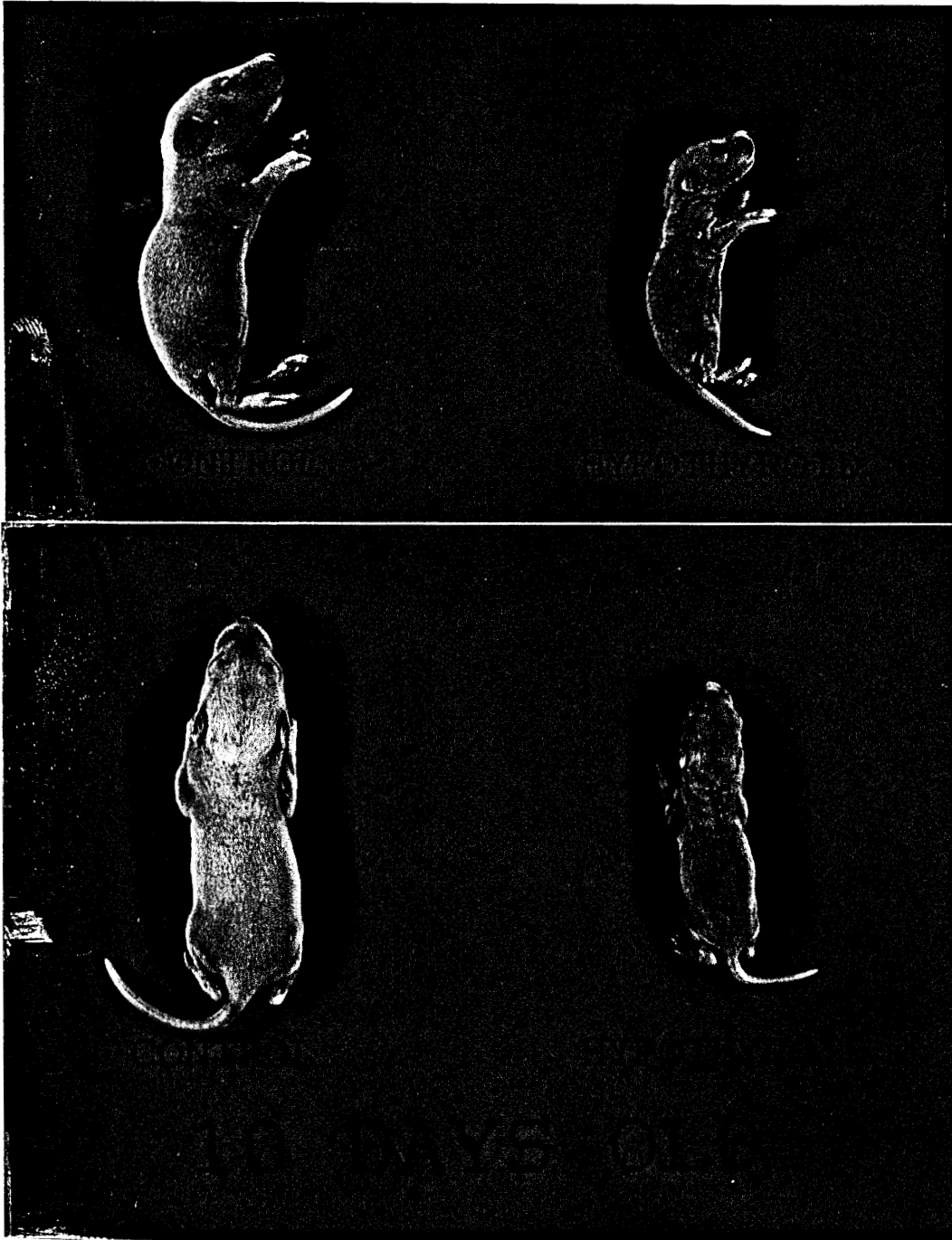


Figure 16. Morphological Alterations at Postnatal Day 10. In addition to reduced growth, the first visible signs of cretinism are apparent. PTU 1 treated animals have delayed hair development, therefore the skin appears dry.



Figure 17. Morphological Alterations at Postnatal Day 20. Twenty day old PTU 1 treated animals exhibit the most extensive signs of cretinism. Eye opening and tooth eruption are delayed. The hair is fine and sparse. The most striking indication of altered skeletal development is expressed as the retention of infantile skull proportions.

Eye opening and tooth eruption were delayed. The most striking indication of altered skeletal development was expressed as the retention of infantile skull proportions, whereby the crown to nose length was reduced and the nose more rounded. Due to delayed skeletal development, diminished muscle tone and delayed tooth eruption, it was necessary to postpone weaning in all hypothyroid animals from PN day 21 to PN day 30. PTU treated animals at 30 days of age still demonstrated signs of cretinism, although the signs were not as obvious as those at 20 days of age (Figure 18). While control animals at this age actively explored their surroundings, treated animals appeared ataxic. Perhaps the ataxia was the result of hypothermia. What reduced activity these animals did perform was manifested as bradykinesia and awkward muscular movements. In order to prevent inadequate nutrition, food was placed directly into the cage, in addition to that supplied within the food bin. By the 60th PN day, the signs of cretinism, other than retarded growth, were barely detectable (Figure 19).

Analysis of Body and Organ Weight

Since hypothyroidism is correlated with delayed developmental states, body and organ weights may be used to gauge the developmental status. Five parameters were investigated: body, brain and cerebellum weights, and weight ratios of

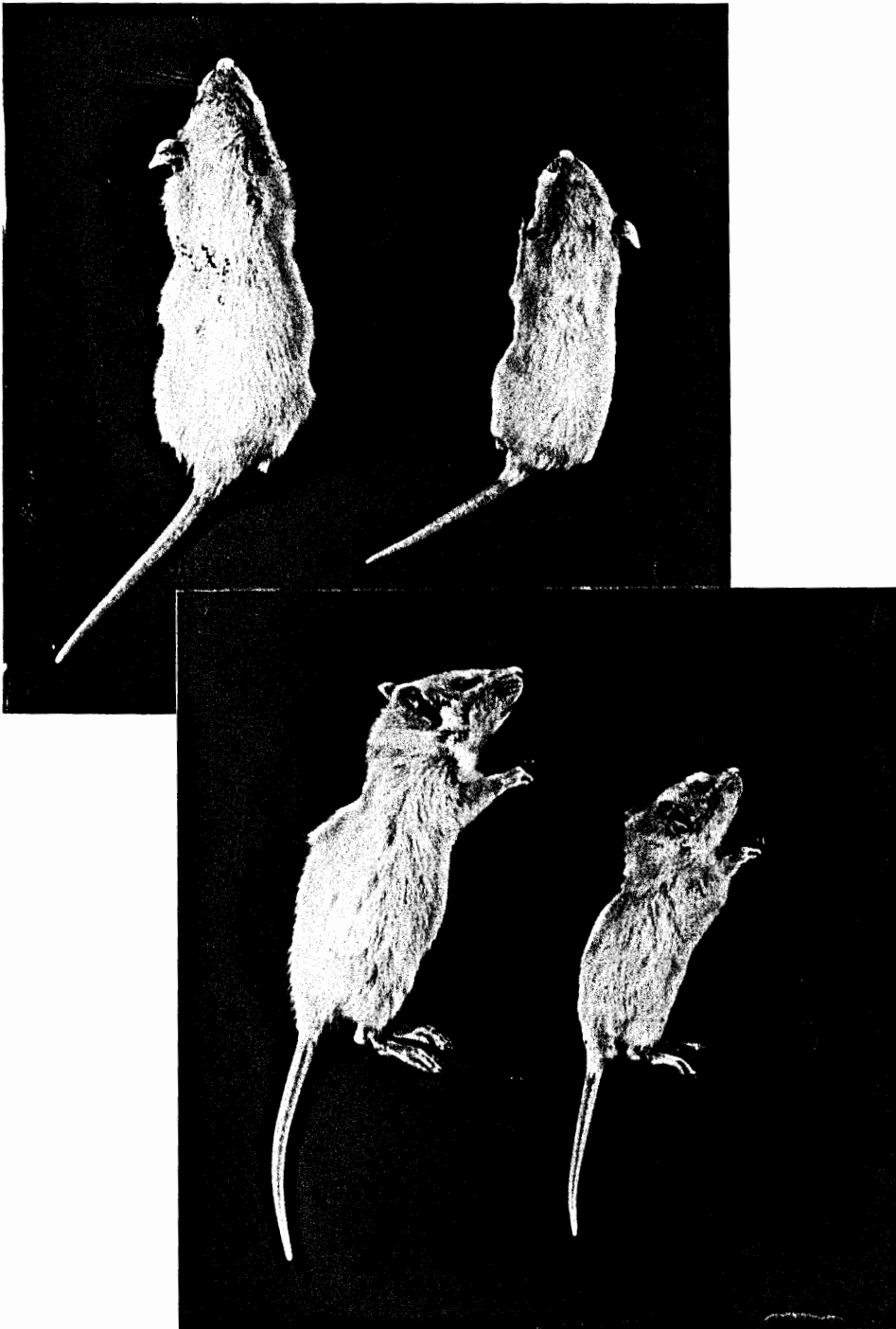
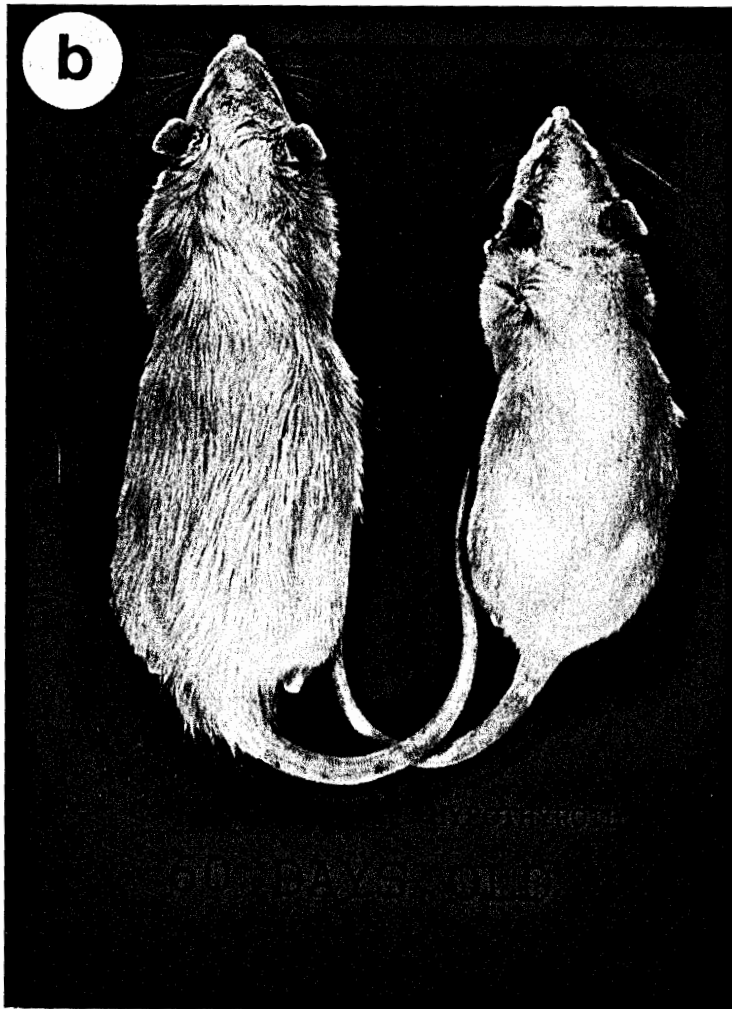


Figure 18. Morphological Alterations at Postnatal Day 30. PTU 1 treated animals at 30 days of age still demonstrate signs of cretinism although they are not as obvious as before.



Figure 19. Morphological Alterations at Postnatal Day 60.
(a) By 60 days of age, recovery seems to occur from the PTU treatment and the signs of cretinism are barely apparent.
(b) Reduced body size is still significant at this stage.



brain:body and cerebellum:brain. Control and hypothyroid values at PN days 10, 20, 30 and 60 were compared. One day old animals were not utilized, since the weighing accuracy was so variable that statistical analysis was inappropriate.

PTU treatment had a significant influence on body weight ($F_{3,237} = 153$ and $F_{2,353} = 654$) (Figure 20). The body weight of PTU 1 treated animals was reduced at all PN days studied, when compared to controls. The greatest difference in body weight was observed at 30 days of age. By 60 days of age a substantial weight gain has occurred; however, PTU 1 animal body weights were still significantly reduced from control body weights.

The body weight of PTU 2 treated animals at PN day 20 was equivalent to control weights, yet different from the other PTU treatment groups. This was not surprising since PTU 2 animals had been subjected to only 10 days of treatment. However, at PN day 30 as the hypothyroid state was established, PTU 2 body weights approached PTU 1 body weights. By PN day 60, the body weight of PTU 2 treated animals was significantly reduced, as compared to control and PTU 1 values.

The body weight of PTU 3 treated animals at PN day 20 was similar to PTU 1 weights, yet different from control and PTU 2 values. Apparently, the additional 10 days of treat-

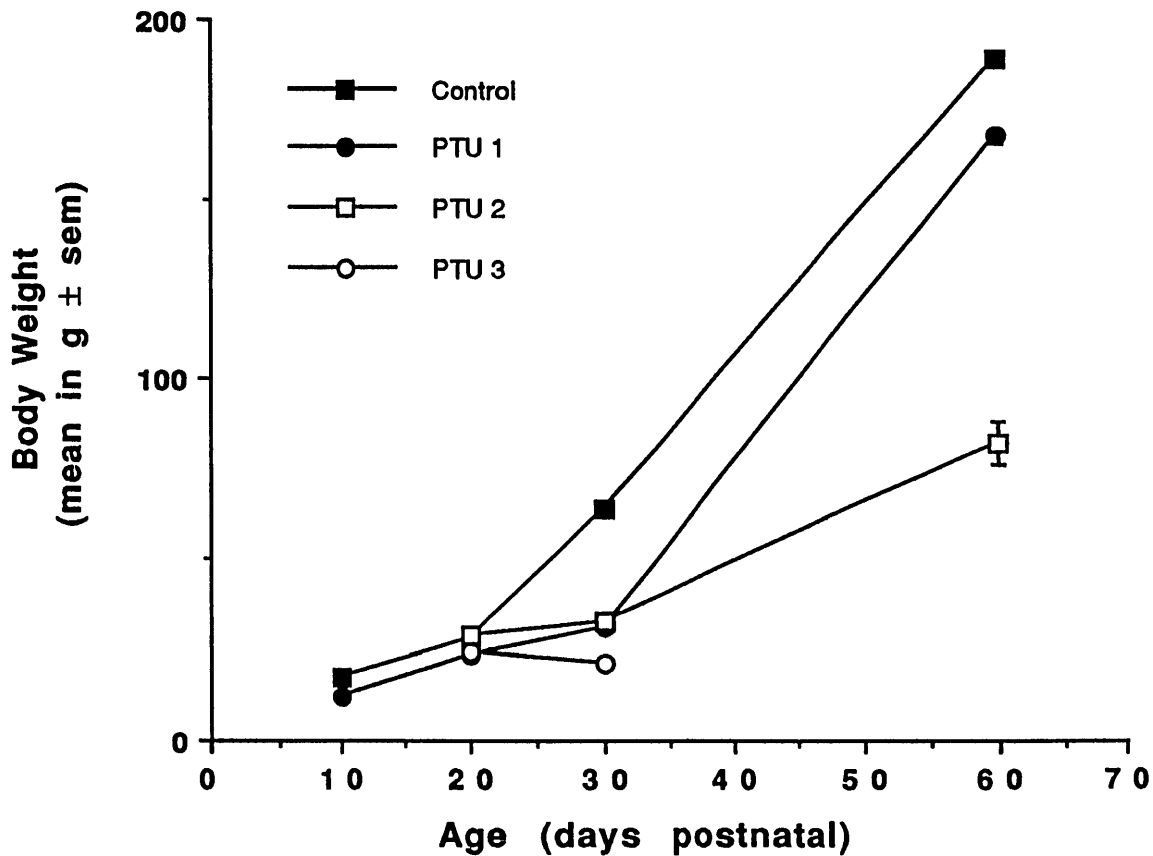


Figure 20. Effect of hypothyroidism on body weight. PTU 1 treated animals show significantly reduced body weights as compared to control animals at all PN days studied. The greatest difference was observed at PN 30. At PN day 20, PTU 2 body weights are equivalent to control values since animals have experienced only 10 days of treatment. Similarly, PTU 3 body weights are equivalent to PTU 1 values since PTU 3 animals have only been subjected to 10 additional days of PTU treatment. By PN day 30, PTU 2 body weights approach PTU 1 values as the hypothyroid state in postnatally treated animals becomes established. The standard error of the mean, although too small to be graphically represented, ranged from 6 to 24 % of the mean.

ment received by PTU 3 animals had no effect on body weight. However, by PN day 30, the body weight of the one remaining PTU 3 animal was substantially reduced from its counterparts.

Like body weight, PTU treatment had a significant effect on brain weight ($F_{3,237} = 308$ and $F_{2,353} = 252$) (Figure 21). Brain development in PTU 1 treated animals appeared to parallel that of the control animals, although reduced brain weights were observed at all PN days studied. As with body weight, the greatest reduction in brain weight was found at 30 days of age. Brain weights began to converge after PN day 30, but were still significantly different at PN day 60.

The brain weight of PTU 2 treated animals was different from all other treatment groups at PN day 20. Therefore, although body weight was not affected by 10 days of treatment, postnatal administration of PTU did effect brain development. By PN day 30, PTU 2 values approached those of PTU 1 treated animals, yet were different from controls and the single PTU 3 value. By PN day 60, the brain weight of PTU 2 treated animals was significantly reduced from control and PTU 1 values.

The brain weight of PTU 3 treated animals at PN day 20 was similar to PTU 1 brain weights. Afterwards, there was a dramatic decline in brain weight for the one remaining PTU 3

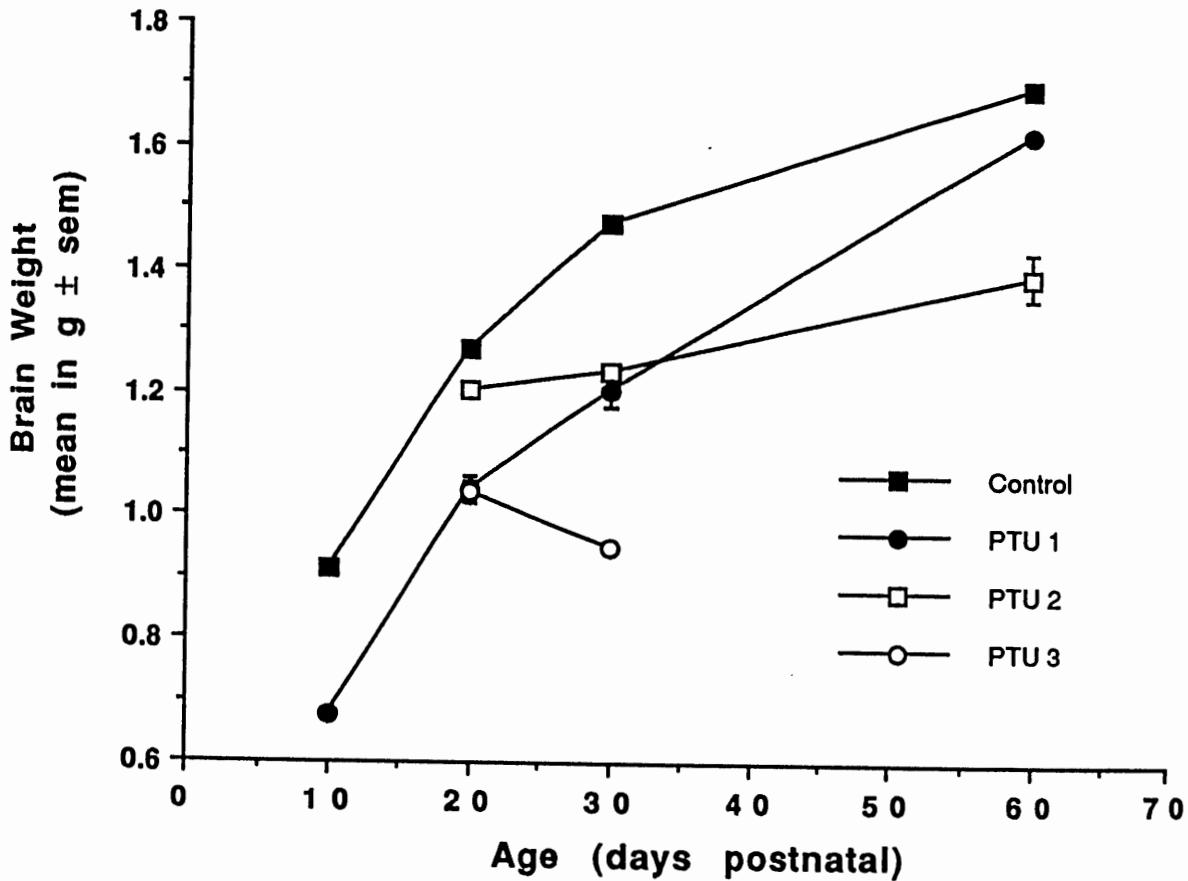


Figure 21. Effect of hypothyroidism on brain weight. PTU 1 treated animals show significantly reduced brain weights at all PN days studied. The greatest difference appears at 30 days of age. The rapid postnatal increase in brain weight is attenuated in PTU 2 treated animals. At PN day 30, PTU 2 brain weights are equivalent to PTU 1 values as the hypothyroid state is established. While PTU 3 brain weights are similar to PTU 1 values at PN day 20, prolonged treatment results in a dramatic decline thereafter. The standard error of the mean, although too small to be graphically represented, ranged from 3 to 14 % of the mean.

animal. The decrease in brain weight induced by prolonged PTU treatment demonstrated the critical role thyroid hormones play in development.

The effect of PTU treatment on cerebellar development, although significant, was not as great as for brain development ($F_{3,237} = 166$ and $F_{2,353} = 135$) (Figure 22). Like brain development, cerebellum development in PTU 1 treated animals appeared to parallel that of control animals, although it was reduced at all PN days studied, except PN day 60. The rapid growth found in control animals between PN days 10 and 20 appeared slightly reduced in hypothyroid animals, so that at 20 days of age the greatest reduction occurred.

The cerebellar weight of PTU 2 treated animals at PN day 20 was equivalent to control animals, yet different from PTU 1 and PTU 3 values. Therefore, like body weight, PTU treatment beginning at day 10 did not seem to affect cerebellum weight. However, by PN day 30, PTU 2 cerebellar weights approached PTU 1 values, as the hypothyroid state was established. By PN day 60, the cerebellum weights of PTU 2 treated animals were significantly reduced, as compared to control and PTU 1 values.

The cerebellar weight of PTU 3 treated animals was similar to PTU 1 animals at PN day 20, yet different from control and PTU 2 values. Like brain weight, the one PTU 3

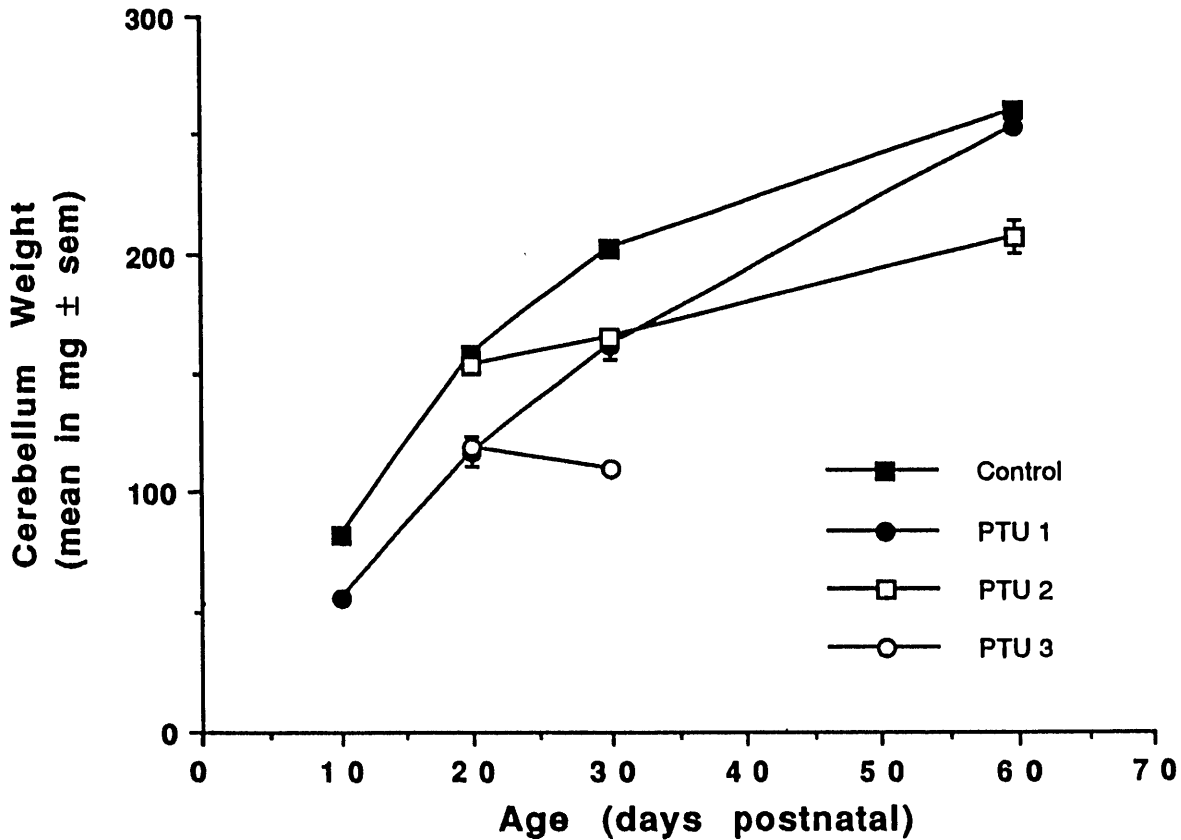


Figure 22. Effect of hypothyroidism on cerebellum weight. PTU 1 treated animals show significantly reduced cerebellum weights at all PN days studied, except PN day 60. The greatest difference appears at 20 days of age. PTU 2 cerebellum weights are similar to control values at PN day 20 and PTU 1 values at PN day 30, but are significantly reduced at PN day 60. While PTU 3 cerebellum weights are comparable to PTU 1 values at PN day 30, there is a rapid decline in cerebellum weight following prolonged PTU treatment. The standard error of the mean, although too small to be graphically represented, ranged from 2 to 25 % of the mean.

treated animal demonstrated a dramatic decline in cerebellar weight following prolonged PTU treatment.

Decreased brain and cerebellum weights of PTU treated animals could be the result of the overall decline in body size and not an organ specific modification. To evaluate this possibility, brain:body and cerebellum:brain weight ratios were calculated. If the ratios were not significantly different it could be hypothesized that the organ weight reduction was a result of decreased body size.

During normal development, the brain:body weight ratio decreases, because the brain, which matures earlier, comprises an even smaller proportion of the total body weight (Figure 23). Both the brain:body weight ratios ($F_{3,237} = 14$ and $F_{2,353} = 15$) and cerebellum:brain weight ratios ($F_{3,237} = 52$ and $F_{2,353} = 28$) were significantly affected by PTU treatment. Since the brain size was less affected by PTU treatment than the body size, the brain:body weight ratio in PTU 1 treated animals was greater than that of control animals. The greatest brain and body weight reductions occurred at 30 days of age, and so it was not surprising that the ratio at PN day 30 showed the most significant alteration. At PN day 20, the control brain:body weight ratio was greater, although not significantly, than the PTU 1 ratio. This could have resulted from either an increase in brain size in

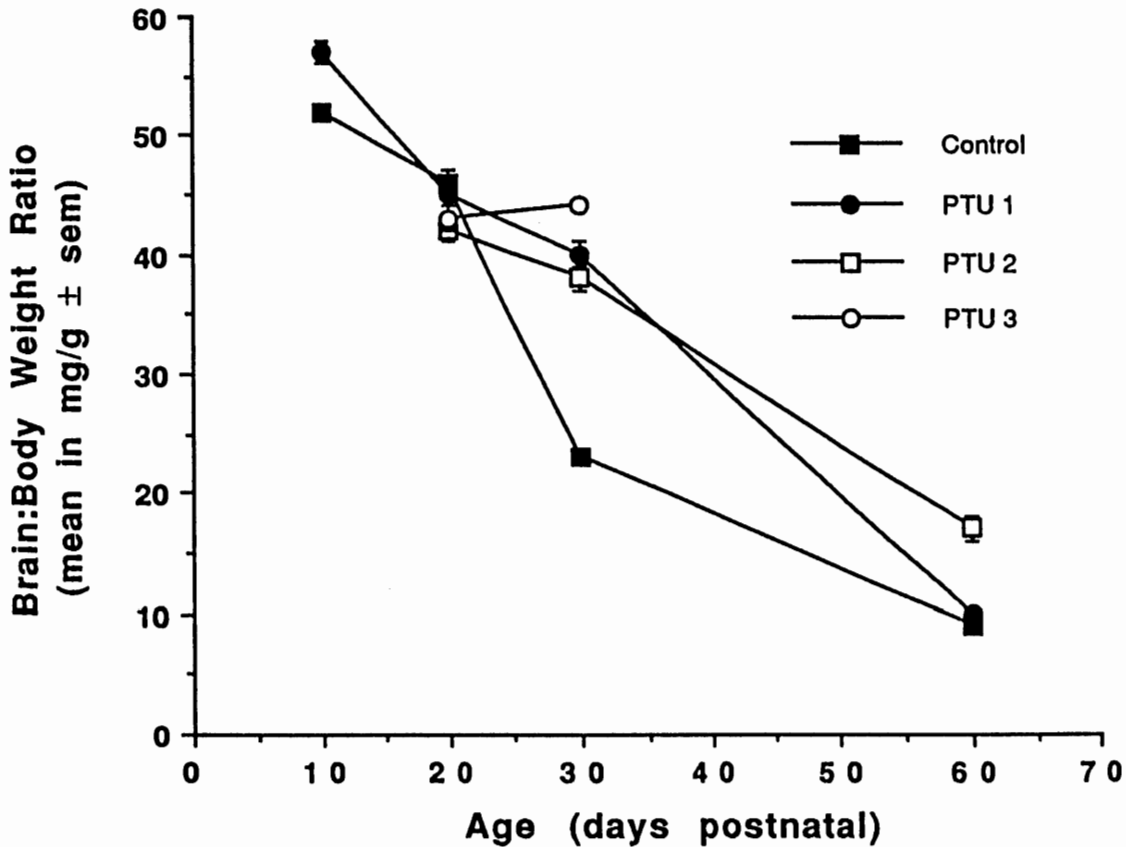


Figure 23. Effect of hypothyroidism on brain:body weight ratio.

Since the brain is less affected than the body by PTU treatment, the brain:body weight ratio of PTU 1 treated animals is greater than the control animals. At PN day 20, only control and PTU 2 ratios are different. At PN day 30, the control ratio differs from all three treatment groups, but all PTU groups are similar. At PN day 60, the PTU 2 ratio differs from control and PTU 1 values, while control and PTU 1 ratios are equivalent. The standard error of the mean, although too small to be graphically represented, ranged from 5 to 24 % of the mean.

relation to decreased body size of control animals or a decrease in brain size in relation to increased body size of hypothyroid animals. By PN day 60, control and PTU 1 treated ratios were similar.

The brain:body weight ratios of PTU 2 treated animals appeared to parallel those of PTU 1 animals, but they became greater at PN day 60. The PTU 2 values differed from the control values at all PN days studied, and also differed from the PTU 1 values at PN day 60, but were similar to the other PTU treatment groups.

The brain:body weight ratio of PTU 3 treated animals only differed from the control value at PN day 30. Therefore, it appeared that the various PTU treatment regimens affected the brain:body weight ratio differently. Since the brain:body weight ratios at PN day 20 were all approximately equal, it could be assumed that the decreased brain weight was due to the overall decrease in body weight at this stage. At other developmental stages, it appeared that the reduction in brain weight was not a result of an overall decrease in body weight, but could be due to other effects.

Histogenesis throughout the rat central nervous system mostly occurs prenatally, but cerebellar neurogenesis largely occurs postnatally. Therefore, as development proceeds the cerebellum:brain weight ratio increases, because the cerebellum continues to develop and accounts for a greater

portion of the brain mass (Figure 24). In control animals, the greatest increase in cerebellum:brain weight ratio occurred between PN days 10 and 20, the normal period of cerebellar neurogenesis. However, the greatest ratio increase in PTU 1 treated animals occurred between PN days 20 and 30, and correlated with the delay in granule cell differentiation. The largest deviation between control and PTU 1 values occurred at 20 days of age, the normal period of external granule layer disappearance. At PN day 30, control and PTU 1 values were similar. By 60 days of age, the PTU 1 cerebellum:brain weight ratio exceeded the control ratio, although not significantly, as the cerebellum accounted for an even greater percent of the total brain.

The increase in the cerebellum:brain weight ratio of PTU 2 treated animals appeared linear over the postnatal stages studied. The PTU 2 ratio was similar to the control value at PN days 20 and 30, but not PN day 60.

Due to the parallel decline in both cerebellum and brain weights, the cerebellum:brain weight ratios in PTU 3 treated animals were the same at PN days 20 and 30. At PN day 20, the PTU 3 ratio was comparable to the PTU 1 value, yet different from the other treatment groups. At PN day 30, the PTU 3 ratio was significantly reduced from all treatment groups. Like the brain:body weight ratio, it appeared that the various PTU treatments affected the cere-

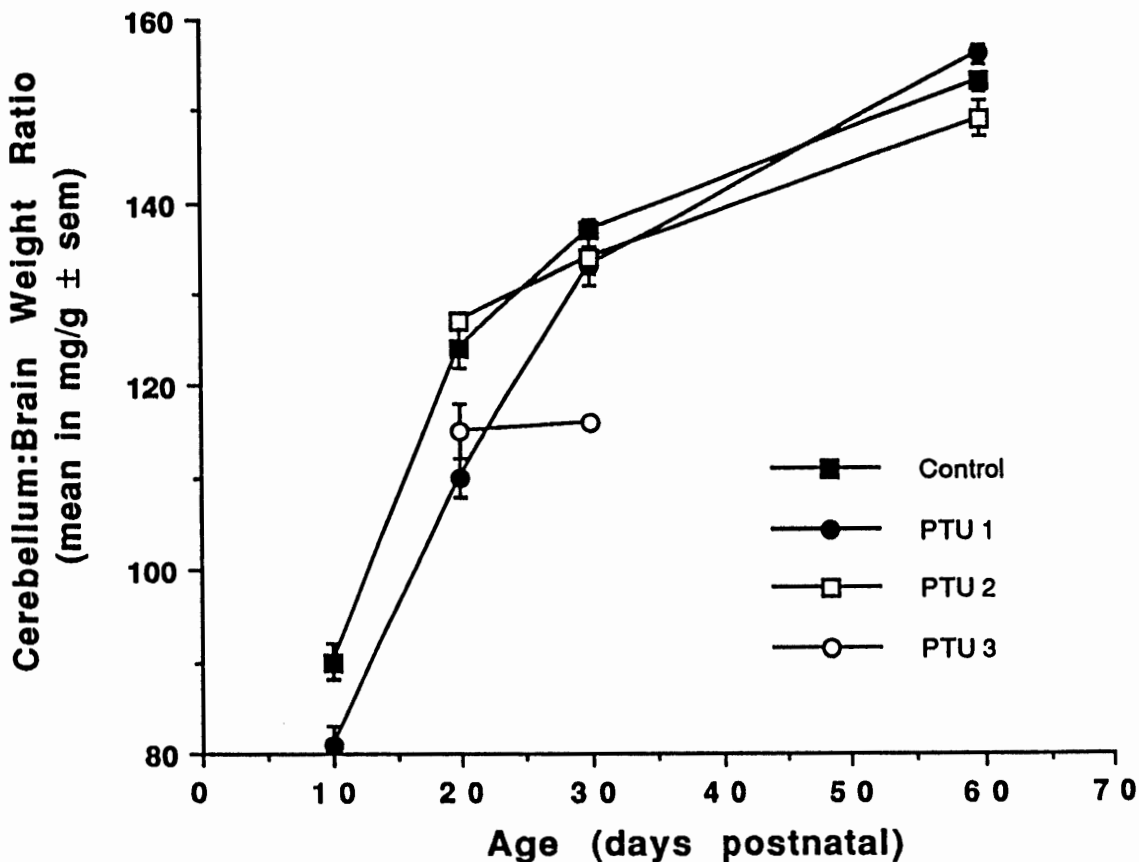


Figure 24. Effect of hypothyroidism on cerebellum:brain weight ratio.

Due to delayed granule cell differentiation within PTU 1 treated animals the greatest increase in cerebellum:brain weight ratio is delayed to PN days 20-30. Control animals show the greatest ratio increase between PN days 10-20, the normal period of cerebellar neurogenesis. Since PTU treatments affect the cerebellum to a greater extent than the brain, the cerebellum:brain weight ratio is decreased in treated animals. At PN day 20, the control and PTU 2 ratios, and the PTU 1 and PTU 3 ratios are equivalent. At PN day 30, only the control and PTU 3 values differ. At PN day 60, only PTU 1 and PTU 2 values are different. The standard error of the mean, although too small to be graphically represented, ranged from 3 to 13 % of the mean.

bellum:brain weight ratio differently. Since the cerebellum:brain weight ratios were similar at PN days 30 and 60, it could be inferred that the reduction in cerebellum weight at these stages in all PTU treatment groups, except PTU 3, was due to the overall decrease in brain weight. However, the reduced ratios observed in PTU treated groups at PN days 10 and 20 could be due to specific thyroid hormone action on cerebellar neurogenesis.

Altered Histogenesis Produces Unique Cerebellar Histology

In addition to the gross morphological alterations induced by PTU treatment, cerebellar histogenesis was modified. The well documented alterations in cerebellar histogenesis may be used to gauge the establishment of a hypothyroid state. In terms of external anatomy, the formation of cerebellar fissures and lobules was not affected by PTU treatment (Figure 25). However, at the cellular level, cerebellar cortical stratification and synaptogenesis were severely affected by PTU treatment.

The first signs of altered histogenesis in PTU 1 tissue were apparent at postnatal (PN) day 1 (Figure 26). Since PTU treatment produced delayed granule cell proliferation, the external granule layer (Egl) was reduced in hypothyroid animals. The Egl consists of the cell bodies of granule,

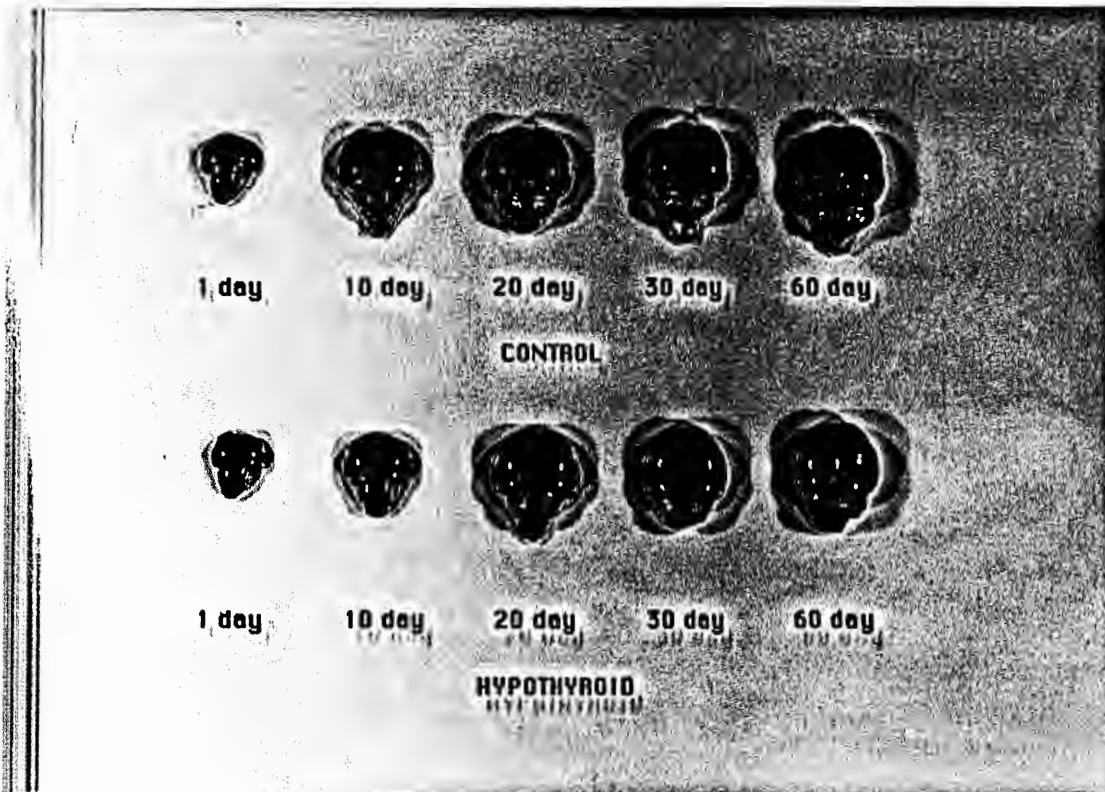


Figure 25. Postnatal Brain Development.
A comparison of total brain and cerebellar size
in control and hypothyroid animals.

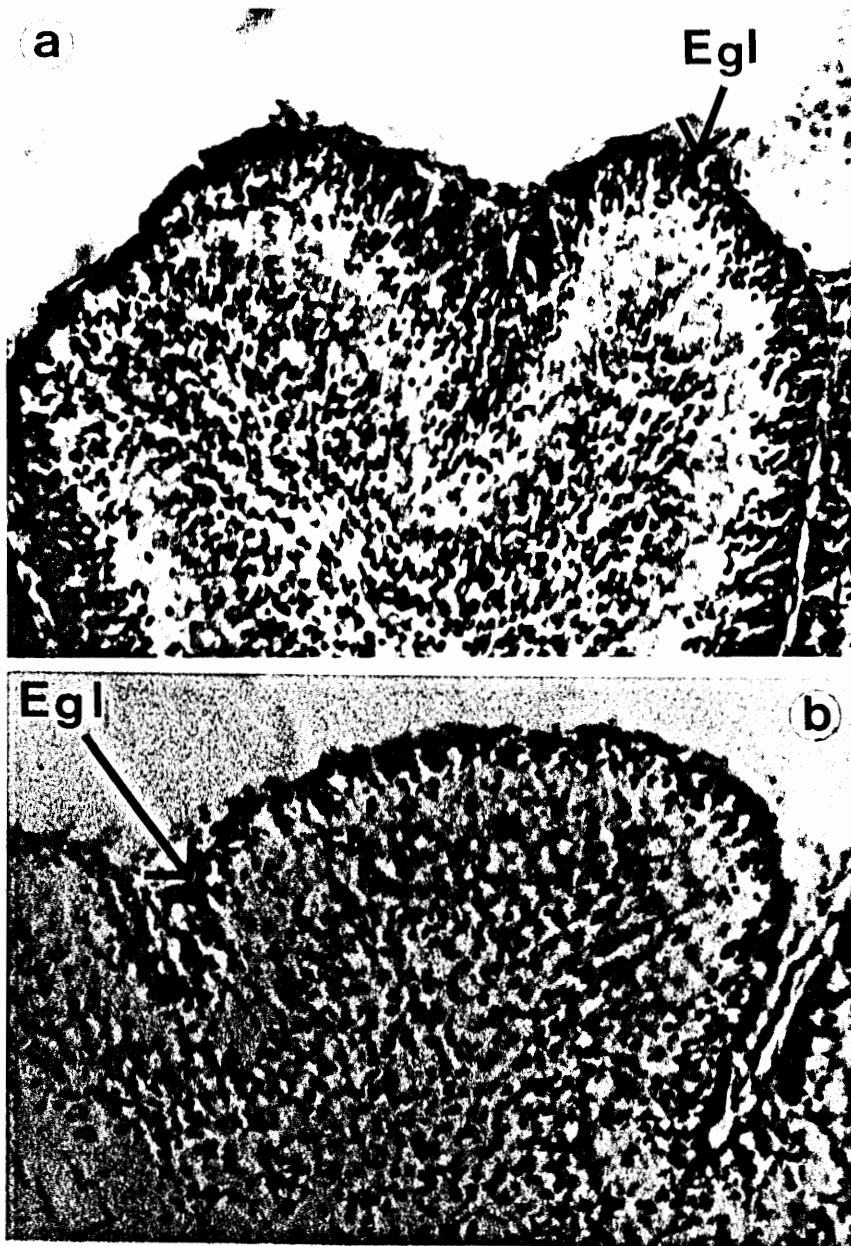


Figure 26. Histological Alterations at Postnatal Day 1.

- (a) The external granule layer (Egl) in control tissue contains densely packed granule cells. (232 X magnification)
- (b) Delayed granule cell proliferation in PTU 1 treated tissue results in a reduced external granule layer (Egl). (232 X magnification)

stellate and basket cells, and lacks intervening neuropil making it difficult to distinguish the various cell types at this stage. However, previous reports indicate the size reduction in the Egl is primarily due to decreased numbers of granule cells, the most numerous cerebellar neuron (Legrand, 1967).

Since granule cell proliferation was delayed beyond PN day 10, the Egl in PTU 1 treated animals remained reduced (Figure 27). By PN day 10 in control animals granule, stellate, and basket cells migrated inward and differentiated, thus forming the molecular layer. At the same time, Purkinje cells migrated outward from the roof of the fourth ventricle, and control tissue began to exhibit typical cortical stratification (Figure 28).

Granule cell differentiation in control tissue was complete by PN day 20 and the cerebellar cortex lacked a distinguishable Egl. Due to delayed granule cell migration, the Egl in PTU 1 treated tissue was still quite prominent (Figure 29). Postnatal PTU treatment (PTU 2) beginning at PN day 10 also resulted in delayed granule cell migration, although not as extensive as that which occurred with prenatal PTU treatment (PTU 1). Continuous PTU treatment (PTU 3) resulted in the most dramatic delay in granule cell migration. Granule cells migrated from the Egl and established synaptic contact with Purkinje cells (Figure 30).

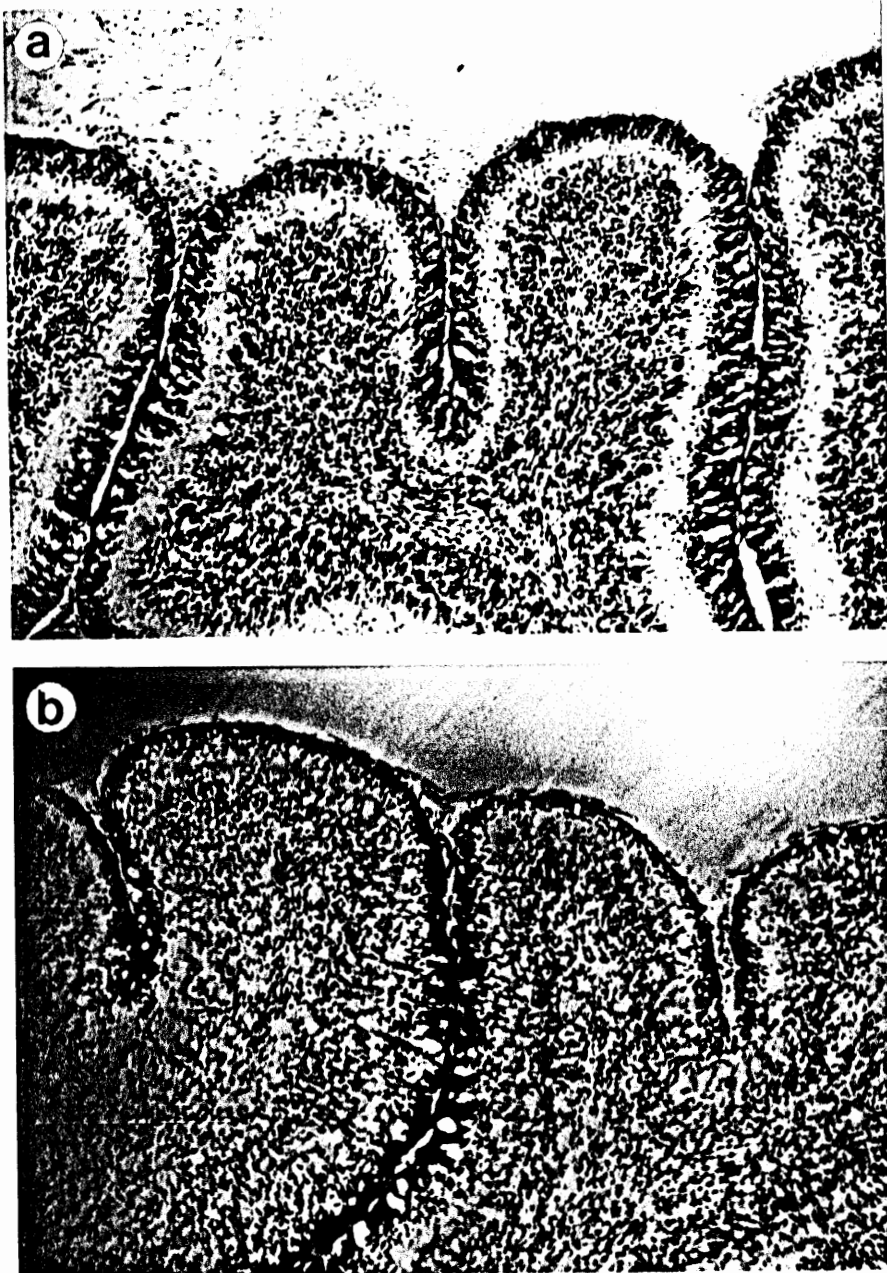


Figure 27. Histological Alterations at Postnatal Day 10.
(a) As granule cells migrate inward, the external granule layer in control tissue is less densely packed. (106 X magnification)
(b) The external granule layer in PTU 1 treated tissue remains reduced. (106 X magnification)

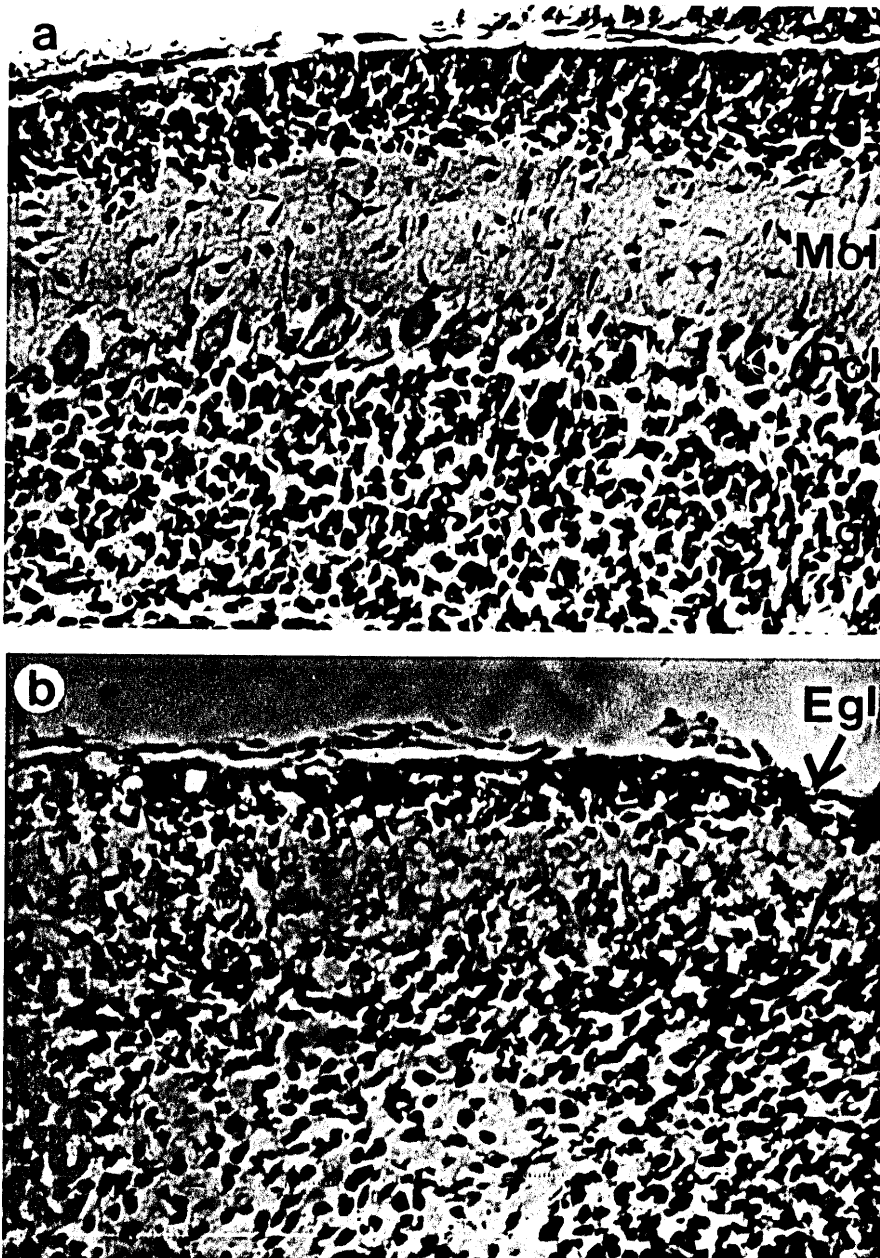


Figure 28. Cortical Stratification at Postnatal Day 10.

- (a) Control tissue begins to exhibit signs of cortical stratification: Egl, external granule layer; Mol, molecular layer; Pcl, Purkinje cell layer; Igl, internal granule cell layer. (320 X magnification)
- (b) PTU 1 treated tissue lacks detectable signs of stratification. (320 X magnification)

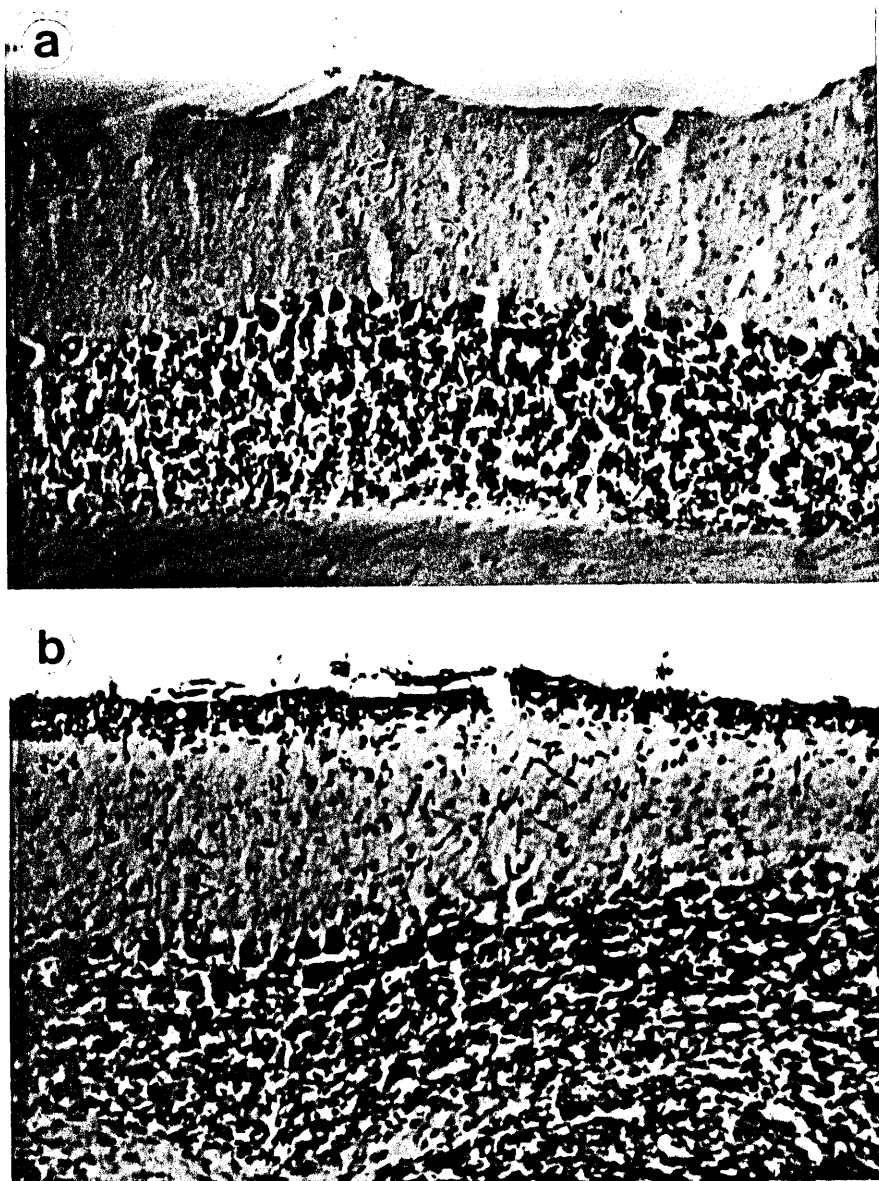


Figure 29. Histological Alterations at Postnatal Day 20.
(a) The external granule layer is thin and barely visible in control tissue. (182 X magnification)
(b) Due to delayed granule cell migration, the external granule layer persists to a greater extent in PTU 1 treated tissue. (182 X magnification)

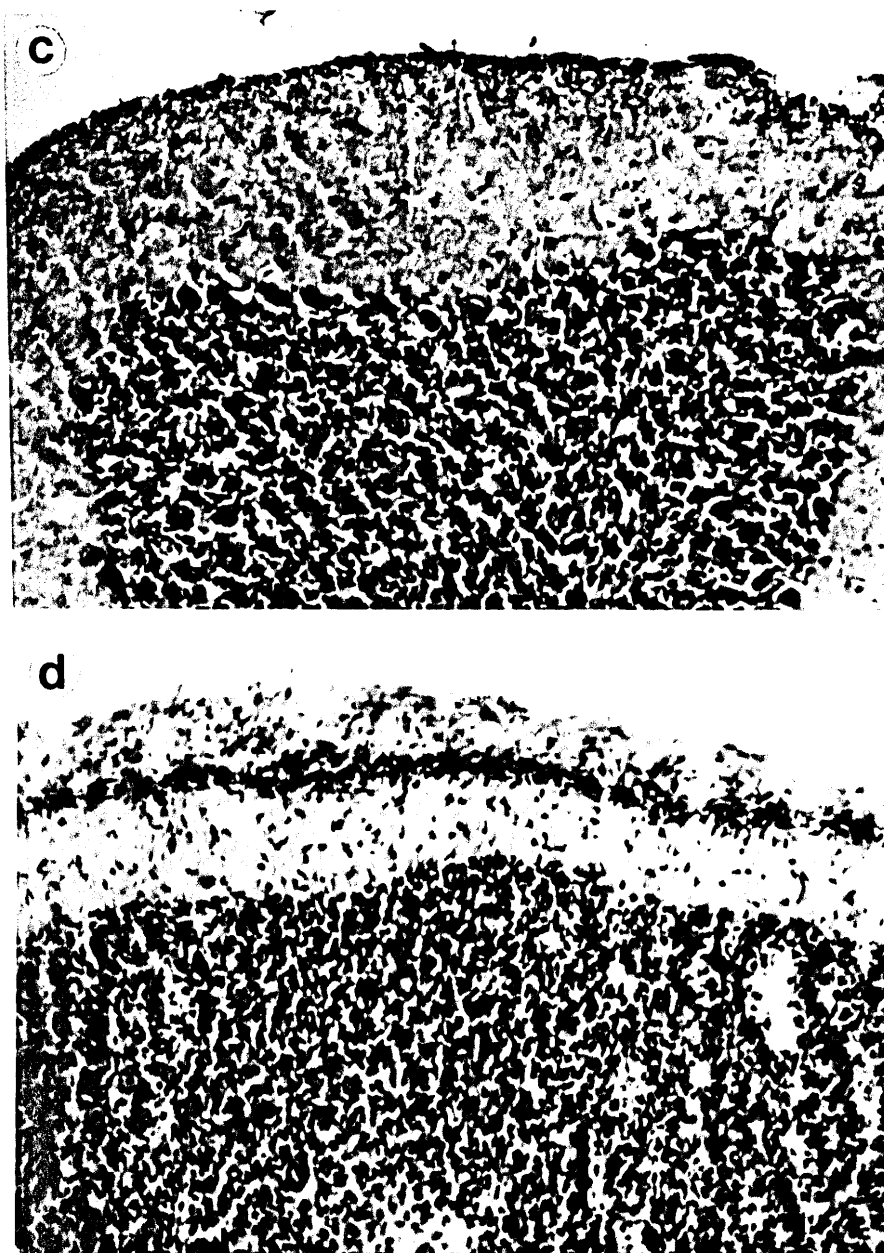


Figure 29. Histological Alterations at Postnatal Day 20.

- (c) Postnatal PTU administration results in delayed granule cell migration and the retention of the external granule layer in PTU 2 treated tissue. (175 X magnification)
- (d) Continuous PTU administration results in the most extensive alterations in granule cell migration. In contrast to the extensive external granule layer, note the diminished size of the molecular layer in PTU 3 treated tissue. (175 X magnification)



Figure 30. Granule cell Migration and Synapsis.
As granule cells (gr) migrate from the external granule layer, they make synaptic contact with Purkinje cells (pc) migrating from the roof of the fourth ventricle.
(1435 X magnification)

The process of synaptogenesis and differentiation must occur within a limited period of time known as the critical period. As a result of delayed granule cell migration and parallel fiber formation, the Purkinje cell misses its "window of opportunity" and forms inappropriate synapses with its nearest "neighbors". Purkinje cell somal morphology appeared to be affected by these altered synaptic contacts. In control tissue, the Purkinje cell soma appeared spherical and possessed one primary dendritic arbor (Figure 31). In PTU 1 treated tissue, the Purkinje cell somata were larger, less regularly shaped and might have contained more than one primary dendritic arbor. The Purkinje cell soma in PTU 2 treated tissue appeared similar in size and shape to those in PTU 1 treated tissue. Continuous PTU treatment in PTU 3 tissue did not seem to severely alter either Purkinje cell somal area or shape, beyond that induced by prenatal treatment.

By PN day 30, both control and hypothyroid tissue exhibited typical cortical stratification (Figure 32). In PTU 1 treated tissue, Purkinje cell dendritic arborization and somal morphology remained hypoplastic even after the disappearance of the external granule layer. In both PTU 2 and PTU 3 treated tissue the molecular layer appeared significantly reduced, while the internal granule layer appeared equivalent in both. The Purkinje cell somal size

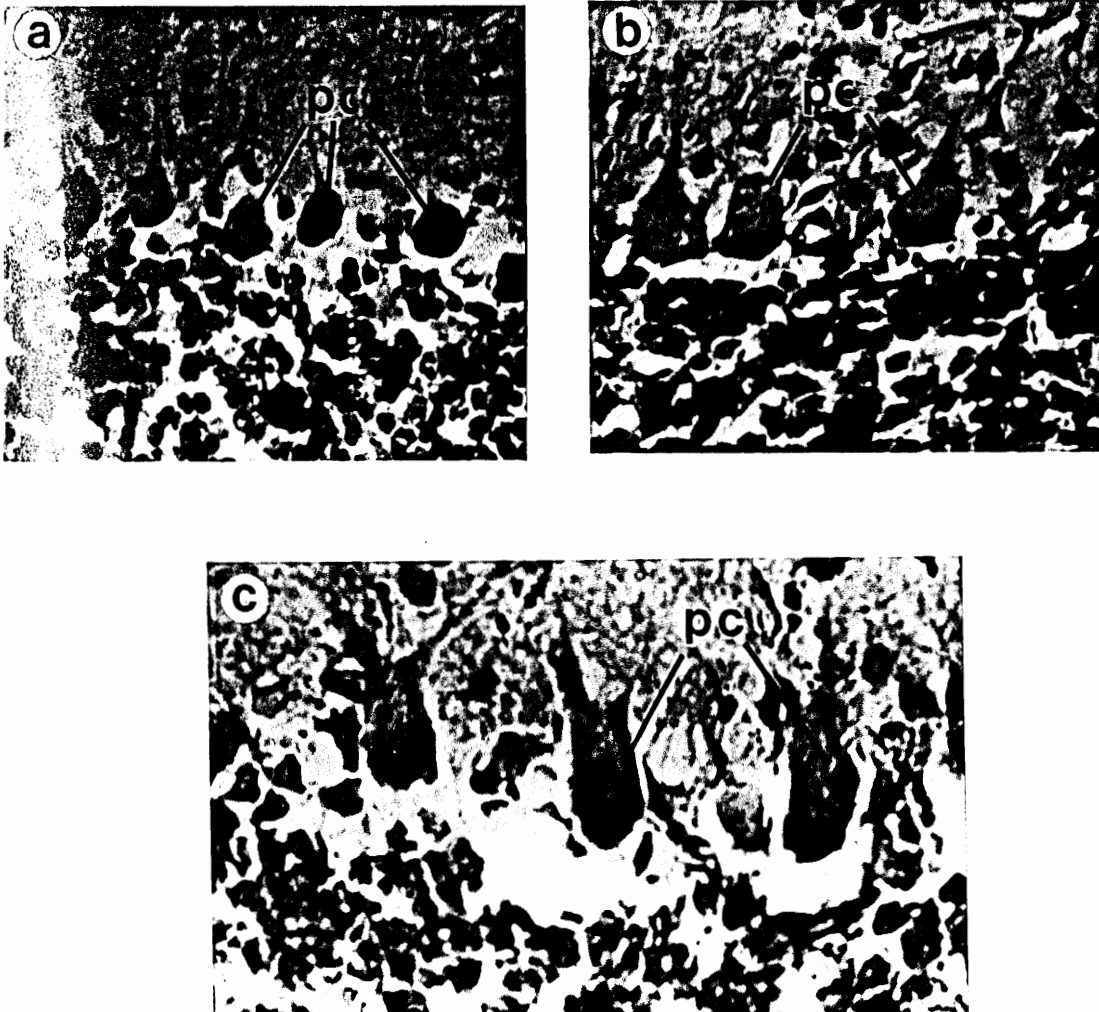


Figure 31. Purkinje cell Morphology at Postnatal Day 20.
 (a) The Purkinje cells (pc) in control tissue exhibit typical somal morphology. (576 X magnification)
 (b) The Purkinje cells (pc) soma in PTU 1 treated tissue are larger and less regularly shaped. (576 X magnification)
 (c) At higher magnification (874 X), it can be seen that the Purkinje cell contains more than one primary dendritic arbor.

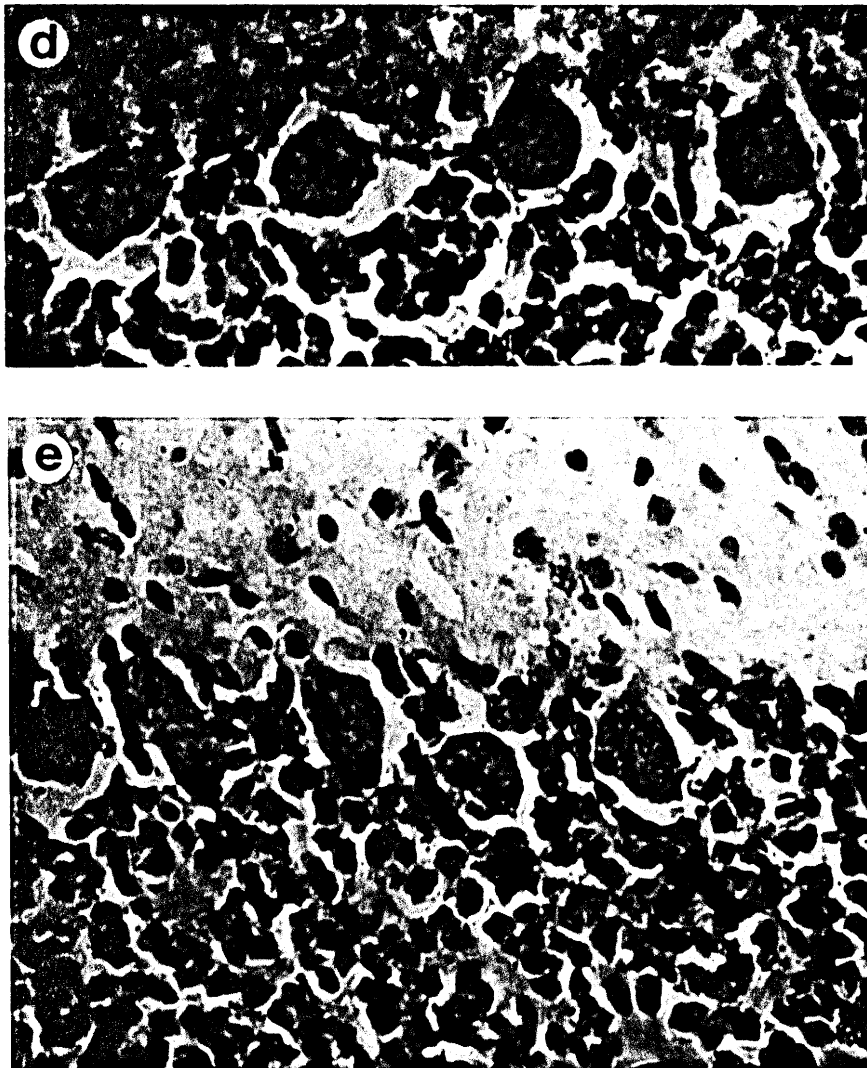


Figure 31. Purkinje cell Morphology at Postnatal Day 20.

- (d) The Purkinje cell somal size in PTU 2 treated tissue appears larger than control tissue, yet exhibit a well defined shape. (696 X magnification)
- (e) While the Purkinje cell soma in PTU 3 treated tissue appear smaller than in other PTU treatments, the shape is less regular. (640 X magnification)

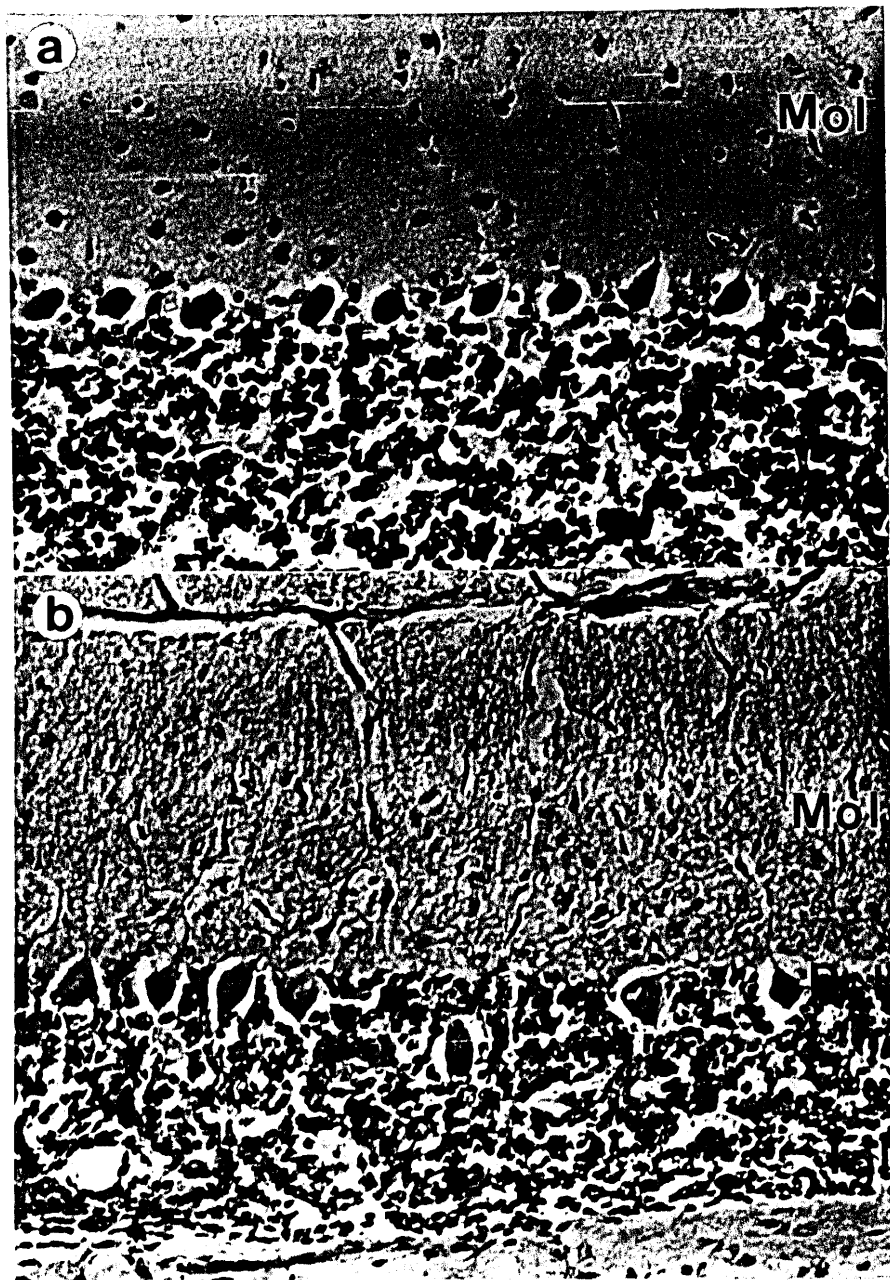


Figure 32. Histological Alterations at Postnatal Day 30.

- (a) Typical cortical strata can be observed in control tissue at this stage. In particular, note the isoplanar character of the Purkinje cell layer (Pcl). (300 X magnification)
- (b) While cortical stratification appears equivalent in PTU 1 treated tissue, Purkinje cells are not aligned at the junction of the molecular (Mol) and internal granule layers (Igl). (300 X magnification)

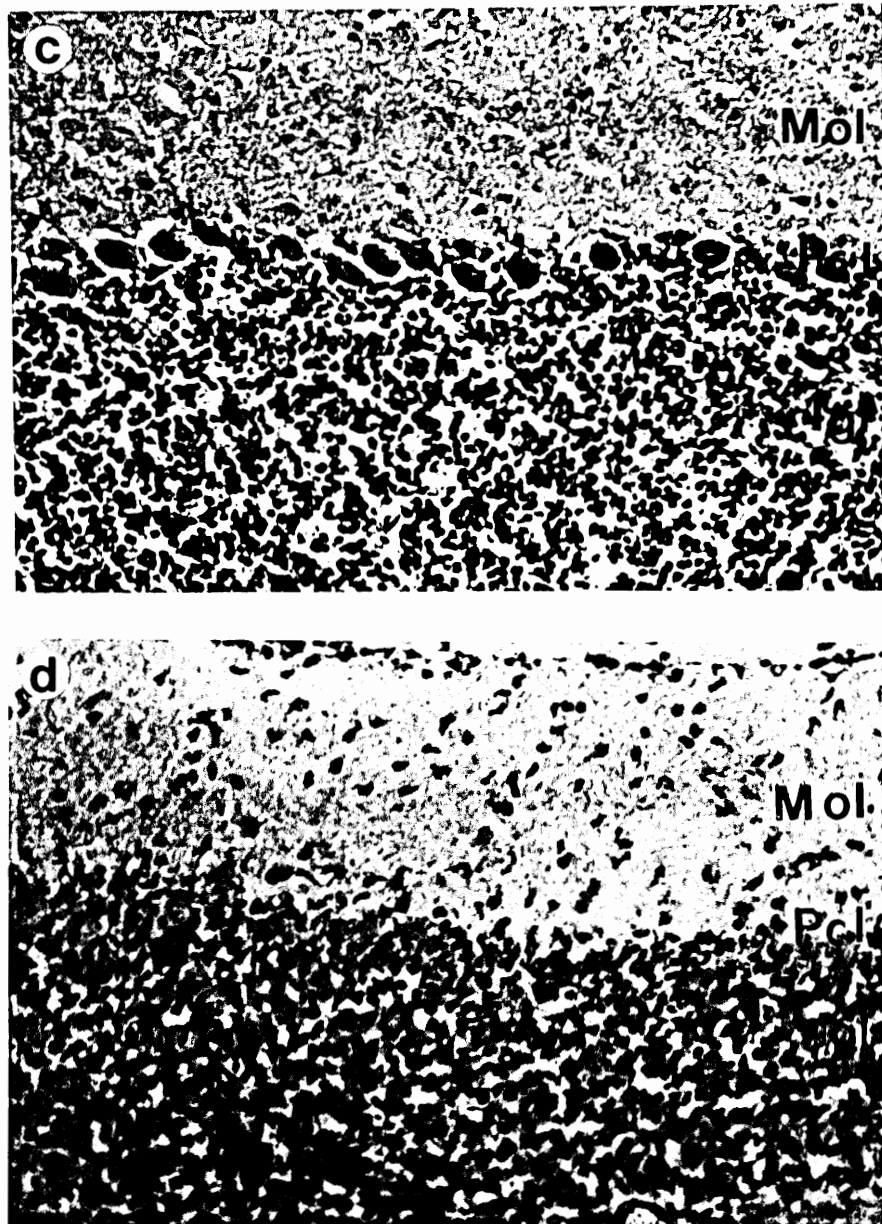


Figure 32. Histological Alterations at Postnatal Day 30.

- (c) Both the molecular and internal granule cell layers appear to be reduced in PTU 2 treated tissue. (278 X magnification)
- (d) While the internal granule cell layer in PTU 3 treated tissue appears similar to PTU 2 treated tissue, the molecular layer in PTU 3 tissue is severely reduced. (278 X magnification)

in control tissue remained considerably larger and less regularly shaped than that of PTU 1 treated tissue. In PTU 2 treated tissue, both the Purkinje cell somal area and shape appeared equivalent to control soma. Continuous PTU treatment to PN day 30 resulted in such severe histological alterations that Purkinje cells were not detectable in the one available histological preparation (Figure 33). In addition to delayed granule cell migration from the external granule layer, PTU treatment also appeared to delay Purkinje cell migration from the roof of the fourth ventricle. Purkinje cells should migrate to the junction of the molecular and internal granule layers, at which point they differentiate to form the isoplanar Purkinje cell layer. Like granule cells found remaining within the external granule layer, Purkinje cells could be found in the internal granule layer of hypothyroid tissue (Figs. 32, 34).

By PN day 60, the histological alterations induced by PTU treatment were barely apparent (Figure 35). The most notable feature in PTU 1 treated tissue was the hypoplasia of the internal granule layer. While PTU 2 treated tissue did not exhibit this hypoplasia, other features of PTU 1 and PTU 2 tissue appeared similar. In control tissue at PN day 60, typical Purkinje cell somal morphology and location were observed. The Purkinje cell somata in PTU 1 treated tissue remained considerably enlarged in size, but were more

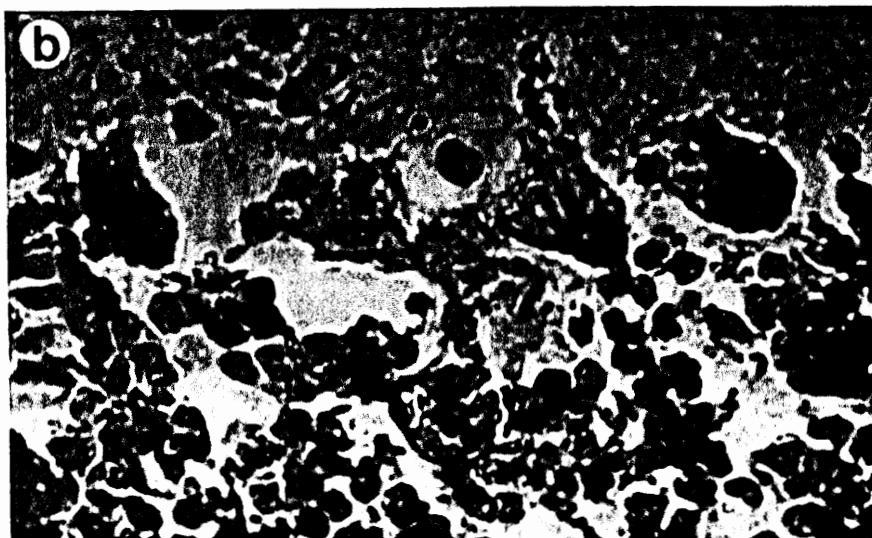
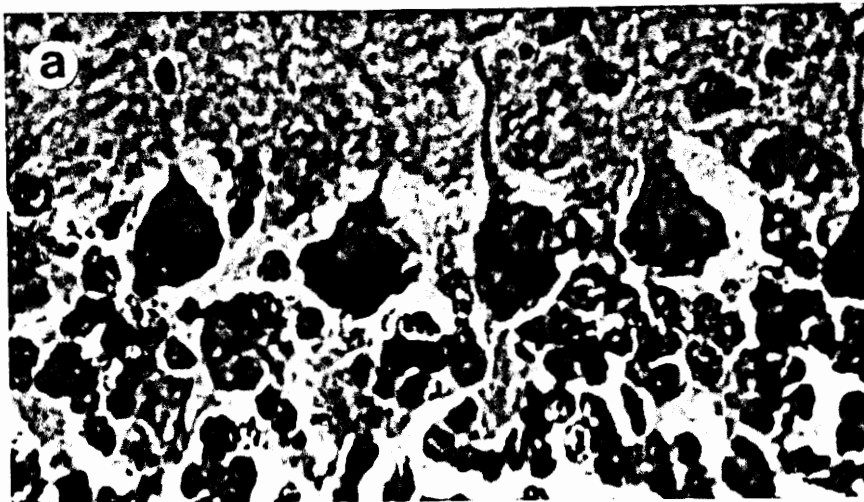


Figure 33. Purkinje cell Morphology at Postnatal Day 30.
(a) Purkinje cells exhibit normal somal morphology in control tissue. (970 X magnification)
(b) Purkinje cells in PTU 1 treated tissue are less regularly shaped. (970 X magnification)

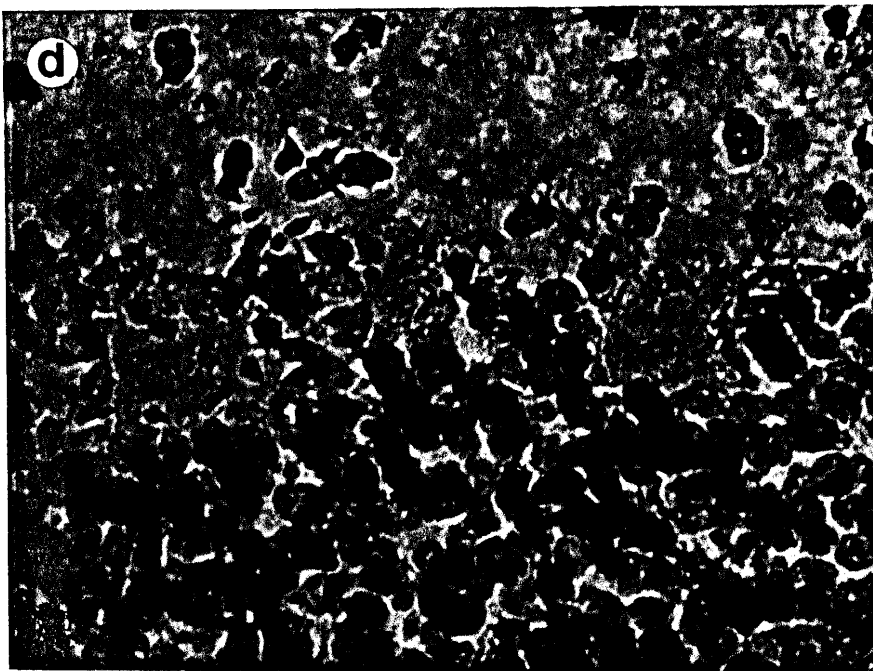
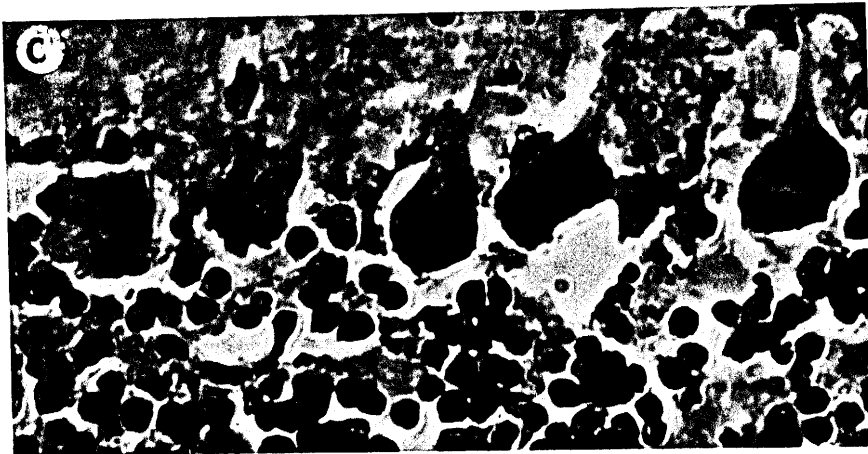


Figure 33. Purkinje cell Morphology at Postnatal Day 30.

- (c) The Purkinje cell soma in PTU 2 treated tissue are smaller in size than PTU 1 treated soma, and appear more regularly shaped. (891 X magnification)
- (d) Continuous PTU treatment results in such severe histological alterations that Purkinje cell soma are not readily detectable at 30 days of age in PTU 3 treated tissue. (891 X magnification)

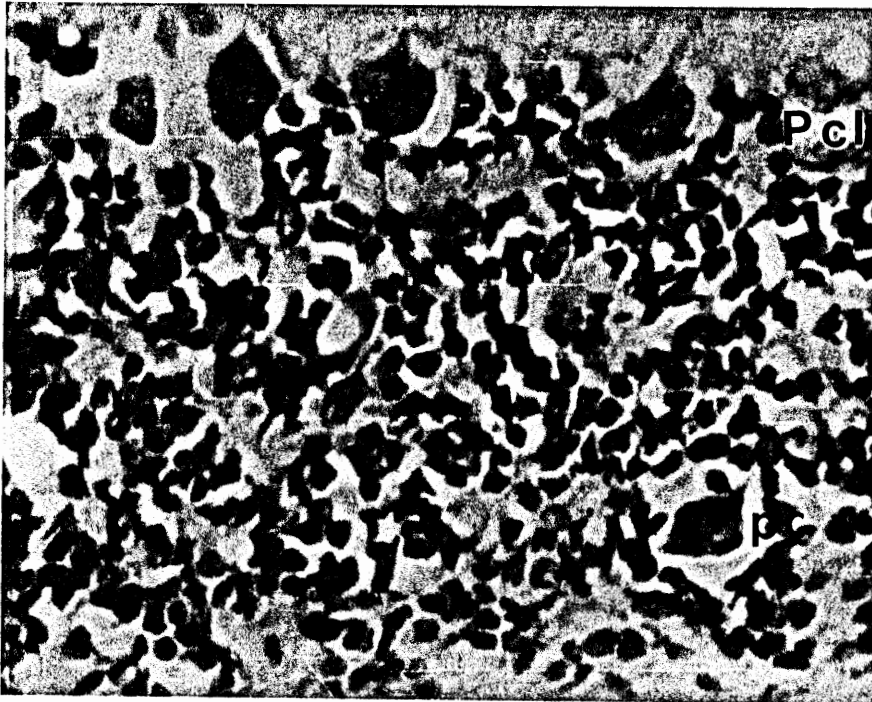


Figure 34. Purkinje cell Soma Displaced by PTU 1 Treatment. Purkinje cell soma should be aligned in a linear fashion within the Purkinje cell layer (Pcl). A putative Purkinje cell (pc) soma can be seen located deep within the internal granule layer of hypothyroid tissue. (784 X magnification)

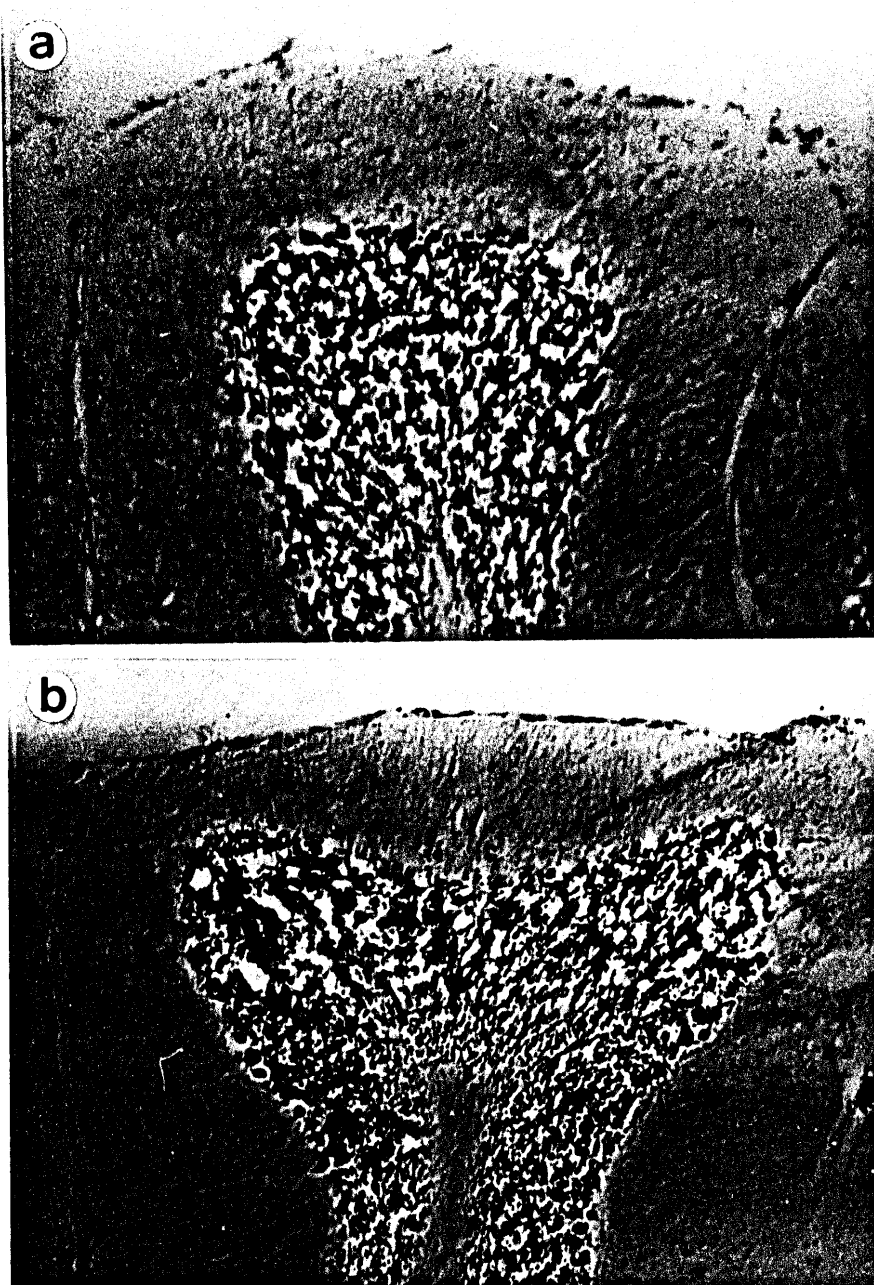


Figure 35. Histological Alterations at Postnatal Day 60.
(a) Typical cortical stratification can be seen in control tissue at this developmental stage.
(166 X magnification)
(b) While cortical stratification appears equivalent to control tissue, the internal granule layer remains hypoplastic in PTU 1 treated tissue.
(113 X magnification)



Figure 35. Histological Alterations at Postnatal Day 60.
(c) All features of cortical stratification in PTU 2 treated tissue appear equivalent to control tissue.
(106 X magnification)

regularly shaped than previously. In PTU 2 treated tissue, the Purkinje cell somal area appeared similar to control tissue, but was less regularly shaped (Figure 36). Using Golgi's silver nitrate method of staining, dendritic arbors could be seen (Figure 37). One primary arbor leads to secondary and tertiary branches, producing the extensive Purkinje cell dendritic arborization that occupies the molecular layer.

To more accurately assess the histological alterations induced by PTU treatment, the Zeiss Video-Plan was used to quantify differences in the cortical strata and Purkinje cell somata. Camera lucida drawings were prepared and digitally analyzed. The thickness of each cortical stratum and two Purkinje cell somal features, somal area and Form PE (defined in Appendix L), were measured.

The increase in cortical depth of both control and hypothyroid tissue paralleled the increase in cerebellar weight (Figure 38). The greatest increase in depth occurred between PN days 10 and 20, and corresponded to the period of most active differentiation. As discussed earlier, PTU treatment was correlated with reduced cerebellar weight, and so it was not surprising to find that cerebellar cortical depth, exclusive of the arbor vitae, was reduced in hypothyroid tissue. Cortical depth at PN day 1 could not be measured, since the cerebellum lacked detectable strata at this

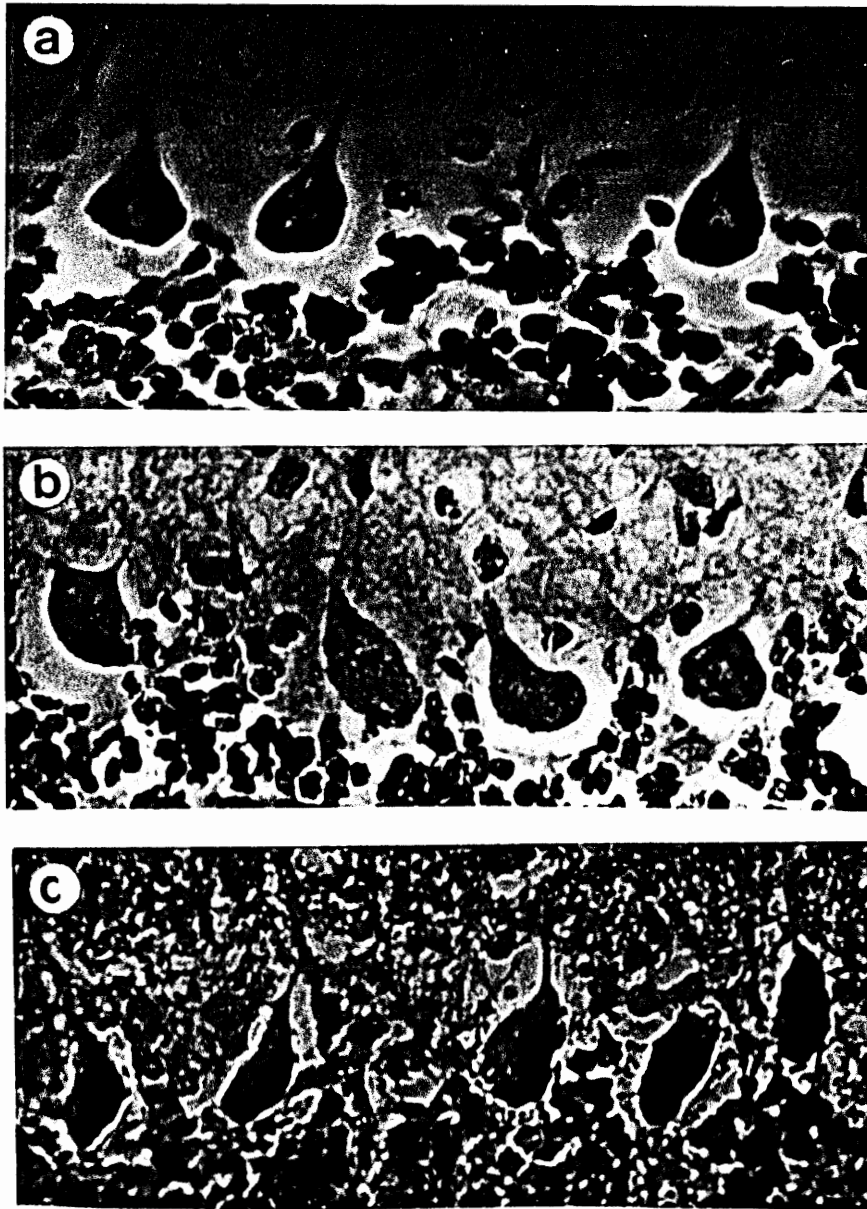


Figure 36. Purkinje cell Morphology at Postnatal Day 60.

- (a) Typical Purkinje cell somal morphology in control tissue. (952 X magnification)
- (b) By postnatal day 60, the Purkinje cell soma in PTU 1 treated tissue appear more regularly shaped than at previous stages. (718 X magnification)
- (c) The Purkinje cell soma in PTU 2 treated tissue appear similar in size, but less regularly shaped than in control tissue (672 X magnification).

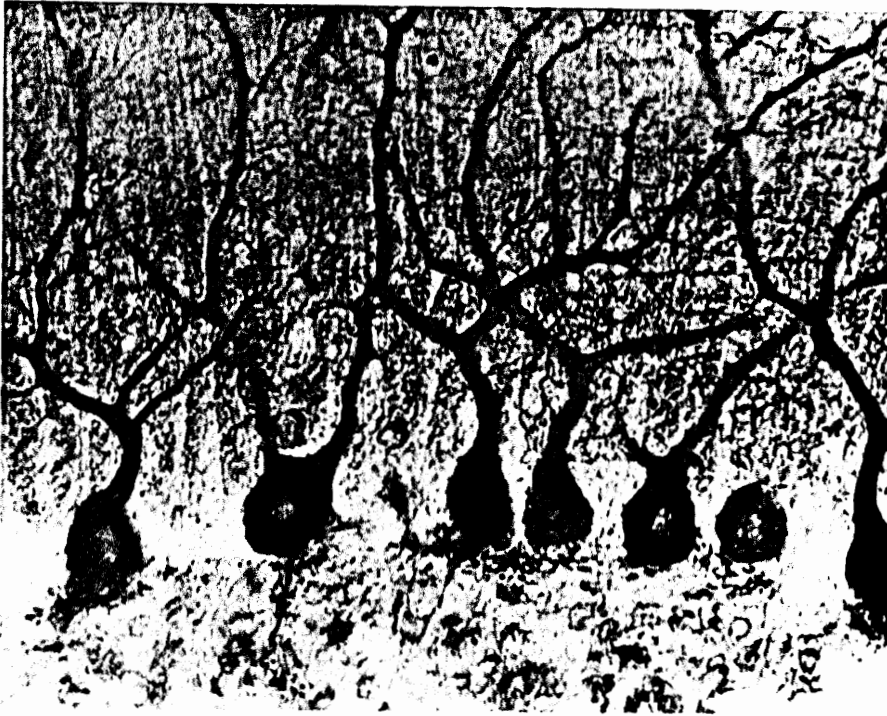


Figure 37. Purkinje cell Dendritic Arborization.
Sixty day postnatal control cerebellum stained by the Golgi method to demonstrate Purkinje cell dendritic arborization into the molecular layer. (470 X magnification)

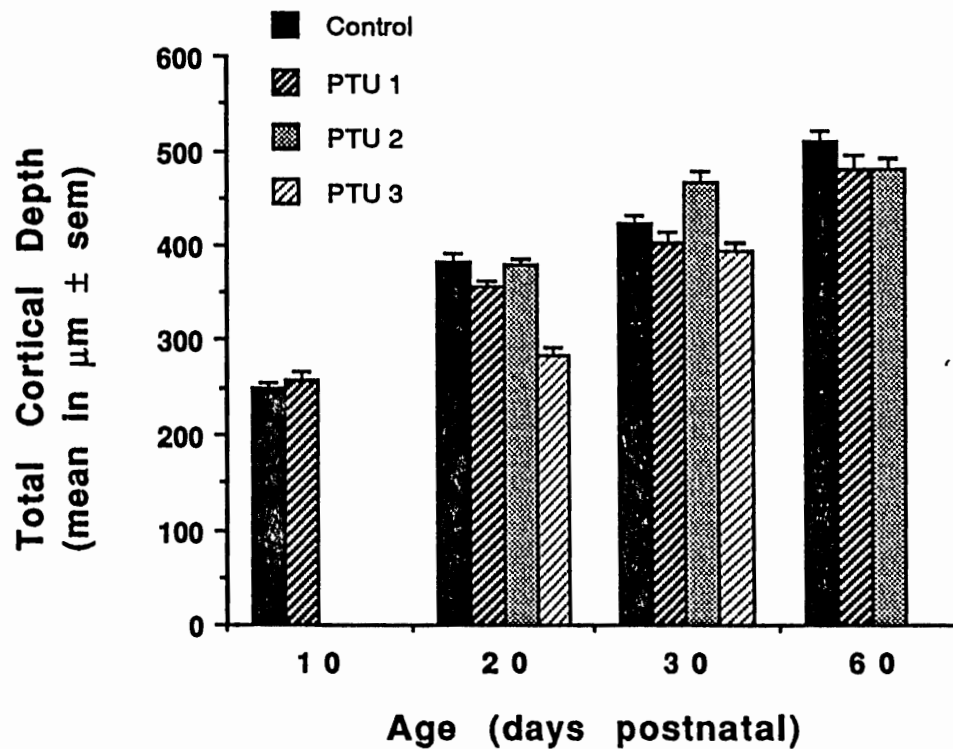


Figure 38. Developmental alterations in total cerebellar cortical depth.

With the exception of PN day 10 (PTU 1) and PN day 30 (PTU 2), the total cortical depth in hypothyroid tissue is smaller than that of control. This is not unexpected since hypothyroidism results in reduced cerebellar size. This reduction is significant for all treatments except: control and PTU 1 (PN 10), control and PTU 2 (PN 20), PTU 1 with control and PTU 2 (PN 30) and PTU 1 and PTU 2 (PN 60).

stage. At PN day 10, the cortical depth in PTU 1 treated tissue was greater, although not significantly, than that of control tissue. The cortical depth at PN day 20 was reduced in both PTU 1 and PTU 3 treated tissues. The PTU 2 cortical depth was equivalent to control values at PN day 20, perhaps because cerebellar weight at this stage was similar. At PN day 30 the cortical depth in PTU 2 treated tissue was inexplicably greater than in control tissue. At this stage PTU 1 values were similar to control and PTU 3 values. At PN day 60 PTU 1 and PTU 2 cortical depth values were equivalent, but remained reduced as compared to controls. Thus it appears that reductions in cortical depth were a general trend of PTU treatment ($F_{3,\infty} = 6$ and $F_{2,\infty} = 13$).

In addition, PTU treatment might have similarly affected the representation of individual strata. When considering the thickness of individual strata, possible differences from controls could be due to an overall reduction in the size of the cerebellum or due to an actual proportional reduction in the particular stratum. The external granule layer (Egl) represents a transitory proliferative zone which accounted for approximately 10% of the total cortical depth at PN day 10. Due to delayed granule cell proliferation, the Egl was dramatically reduced in PTU 1 treated tissue at PN day 1 (Figure 39). Due to delayed granule cell migra-

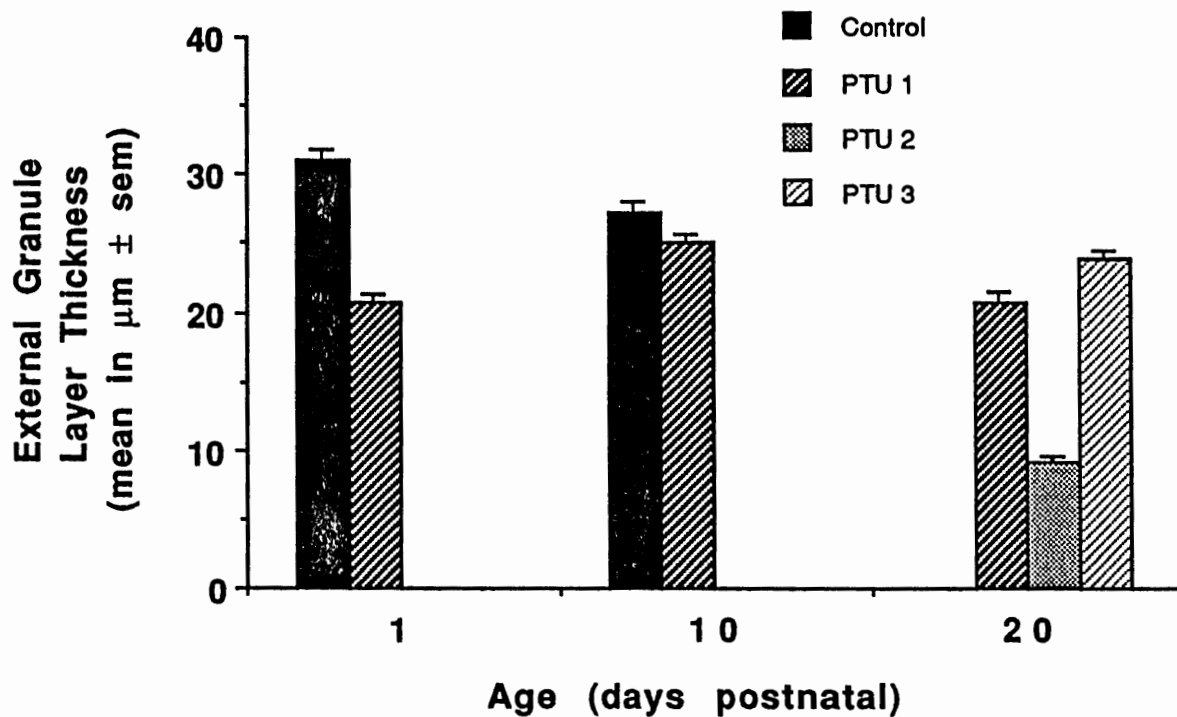


Figure 39. Developmental alterations in the cerebellar external granule layer (Egl).

In control tissue, the Egl disappears rapidly, and is not detectable at PN day 20. Delayed granule cell proliferation in hypothyroid tissue results in a severe reduction in the Egl at PN day 1. Delayed granule cell migration in hypothyroid tissue deters Egl disappearance so that it persists at PN day 20. Even postnatal PTU administration (PTU 2) results in delayed granule cell migration, while prolonged treatment (PTU 3) results in the most significant retention of the Egl.

tion, the Egl in PTU 1 treated tissue did not disappear and persisted at least until PN day 20. The most rapid disappearance of the Egl in control tissue occurred between PN days 10 and 20, and corresponded to the migration and differentiation of stellate and basket cells, as well as granule cells. Since the Egl was still present, although barely, in PTU 2 treated tissue it was demonstrated that even postnatal administration of PTU could affect cerebellar development and granule cell migration. Prolonged PTU treatment resulted in the greatest retention of the Egl. Statistics indicate significant differences in Egl depths at all PN days studied ($F_{3,\infty} = 47$) showing that PTU did affect the representation of the Egl within the cerebellar cortex.

As stellate and basket cells migrate inward from the Egl they differentiate and establish the molecular layer. In addition, the molecular layer contains the dendritic arbors of Purkinje cells, the parallel fibers of granule cells, and intervening glial neuropile. Due to delayed granule cell migration and parallel fiber formation, the molecular layer in all PTU treated tissue at PN day 20 was dramatically reduced, with equivalent PTU 1 and PTU 2 values ($F_{3,\infty} = 61$ and $F_{2,\infty} = 16$) (Figure 40). By PN day 30, the Egl in hypothyroid tissue had disappeared and the molecular layer was equivalent in both control and hypothyroid tissue,

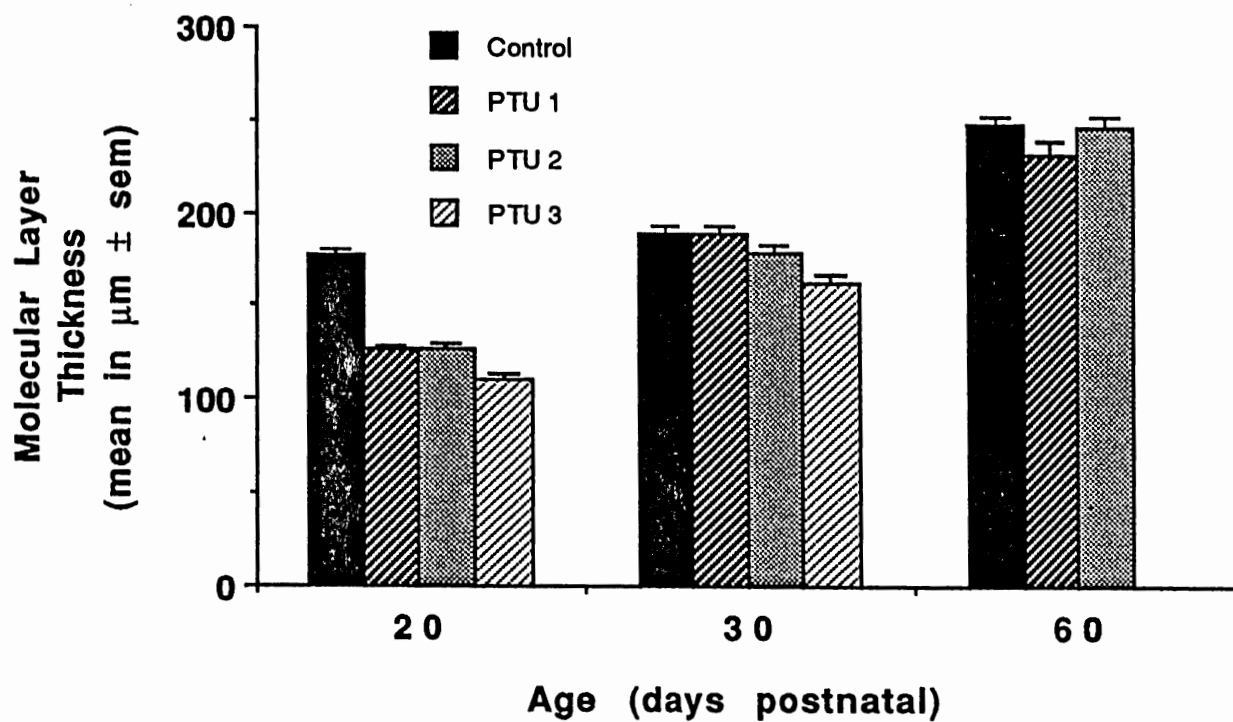


Figure 40. Developmental alterations in the cerebellar molecular layer.

Due to the retention of the Egl in hypothyroid tissue at PN day 20, the molecular layer is significantly reduced. By PN day 30, the Egl has disappeared and the molecular layer in control tissue is equivalent to hypothyroid, except in PTU 3 treated tissue. At PN day 60, the molecular layer of PTU 1, but not PTU 2 treated tissue is reduced.

except PTU 3 treated tissue. PTU 1 and PTU 2 values were similar, but all other hypothyroid values were different. The molecular layer at PN day 60 in PTU 1, but not PTU 2 treated tissue, was significantly reduced. However, when the molecular layer was represented as a proportion of the total cortical depth (remembering that the cortical depth is reduced in PTU treated tissue), no differences were observed.

The internal granule layer (Igl) consists of Golgi cells, Purkinje cell axons and climbing and mossy fibers. The Igl at PN day 20 was equivalent in control and hypothyroid tissue, except PTU 3 treated tissue (Figure 41). However, the Igl was significantly reduced at PN days 30 and 60, even when represented as a proportion of total cortical depth ($F_{3,\infty} = 10$ and $F_{2,\infty} = 16$). It is known that the inability of granule cells to establish proper synaptic contact with Purkinje cell dendritic arbors results in granule cell death. At PN day 20, most granule cells remained in the Egl of hypothyroid tissue and, therefore, have not as yet established the Igl. In control tissue, granule cells established maximum Purkinje cell contact at PN day 21 thus, the greatest Igl increase in control tissue was attained between PN days 20 and 30. As development proceeded,

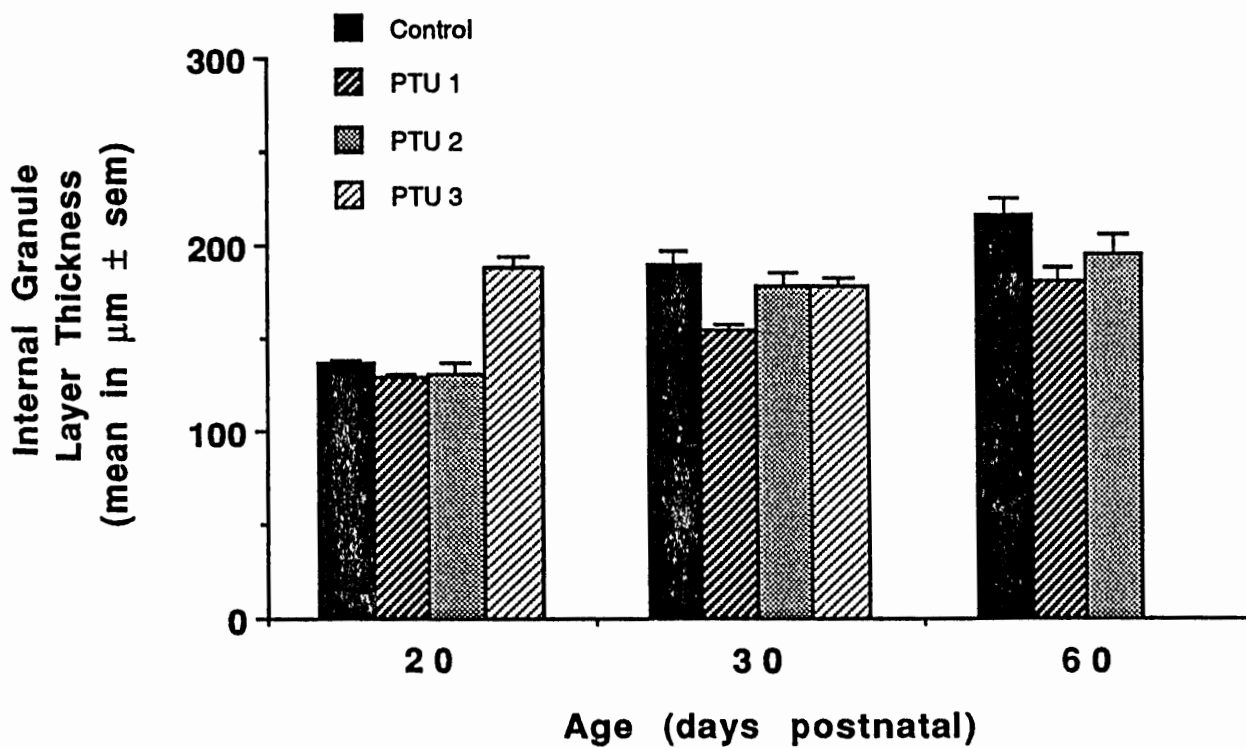


Figure 41. Developmental alterations in the cerebellar internal granule layer (Igl).

Since granule migration is not yet complete at PN day 20, the Igl is equivalent in control and hypothyroid tissue, except PTU 3 treated tissue. Due to increased granule cell death in hypothyroid tissue, the Igl is reduced in all PTU treatment groups at PN days 30 and 60.

Igl depth increased in hypothyroid tissue, but its establishment was diminished due to increased granule cell death.

The statistical analysis of PTU effects on cortical stratification only substantiated the histological alterations observed. It appeared that PTU altered total cortical depth and affected strata differentially at critical developmental periods. Only the external granule layer was affected at all postnatal stages studied. This was to be expected, due to its transient nature and PTU's effect on delaying granule cell proliferation and migration. No other cortical layer was affected at all developmental stages suggesting that PTU exerted its effect at specific developmental stages. Assuming the locus of action of PTU is the thyroid, leading to reduction or elimination of thyroid hormone output, then the observed alterations of the cortical strata in treated tissue could be due to the resultant deficiency of thyroid hormone.

While it was clearly demonstrated that PTU treatment influences cortical stratification within the cerebellum, it also appeared as though PTU treatment produced severe histological alterations in Purkinje cells. Unlike PTU's effect on cortical stratification, its effect on Purkinje cell morphology was more blatant. Purkinje cell somal areas were significantly greater at all postnatal stages and PTU treat-

ments studied, except PTU 2 treated tissue at PN day 60 ($F_{3,\infty} = 33$ and $F_{2,\infty} = 93$). An average Purkinje cell in hypothyroid tissue was 36% larger than its control counterpart. As development proceeded in control tissue, Purkinje cell somal area declined. The somal area in hypothyroid tissue exhibited greater fluctuations (Figure 42). Purkinje cell soma were not only larger in PTU treated tissue, but they were also less regularly shaped. Form PE is a measure of "circularity". A perfect circle has a Form PE equal to one. As objects deviate from this spherical shape the Form PE decreases. While soma are generally not considered spherical in nature, the Form PE was used as a gauge of alterations in shape ($F_{3,\infty} = 32$ and $F_{2,\infty} = 93$). As development proceeded, Purkinje cell somal Form PE increased in both control and hypothyroid tissue, except in PTU 2 treated tissue at PN day 60. Synaptogenesis involves a temporary redundancy of synapses. As inappropriate synapses are eliminated and appropriate ones stabilized, Purkinje cell soma approach a spherical nature. PTU treatment affected somal shape, since the Form PE was significantly reduced at all postnatal stages and PTU treatments, except PTU 2 treated tissue at PN day 20 and at PN day 30 where PTU 2 values were significantly greater (Figure 43). Therefore, even though the other histological alterations induced by PTU

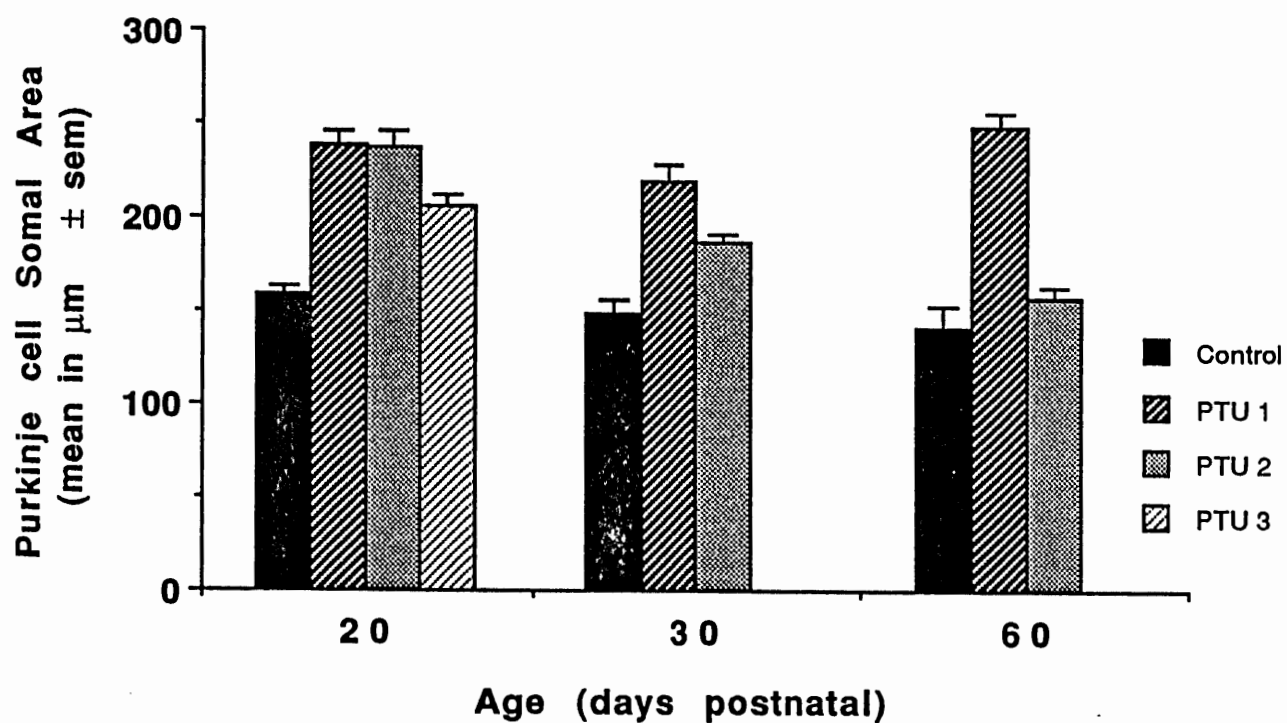


Figure 42. Developmental alterations in Purkinje cell somal area.

Purkinje cell somal area in control tissue decreases in a linear fashion as development proceeds. In hypothyroid tissue, Purkinje cell somal area fluctuates during development. The Purkinje cell somal area in all PTU treatment groups is significantly larger at all postnatal stages studied.

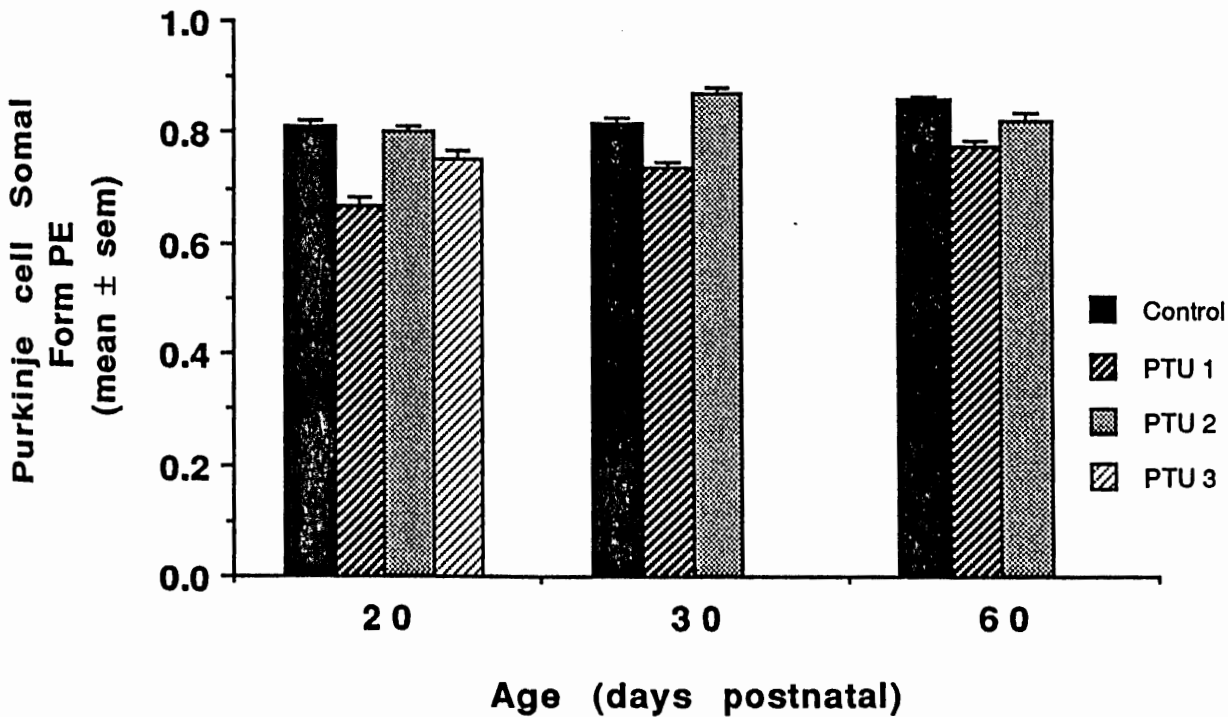


Figure 43. Developmental alterations in Purkinje cell Form PE.

Form PE is a measure of "roundness", such that a Form PE = 1 represents a perfect circle. As the Form PE decreases, objects may be considered less spherical. As development proceeds and synaptic contacts are stabilized, the Form PE of the Purkinje cell soma in both control and hypothyroid tissue increases. The Purkinje cell soma in hypothyroid tissue may be considered less spherical (or more irregularly shaped) since the Form PE is significantly reduced at all postnatal stages studied, except PTU 2 treated tissue at PN day 20.

treatment became less apparent during development, Purkinje cell somal area and shape remained affected throughout development.

Serum PTU and Free T₃ Analysis

While the morphological and histological alterations induced by hypothyroidism were quite obvious, alternate biochemical means of gauging the hypothyroid state were sought. To verify the establishment of the hypothyroid state, one could either monitor plasma PTU or free T₃ concentration. The large population of animals used in this study made the initial use of a free T₃ radioimmunoassay unfeasible, necessitating the use of the 2,6-dichloroquinone-4-chloroimide PTU assay of Ratliff and coworkers (1972). Unfortunately, this assay requires two milliliters of serum. Since it is impossible to obtain that quantity of serum from one animal it was necessary to pool sera from littermates and generate a litter PTU profile. At PN day 1, the dam's serum PTU concentration was determined, since the eight or fewer pups within a litter could not supply the necessary serum. Likewise, control serum was collected and pooled from 60 day old male animals and PTU added to prepare a standard calibration curve. Even when using freshly prepared PTU, the calibration curves varied by as much as 79%,

yet each curve remained linear over the 2.5 - 7.5 $\mu\text{g/ml}$ concentration range. Initially, the serum PTU concentration of PTU 1 treated animals was measured to determine the effective dose for treatment. The compound 2,6-dichloroquinone-4-chloroimide reacted with thioureylene derivatives to produce a yellow compound. Since this colored complex was preferentially soluble in chloroform it was separated from aqueous solutions for colorimetric analysis. To increase the specificity of the assay, the solution was buffered to pH 8.0. According to Ratliff and coworkers (1972), only the nonphysiological thioureylene compounds are extracted into chloroform at this pH. With the exception of PN day 30, serum PTU levels steadily declined postnatally (Table 1). Previous reports have indicated that PTU levels in excess of 0.18 $\mu\text{g/ml}$ completely inhibited thyroid hormone synthesis in the adult rat (Francis and Rennert, 1980). While the data clearly indicated sufficient PTU levels to prevent T_3 synthesis, other factors may have interfered with the colorimetric assay. Therefore, a more sensitive, reliable and direct T_3 assay was sought.

Most T_3 is transported bound to serum proteins, and concentrations of free T_3 in serum are quite low (pg/ml). However, the free T_3 is the physiologically active form;

Standard Calibration Curve

$A_{435 \text{ nm}}$	[PTU] in $\mu\text{g/ml}$
0.028	2.5
0.045	5.0
0.060	7.5
0.071	10.0
0.090	12.5

PTU Assay

PN day	$A_{435 \text{ nm}}$	[PTU] in $\mu\text{g/ml}$	N
1	0.060	7.63 ± 4.64	28
10	0.033	3.13 ± 0.80	6
20	0.030	2.50 ± 1.34	9
30	0.035	3.31 ± 1.07	10
60	0.018	0.38 ± 0.54	9

Table 1. Serum PTU Concentration.

A standard calibration curve was prepared and serum PTU levels in PTU 1 treated animals determined by interpolation. Values in excess of $0.18 \mu\text{g/ml}$ are required to inhibit thyroid hormone synthesis. While the data, presented as mean \pm sem, indicates values clearly in excess of this, other physiological substances might interfere with the assay.

therefore, the most direct means of assessing the hypothyroid state was to measure serum free T_3 levels.

The thyroid gland in control animals begins to function at embryonic day 18; however, measured free T_3 levels remained low even after birth (Table 2). Both age ($F_{4,40} = 179$) and PTU treatment ($F_{3,40} = 38$) had significant effects on free T_3 levels. As neonate development proceeded, thyroxine concentrations steadily increased, peaked at PN day 30 and then declined. In PTU 1 treated animals, where treatment was administered both prenatally and postnatally until day 10, free T_3 was not detectable at PN day 1 or PN 10. After cessation of PTU treatment, thyroxine synthesis occurred even while it appeared that PTU was present in sufficient quantities to prevent iodide organification. In addition, on PN day 20 the thyroid gland of PTU 1 treated animals appeared to hypersecrete T_3 , since assayable serum free T_3 levels were almost two times that of control values. Thereafter, the T_3 levels were similar to control values.

Since PTU 1 treated animals exhibited recovery of free T_3 serum levels, two other PTU treatment regimens were established. In PTU 2 treated animals, where treatment was initiated at PN day 10 thereby avoiding developmental influences, T_3 levels were significantly reduced from their control counterparts at PN days 30 and 60.

Standard Calibration Curve

% Bound	[free thyroxine] (pg/ml)
100%	0
90%	0.5
78%	1.5
65%	3.0
51%	6.6
32%	21
19%	44

Free T₃ Concentration
mean (in pg/ml) ± sem

PN	Control	N	PTU 1	N	PTU 2	N	PTU 3	N
1	< 0.1	3	< 0.1	3				
10	1.1±0.05	3	< 0.1	2				
20	1.8±0.10	3	3.1±0.14	3	0.4±0.07	4	< 0.1	4
30	3.0±0.13	3	3.0±0.21	4	1.5±0.10	4	< 0.1	1
60	2.5±0.08	3	2.5±0.11	4	1.5±0.12	4		

Table 2. Free T₃ concentrations.

Free T₃ concentrations were measured by radioimmunoassay and values were interpolated from prepared standards. T₃ levels in control animals steadily increase as development proceeds, to plateau at PN day 30. T₃ levels in PTU 1 treated animals were not detectable at PN days 1 and 10. After treatment ceased at PN day 10, the thyroid gland begins to function and initially hypersecrete T₃. Afterwards, the T₃ levels of PTU 1 animals are equivalent to controls. PTU 2 treated animals have significantly reduced T₃ levels at all PN days studied. T₃ levels were not detectable in PTU 3 treated animals which received continual treatment.

Since PTU 3 treated animals received treatment continually until sacrificed, it was not surprising that T_3 was not detectable within assay limits.

From the data presented, it can be seen that the PTU model system developed and used in this study is effective in producing and maintaining the hypothyroid state. PTU 1 treatment produced a neonatal hypothyroid state which allows evaluation of T_3 's role in early postnatal cerebellar development. PTU 2 treatment partially suppressed T_3 levels which demonstrates that PTU is somewhat effective in pubertal and adult rats at suppressing T_3 . PTU 3 treatment demonstrated the effect of long-term deprivation of T_3 on the rat. With the establishment of the hypothyroid state via PTU treatment, molecular investigations of the synthesis and regulation for apolipoprotein E (apo E) and transferrin (T_f) were undertaken.

Cerebellar *In Vitro* Translation Profile

To ascertain the types of proteins synthesized within the cerebellum, a total protein profile was generated by *in vitro* translation of Poly A⁺ RNA in a micrococcal nuclease treated reticulocyte lysate system. After synthesis, protein profiles were prepared by electrophoretic separation of proteins by molecular weight on polyacrylamide gels contain-

ing SDS. Since equal amounts of incorporated counts were loaded on each lane, band intensities could be compared. The two parameters investigated were the developmental expression of cerebellar proteins and the alterations in protein synthesis induced by the hypothyroid state.

It was first necessary to verify that subcutaneous administration of 0.5 N NaOH titrated to pH 10.0 (vehicle for PTU 1 treatment) did not influence the protein profiles obtained from Poly A⁺ translatable RNA (Figure 44). The cerebellar protein profile of untreated (control) and vehicle treated animals appeared similar, with some bands being accentuated at PN days 1, 10, 20, when compared to 30 and 60 days. Since both profiles exhibited enhanced ³⁵S-met incorporation into specific protein bands during development, it was assumed that the alkaline vehicle had not affected the developmental pattern of cerebellar *in vitro* translation.

The cerebellar protein profile for PTU 1 treated animals appeared to have large numbers of proteins influenced by the lack of thyroid hormone (Figure 45). Radioactive amino acid incorporation into specific protein bands appeared reduced at PN day 1 and 10, correlating with the decreased T₃ concentrations. It is not likely that this phenomenon is the result of the translation system, since proteins of varying molecular masses over the entire range

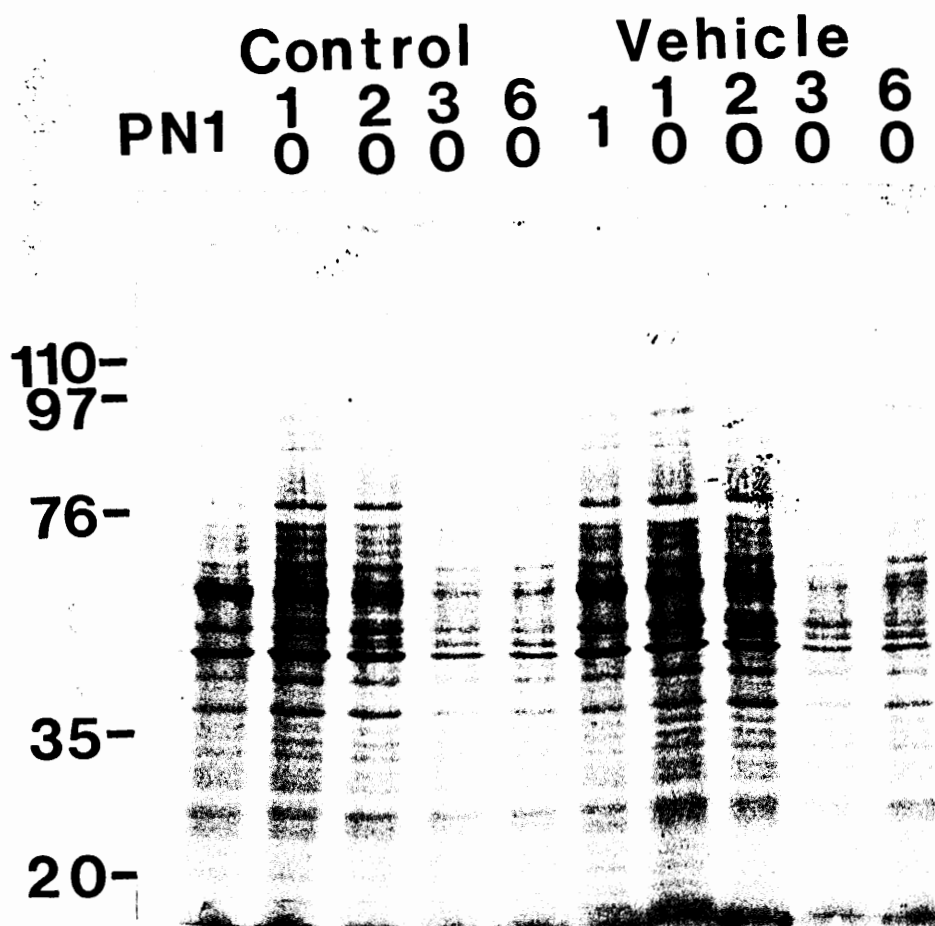


Figure 44. Vehicle treated cerebellar protein profile.
³⁵S-met incorporation appears more prominent at the early developmental stages (PN days 1, 10 and 20). Since the protein profile for vehicle treated tissue resembled control tissue, it can be assumed that subcutaneous injections of 0.5 N NaOH titrated to pH 10.0 has no major readily observable effect on cerebellar protein synthesis. Each lane represents 1×10^5 cpm *in vitro* translated proteins exposed to x-ray film for 48 hr.

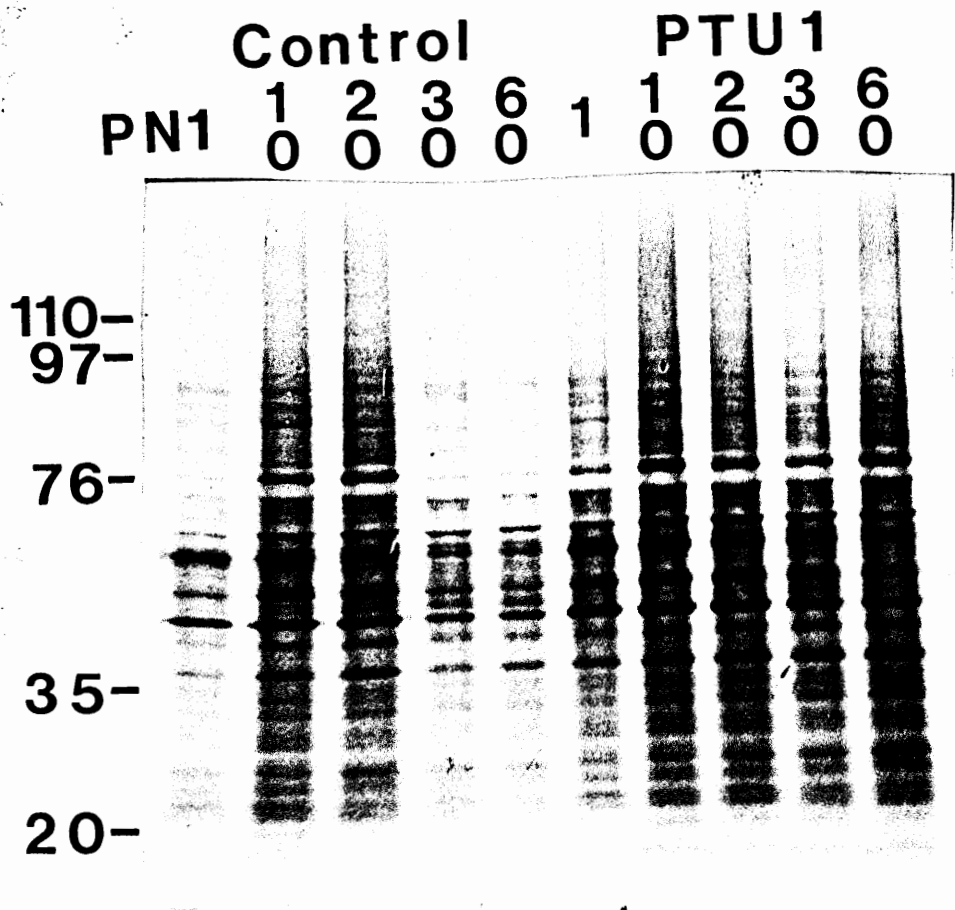


Figure 45. PTU 1 treated cerebellar protein profile.

Prenatal PTU treatment lead to slight decreases in ³⁵S-met incorporation at PN days 1 and 10. At PN day 20, as T₃ synthesis occurred, specific proteins begin to appear. By PN day 60, increased radioactive amino acid incorporation and the presence of previously undetected proteins occurs, particularly at masses of approximately 28, 32, and 85 kDa. Each lane represents 1 x 10⁵ cpm *in vitro* translated proteins exposed to x-ray film for 48 hr.

from 20 to 110 kDa were translated. After PTU treatment ceased at PN day 10, free T_3 serum levels increased and there appeared to be an increase in ^{35}S -met incorporation in a considerable number of proteins. Although free T_3 levels were comparable in control and PTU 1 treated animals at PN days 30 and 60, the protein profile of PTU 1 treated animals appeared to demonstrate increased band intensities as compared to control proteins.

A substantial number of proteins appeared to be affected in the cerebellar protein profile of PTU 2 and PTU 3 treated animals (Figure 46). In PTU 2 treated animals, translated proteins of molecular mass greater than approximately 85 kDa were not readily detectable. The overall control and PTU 2 protein profiles appeared similar at PN day 20. Conversely, the profile of PTU 2 treated animals appeared enhanced over comparable control proteins at PN days 30 and 60. In the most severe PTU treatment, PTU 3, specific band intensities appeared diminished or absent as compared to control and PTU 2 treated profiles, particularly in the 20 - 35 kDa range.

While overall developmental trends were appraised by analysis of a total protein profile, it was difficult to assess the effects of thyroid hormones on specific proteins.

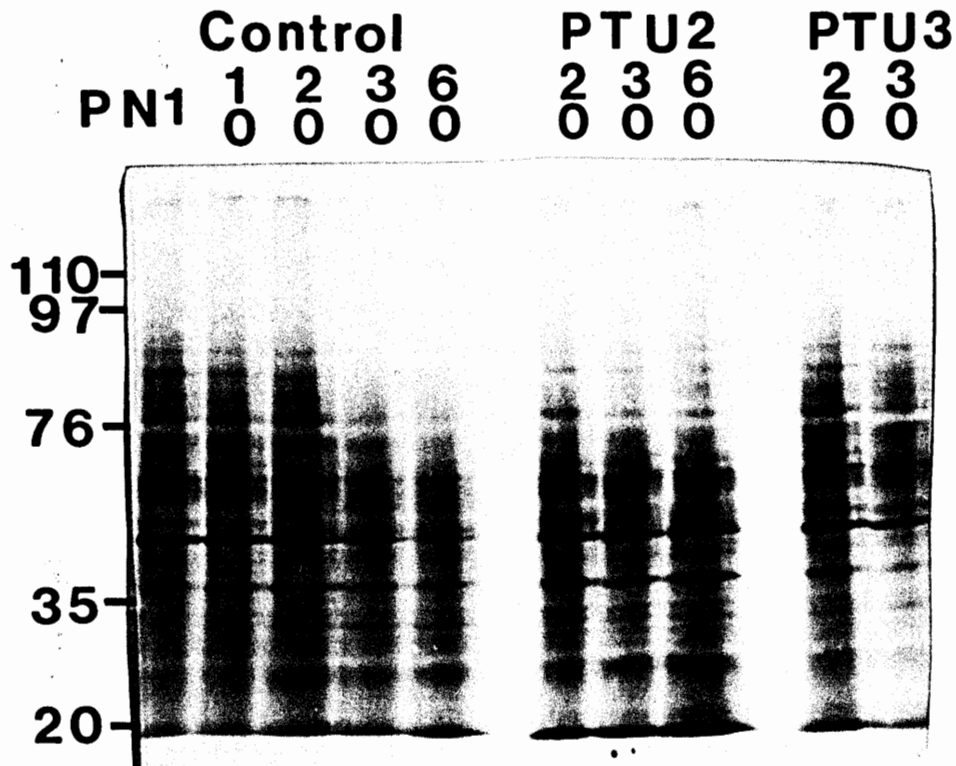


Figure 46. PTU 2 and PTU 3 treated cerebellar protein profile.

³⁵S-met incorporation in certain protein bands between 20 and 50 kDa appear accentuated in the PTU 2 treated profile at PN days 30 and 60 as compared to controls. In comparison, continual PTU treatment (PTU 3) produces declines in both the number and extent of proteins translated *in vitro*, especially of proteins less than 20 kDa and greater than 85 kDa. Each lane represents 1×10^5 cpm *in vitro* translated proteins exposed to x-ray film for 48 hr.

Specific polyclonal antibodies were used to immunoprecipitate apolipoprotein E (apo E) and transferrin (T_f) from the *in vitro* translation mixture. The aim was to characterize the developmental profile for apo E and T_f and determine thyroid hormone's role on the regulation on these proteins within the cerebellum. Both proteins have been shown to be regulated by T_3 in the liver. Apo E increases as a result of PTU treatment, while T_f decreases.

The immunoprecipitation of *in vitro* translated transferrin was hindered by the large amount of nonspecific binding of the lysate mixture to the staph A protein of Pansorbin. To determine background binding to Pansorbin, 2×10^5 cpm reticulocyte lysate, translated in the absence of mRNA, was immunoprecipitated (Figure 47). This profile contained numerous bands in the 50 - 65 kDa range and was used for comparison with cerebellar and liver immunoprecipitated *in vitro* translation products, since both apo E and T_f are known to be hepatically synthesized. Regardless of whether 2 or 4×10^5 cpm cerebellar translation product was used, the apo E protein band was always readily detectable. In order to aid in the detection of transferrin, purified transferrin was used as a molecular weight standard. Since the proteins translated *in vitro* are not posttranslationally modified, transferrin's mass is 74 kDa rather than 76 kDa.

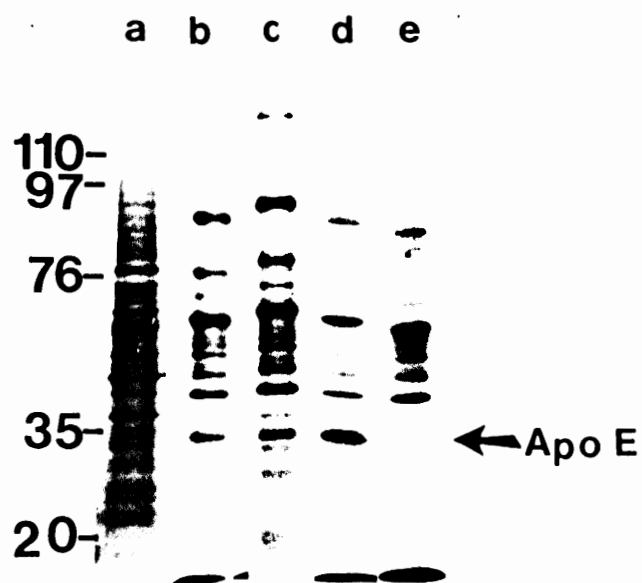


Figure 47. Comparison of total protein profile with immunoprecipitated protein profile.

- a) Total protein profile of PN day 20 control tissue.
- b) Immunoprecipitated profile with 2×10^5 cpm.
- c) Immunoprecipitated profile with 4×10^5 cpm.
- d) Liver immunoprecipitated profile.
- e) Reticulocyte lysate immunoprecipitated profile.

Unfortunately two prominent bands appeared in the reticulocyte profile at this molecular mass. However, a band at 76 kDa appeared in the hepatic profile which was absent in the reticulocyte profile. It was this band that was assumed to be transferrin.

To quantify the amount of proteins immunoprecipitated, densitometric scanning of the autoradiograms was performed. These scans were photocopied, the peak corresponding to the apo E and T_r band was cut out and weighed. Therefore, the data represent a relative comparison of total area under the peak. Since it was necessary to cut the autoradiograms into strips to place on the linear drive apparatus of the scanner, only one autoradiogram was analyzed. The immunoprecipitation experiments were repeated four times and a representative autoradiogram was selected for scanning. Therefore, statistical analysis and comparison is wholly inappropriate since meaningful conclusions cannot be drawn from a single member of the population.

Even though it appeared that PTU treatment had no overall affect on apo E concentrations, interesting developmental trends may be inferred from the immunoprecipitated protein profile (Figure 48). In control tissue, translatable mRNA for apo E increased as development proceeded and plateaued at PN day 20. Afterwards, apo E levels appeared

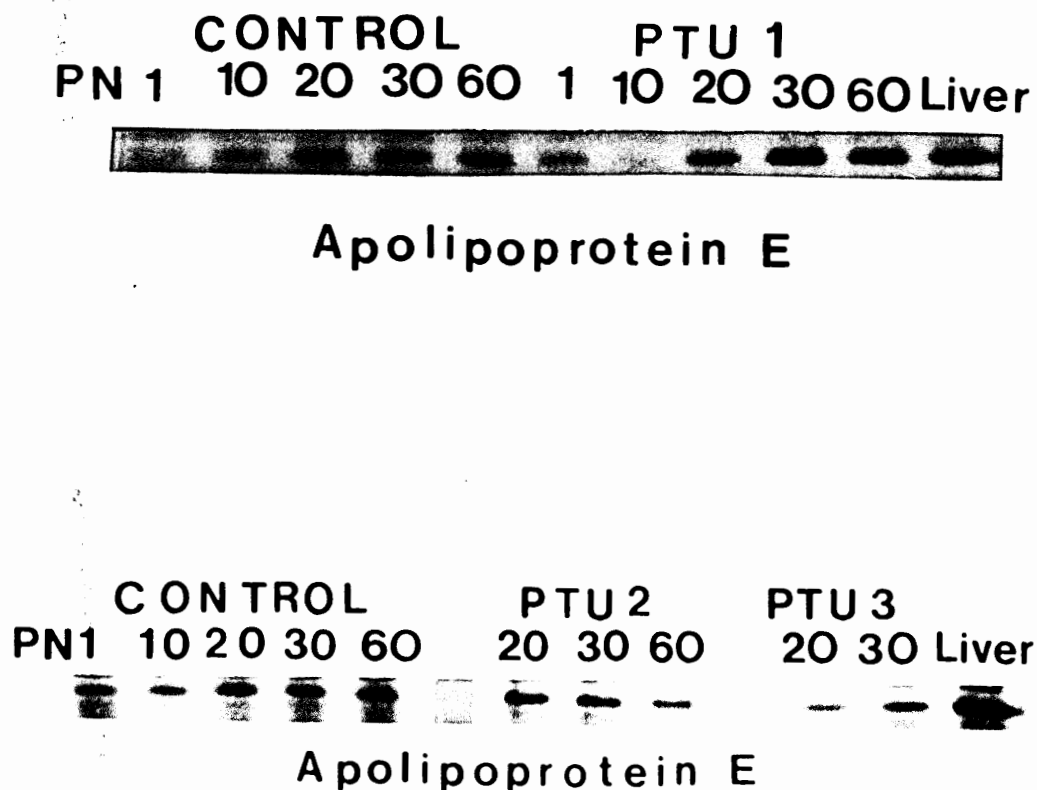


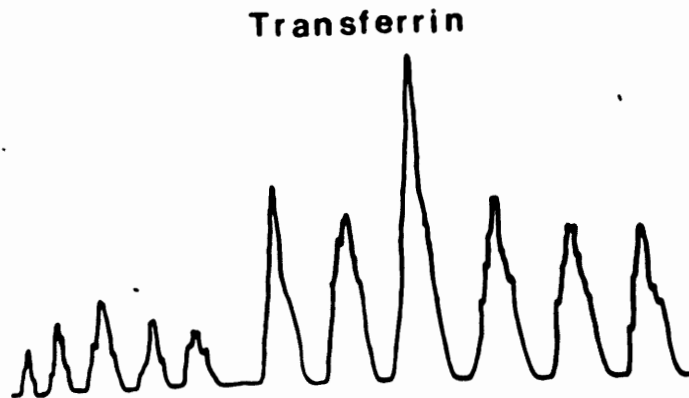
Figure 48. Apolipoprotein E protein profile.

In control tissue, immunoprecipitable apo E levels increase to PN day 20 and then remain relatively constant. In PTU 1 treated tissue, apo E levels decline to PN day 10, then increase to approach the immunoprecipitable hepatic apo E levels at PN day 30. The PTU 1 profile represents 2×10^5 cpm *in vitro* translated proteins exposed to x-ray film for 2 weeks. Immunoprecipitable apo E declines developmentally in PTU 2 and PTU 3 treated tissues. The PTU 2/3 profile represents 4×10^5 cpm proteins exposed for 10 days.

relatively constant. In PTU 1 treated tissue, immunoprecipitable apo E appeared to decline from PN day 1 to PN day 10 as animals were maintained in the hypothyroid state. After the PTU treatment ceased and free T_3 serum levels increased, there appeared to be a large increase in immunoprecipitable apo E. By PN day 30, and continuing to PN day 60, translatable cerebellar apo E mRNA appeared similar to hepatic levels. In PTU 2 treated tissue, apo E levels, as compared to control, appeared 40% greater at PN day 20, similar at PN day 30 and 50% reduced at PN day 60. In PTU 3 treated tissue, apo E levels at PN day 20 appeared similar to control and PTU 2 values. At PN day 30, the apo E concentrations in PTU 3 treated tissue appeared 25% less than both control and PTU 2 values.

Immunoprecipitable T_r concentrations from *in vitro* translation of cerebellar mRNA were so low that it was difficult to depict the autoradiogram bands photographically (Figure 49a). Since the sensitivity of detection for T_r was low using 2×10^5 cpm translation mixture, the experiment was repeated using 4×10^5 cpm (Figure 49b). Even with the use of twice the amount of translation product, the T_r protein bands could not be detected photographically; however, quantitation was made possible by densitometric scanning.

CONTROL PTU 1
 PN1 10 20 30 60 1 10 20 30 60 Liver



CONTROL PTU 2 PTU3
 PN1 10 20 30 60 20 30 60 20 30

Transferrin

Figure 49a. Transferrin protein profile.

The autoradiogram of 2×10^5 cpm *in vitro* translated products exposed to x-ray film for 3 weeks demonstrates low cerebellar T_r levels. Densitometric scanning of the autoradiogram shows that T_r levels in control tissue increases to PN day 20 and then declines. In PTU 1 treated tissue, where free T_3 was present, *in vitro* T_r translation was increased and even greater than that of the liver.

	CONTROL				PTU 2			PTU3	
PN1	10	20	30	60	20	30	60	20	30

Transferrin



Figure 49b. Transferrin protein profile.

Even the use of 4×10^5 cpm *in vitro* translated protein exposed to x-ray film for 3 weeks did not assist the photographic detection of the T_r protein band. Immunoprecipitable T_r was reduced in both PTU 2 and PTU 3 treated tissue. It was necessary to enlarge all scans to depict the diminished PTU 2 and PTU 3 peaks.

From the gels analyzed, T_f values were one-tenth that of cerebellar apo E or hepatic T_f levels. In control tissue, T_f protein levels appeared to increase as development proceeded, peaked at PN day 20 and then declined thereafter. Like apo E, T_f proteins levels in PTU 1 treated tissue exhibited a large increase of immunoprecipitable T_f as free T_3 levels increased. Conversely, T_f levels appeared reduced in both PTU 2 and PTU 3 tissue, as compared to controls, at all postnatal stages investigated. Therefore, unlike apo E, the *in vitro* synthesis of T_f appeared to be affected by PTU treatment and the hypothyroid state.

Polymerase Chain Reaction Amplification

In order to perform northern hybridization, specific cDNA probes are required. These cDNAs must be isolated from the host vector's nucleic acids and labelled to provide detectable markers for the presence of expressed RNA sequences in cerebellar tissue via hybridization. Polymerase chain reaction (PCR), which amplifies the amount of cDNA, was used to increase the available quantity of the specific cDNAs, the cDNA was then radioactively labelled by random priming.

The initial step of PCR involved denaturation of the two cDNA strands. Since the cDNA was GC tailed for inser-

tion into the host vector, and the cDNA itself is GC rich (68% GC content), the standard PCR denaturation protocol was insufficient. Longer periods of denaturation and/or higher denaturation temperatures either reduced or completely eliminated polymerase activity. Prolonged preheating of the template in the absence of enzyme aided amplification and the use of 4.0% DMSO proved most beneficial in the initial amplification (Figure 50). This PCR product was then reamplified. The best amplification was obtained when the initial apo E PCR product, amplified in the presence of DMSO, was reamplified in the absence of DMSO. Transferrin amplification and subsequent reamplification did not require the addition of DMSO.

Northern Hybridization

The PCR amplified cDNA products were radioactively labelled by random priming to specific activities of 1×10^8 cpm/ μ g DNA, with the percent of $^{32}\text{P}[\alpha \text{ dCTP}]$ incorporation ranging from 28 - 52%. Electrophoresis of varying amounts of RNA was attempted, including 5 μ g poly A⁺ RNA, and 10, 15 and 20 μ g total RNA. Ten micrograms total RNA provided the best results with the apo E probe (Figure 51). Like the immunoprecipitation experiments, the northern hybridization experiments were repeated, but only one representative

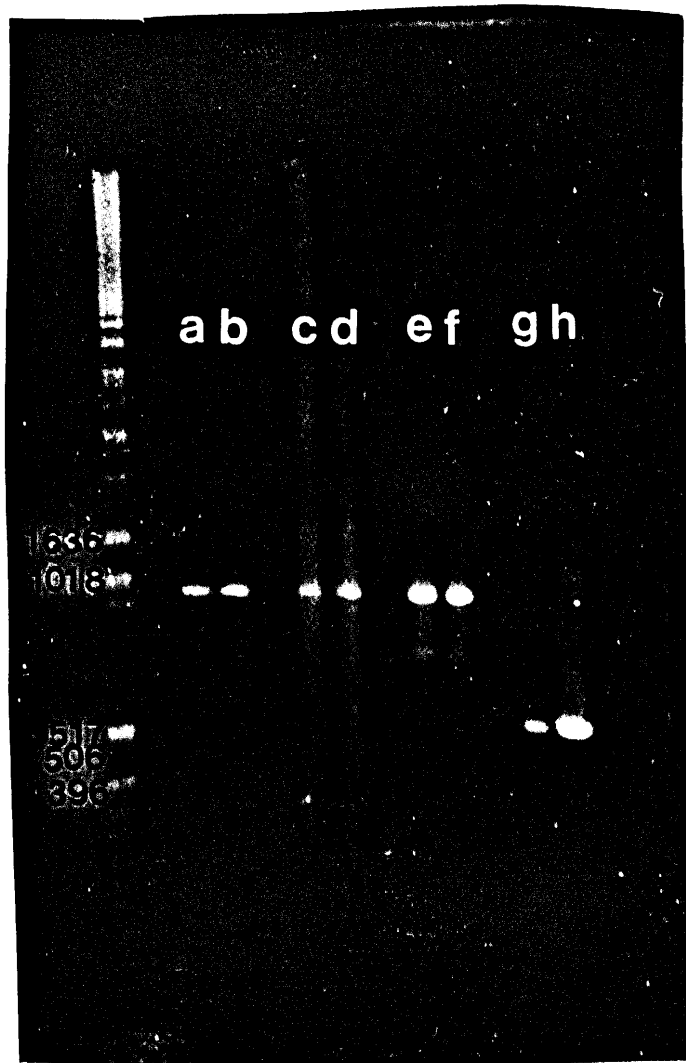


Figure 50. Electrophoresis of PCR amplified products.

To determine size and purity of PCR amplified products, 8 μ l PCR product was electrophoresed in a 1.0% agarose gel, stained with ethidium bromide and nucleic acids visualized using UV transmission.

- a) apo E amplified without the addition of DMSO
- b) apo E amplified with the addition of 4.0% DMSO
- c) apo E amplified without DMSO, reamplified without DMSO
- d) apo E amplified without DMSO, reamplified with 4.0% DMSO
- e) apo E amplified with DMSO, reamplified without DMSO
- f) apo E amplified with DMSO, reamplified with 4.0% DMSO
- g) initial transferrin amplification
- h) transferrin reamplified

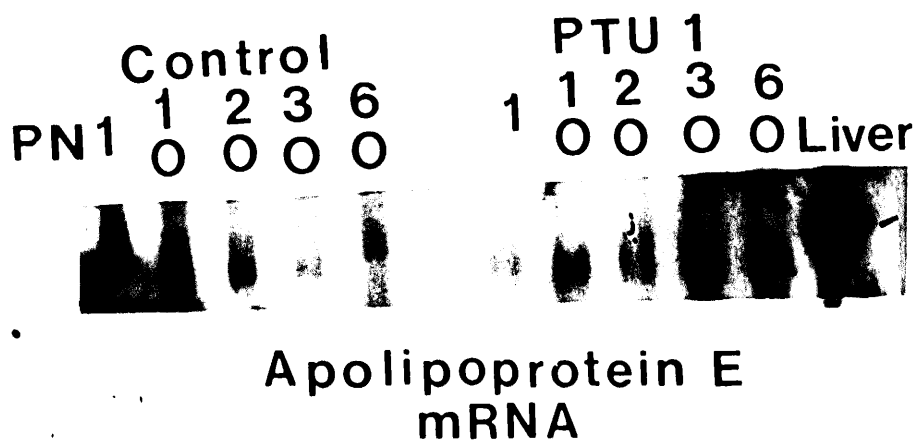


Figure 51. Northern hybridization of apo E mRNA.

In control tissue, apo E mRNA levels decline as development proceeds. In PTU 1 treated tissue, apo E mRNA levels are low during PTU treatment, but increase with increased free T_3 in serum at PN day 20. Each lane represents 10 μg total RNA hybridized with 1×10^8 cpm/ μg apo E cDNA probe and exposed to x-ray film for 24 hours.

autoradiogram was scanned for quantitation. Apo E mRNA levels appeared to decline as development proceeded in control tissue. In PTU 1 treated tissue, apo E mRNA appeared reduced during the period of PTU administration. Thereafter, free T_3 in serum increased and apo E mRNA concentrations appeared to increase, although not nearly to those levels found in the liver.

The *in vitro* translatable T_r protein was present in very small amount when mRNA from cerebellar tissue was used; therefore, it was anticipated that T_r mRNA levels would also be reduced. Therefore, northern hybridization for transferrin was performed with 15 μ g total RNA (Figure 52). In control tissue, the greatest mRNA level appeared at PN day 20 and thereafter levels appeared to decline. Even with longer exposure of the hybridized blot to x-ray film (up to 7 days), T_r mRNA could not be detected at PN day 1. Like apo E, transferrin mRNA levels in PTU 1 treated tissue appeared reduced while animals received PTU treatment. At PN day 20, when serum levels of T_3 were elevated, the transferrin mRNA concentration appeared to increase dramatically.

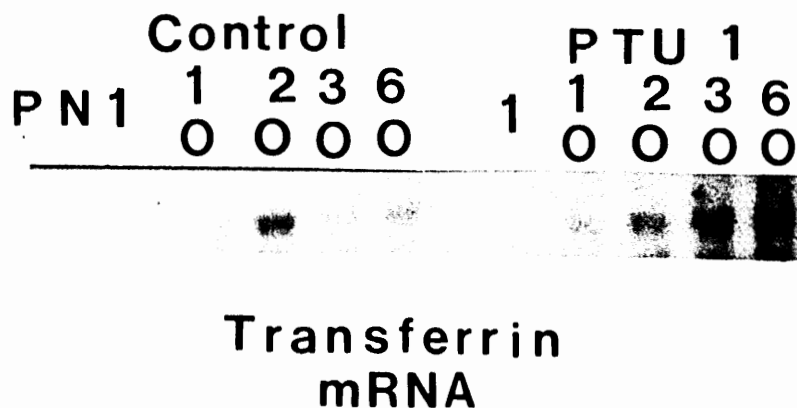


Figure 52. Northern hybridization of transferrin mRNA.

Like T_f protein levels in the cerebellum, T_f mRNA levels are low. In control tissue, T_f mRNA appears greatest at PN day 20. In PTU 1 treated tissue, T_f levels are low during PTU treatment. With free T_3 present, T_f mRNA levels increase dramatically. Each lane represents 15 μg total RNA, hybridized with 1×10^8 cpm/ μg T_f cDNA probe and exposed for 72 hours.

CHAPTER IV

DISCUSSION

It is clear from the data presented that propylthiouracil (PTU) treatment during critical developmental periods severely alters neurogenesis, cellular migration and synaptogenesis within the cerebellar cortex. The investigation of thyroid hormone effects on the availability of apo E and T_f mRNA's for *in vitro* translation was constrained by the fact that thyroid hormones are required for normal cerebellar development. To distinguish between thyroid hormone's effect on eukaryotic development and its effect on cerebellar gene expression, PTU was administered only postnatally. Legrand (1967) administered PTU at various embryonic stages and found no variation in cerebellar histology regardless of the extent of embryonic treatment. Therefore, thyroid hormones did not appear to affect embryonic development within the cerebellum. This is not surprising, because most cerebellar development in rats occurs postnatally. Since most cerebellar differentiation has occurred by PN day 10, administration of PTU after this stage should avoid developmental effects of PTU treatment. Therefore, 0.1% PTU in drinking water was administered from PN day 10 to sacrifice (PTU 2). Unfortunately, even postnatal PTU administration

produced altered cortical stratification. Therefore, the use of the cerebellar model, which requires thyroid hormone for normal development, to investigate thyroid hormone effects on gene regulation is tenuous at best.

PTU is transported to and concentrated within the thyroid gland, where it interacts with and is degraded by thyroid peroxidase. The balance between PTU administration and degradation determines PTU levels within the thyroid gland. Since PTU's inhibition of thyroid hormone synthesis is reversible, the extent of inhibition is directly proportional to the intrathyroidal PTU concentration, which, in turn, is dependent upon plasma concentrations. Francis and Rennert (1980) reported that serum PTU concentrations in excess of 0.18 $\mu\text{g/ml}$ were required to completely inhibit thyroid hormone synthesis. The dose administered to PTU 1 treated animals was ten-fold higher than that administered by Francis and Rennert. Therefore, it was expected that serum PTU levels would also be ten times greater than the 0.18 $\mu\text{g/ml}$ required to inhibit thyroid hormone synthesis. Even though PTU levels were in excess of 0.18 $\mu\text{g/ml}$, the morphological and histological features of hypothyroidism diminished at the later developmental stages (PN days 30 and 60). Either the critical period of thyroid hormone action

on these features had passed or other factors were interfering with the PTU assay. Because PTU is oxidized by the enzyme thyroid peroxidase (Lindsay et al., 1978), this PTU assay might detect PTU oxidation products, as well as active PTU. In addition, there was a precipitous drop in assay sensitivity at low PTU concentrations, as demonstrated by the PN day 60 concentration of 0.38 $\mu\text{g}/\text{ml}$ when compared to other PN levels. This drop is probably due to the assay itself since each calibration curve demonstrated diminished sensitivity at low PTU concentrations.

An alternate means of detecting PTU is high-performance liquid chromatography (HPLC). Rosseel and Lefebvre (1990) reported the detection limit of 50 ng/ml in only 100 μl of plasma by a HPLC method using ion-pair reversed-phase chromatography and UV detection at 300 nm. As with the PTU assay of Ratliff et al., it is possible, although less likely since HPLC is more sensitive than colorimetric analysis, that PTU oxidation products would also be detected. In addition, the authors presented data on PTU stability. PTU stability was maintained for at least 14 days at $-20\text{ }^{\circ}\text{C}$ and at least one month at $-80\text{ }^{\circ}\text{C}$. Some of the serum samples used throughout this experiment were stored at $-20\text{ }^{\circ}\text{C}$ for

longer periods of times. This might explain the great variability obtained with the PTU assay utilized.

While in theory the determination of PTU concentrations may be an effective means of gauging the efficacy of treatment, in practice it is more appropriate to measure thyroid hormone levels directly by radioimmunoassay (RIA). RIA has but one limitation, highly lipemic serum samples may yield erroneous results. Since hypothyroidism is associated with hyperlipidemia one might question the accuracy of this assay. While nonesterified fatty acids have no effect on the assay, no data are available for other lipid components which might interfere with the assay. Even with this flaw, it would appear that the free T_3 radioimmunoassay is the most direct and appropriate means of determining the establishment of the hypothyroid state.

The data presented in Table 2, show the thyroid hormone status of the three PTU treatment groups. Thyroid hormone levels gradually increased, until a surge of synthesis occurred shortly after parturition (Griffin and Ojeda, 1988). After birth, neonates are independent of maternal thermoregulation and must establish an autonomous metabolism. Following this initial postnatal surge, thyroid hormone levels declined rapidly, so that when serum samples were

obtained at PN day 1, T_3 was not detectable within the limits of the radioimmunoassay. Afterwards, T_3 levels increased as development proceeded and reached a plateau at PN day 30. Since samples were not obtained at intermediate stages, perhaps the T_3 peak actually occurred elsewhere during development.

In PTU 1 treated animals, T_3 was not detected during the period of PTU treatment. However, by PN day 20 elevated serum T_3 levels were probably due to a substantial increase in T_3 synthesis. Elevated thyrotropin concentrations in the presence of sufficient PTU maintains follicular hypertrophy (Griffin and Ojeda, 1988). If indeed the locus of PTU action is iodination, there conceivably could have been a burst of iodide organification of thyroglobulin once PTU levels declined. This could then result in the hypersecretion of thyroid hormones, until the hypothalamic-pituitary-follicular feedback system became regulated. This would explain why at PN days 30 and 60 the T_3 concentrations in control and PTU 1 treated animals were equivalent.

In PTU 2 animals, T_3 concentrations were significantly reduced from control counterparts at all developmental stages studied. It was anticipated that T_3 would decline with prolonged PTU treatment, but the data indicated other-

wise. Although this reduction was not as large as anticipated, it was significant. Since serum T_3 was not completely absent, caution must be exercised in drawing conclusions concerning the role of thyroid hormones on the regulation of apo E and T_f expression in PTU 2 treated animals. It is not surprising that T_3 was not detected in PTU 3 treated animals, since they were continually exposed to PTU treatment.

While statistics indicated that the hypothyroid state was established in both PTU 2 and PTU 3 animals, it was clearly demonstrated that subcutaneous PTU administration was superior to oral administration since serum free T_3 levels were not detectable. Even though PTU may be absorbed via the gastrointestinal tract, its absorption rate might be limited by its solubility. However, once in solution, the PTU is readily available for absorption into subcutaneous capillaries. Unabsorbed orally administered PTU would probably pass through the gastrointestinal tract, but subcutaneously administered PTU would have to be eliminated renally. In addition, if the PTU solution is lipid soluble, it might be stored in subcutaneous adipose tissue. This indeed might explain the increased toxicity of subcutaneously administered PTU.

In light of the caveats concerning the observed serum PTU and T_3 levels discussed above, it is now possible to analyze the morphological, histological and molecular phenomena observed. The gross morphological features of only PTU 1 treated animals were observed. Although most of the early signs of cretinism disappeared as recovery from the hypothyroid state occurred, skeletal maturation remained affected. Thyroid hormones are known to play a permissive role in the regulation of a number of hormonal systems, so perhaps other hormones were involved in the morphological alterations observed. For example, the retardation in skeletal development could be the result of decreased somatotropin, since both somatotropin mRNA (Wood et al., 1987) and protein (Oppenheimer and Samuels, 1983) concentrations are decreased in the hypothyroid state. It has been demonstrated that somatotropin induces insulin-like growth factor in culture (Ceda et al., 1985) and that the number of follicular insulin-like growth factor receptors is increased following PTU treatment (Polychronakos et al., 1986). Increased follicular insulin-like growth factor binding could explain the thyrotropin-mediated hyperplasia of the thyroid gland observed in PTU treatment. Whereas the skeletal alterations may be mediated by somatotropin, the alter-

ations in hair and nails, which are both epidermal derivatives, may be regulated by epidermal growth factor. In culture, epidermal growth factor was shown to modulate thyroid growth and function (Westermarck et al., 1983). Perhaps a reciprocal relationship exists, whereby thyroid hormones regulate epidermal growth factor. Therefore, PTU treatment may not only alter thyroid function, but may also involve complex, interrelated hormonal systems.

There clearly was delayed development as evidenced by altered morphology, but a more accurate assessment required the quantitation of these differences. Generally, body, brain and cerebellum weights were reduced in PTU treated animals, regardless of the treatment type. The reduction in body weight observed in PTU 1 treated animals may have been due to the dam's inability to provide sufficient milk for her pups. Hypothyroid pups were not weaned until 30 days of age, and even though pups had access to an adequate food supply, they probably relied more heavily on maternal nutrition due to their decreased motor activity. Once weaned, the animals must actively procure food for proper nutrition. Therefore, the weight gain observed at the later developmental stages in PTU 1 treated animals was probably due to increased food consumption and/or thyroid hormone recovery.

It was suspected that the reduction in brain and cerebellum weights was the result of the overall smaller body size in PTU treated animals. This possibility was eliminated by calculating weight ratios of brain:body and cerebellum:brain. Because these ratios varied considerably with the treatment type and developmental stage, it was concluded that thyroid hormones exert their action at specific developmental stages. Moreover, the basic trend also demonstrated that the reduced brain and cerebellum weights were not just the result of decreased body size. Even in PTU 1 treated animals, thyroid hormones synthesized at PN day 20 could not overcome the developmental alterations induced at earlier stages.

The role thyroid hormones play in cerebellar development has been well characterized. The intent of this project was to administer the goitrogen propylthiouracil via different routes and at various developmental stages to investigate developmental effects on gene regulation. Histological observations were simply used to replicate prior neural effects of the presumed hypothyroid state.

As previously reported, delayed granule cell proliferation and migration associated with hypothyroidism results in altered cortical stratification (Legrand, 1967; Nicholson

and Altman, 1972b). While it was anticipated that prenatal PTU administration would result in prolonged retention of the external granule layer (Egl), it was surprising that postnatally administered PTU produced similar results, although less blatant. Since the establishment of synapses within the molecular and internal granule layers requires the migration of granule cells from the Egl, both layers are affected by PTU treatment (Lauder, 1977).

As granule cells migrate from the Egl, their axons bifurcate and emit tangentially directed parallel fibers which establish synaptic contact with the Purkinje cells' dendritic arbors. Previous reports have attributed the heterologous synapses generated by the hypothyroid state to retarded granule cell mobility (Legrand, 1967; Lauder, 1977). It is possible that thyroxine regulates the growth of parallel fibers, not the mobility of granule cells. Therefore, the granule cell migration rate may depend on parallel fiber growth rate and the later, in turn, might be regulated by cerebellar water content. By subjective observation upon dissection, it appeared that the water content in PTU treated animals decreased more slowly. While this could allow for increased plasticity and the ability to correct for some of the abnormal synapses, it cannot explain

retarded parallel fiber growth. Alternatively, myelination of parallel fibers could regulate their growth rate. The extent of myelination is inversely proportional to water content (Balázs et al., 1969). The greater water content in hypothyroid tissue could result in decreased myelination and retarded parallel fiber growth. This would affect the molecular layer only at the early developmental stages, when the water content is greater. At PN day 20, all PTU treatment types exhibited reduced molecular layers. As water content diminished and myelination was established, parallel fiber growth could occur. Perhaps due to greater water retention in PTU 3 treated animals, the molecular layer remained reduced throughout development.

The internal granule layer (Igl) appeared to be affected by PTU to a greater extent than the molecular layer. Granule cells die when they fail to establish appropriate synapses during their migration. At PN day 20, the Igl's in control, PTU 1, and PTU 2 tissues were equivalent. This could be due to the retention of the Egl in PTU treated tissue at this stage. Afterwards, the diminished Igl in PTU treated tissue probably was due to granule cell death.

In addition to altered cortical stratification, synaptogenesis was affected by PTU treatment. The principle

synapsis within the cerebellar cortex is that between granule and Purkinje cells. It has been reported that due to delayed granule cell migration and the consequent unavailability of their primary targets, Purkinje cells form heterologous synapses (Nicholson and Altman, 1972 a & b). These anomalous synapses severely alter Purkinje cell somal morphology. Regardless of the type of PTU treatment, the Form PE was reduced and the somal area greater than that of controls. In addition, these characteristics remained affected throughout development.

Another striking feature observed in PTU treated tissue was the failure of Purkinje cell somata to establish an isoplanar cell layer at the junction of the molecular and internal granule cell layers. Putative Purkinje cell somata could be found deep within the Igl. Another cell type located within the Igl is the Golgi type II cell. Cell specific markers should be used to immunocytochemically characterize the nature of this unknown cell type. Purkinje cells may be identified by the proteins cerebellin (Slemmons et al., 1985), calbindin (Jande et al., 1981), and PEP-19 (Ziai et al., 1988). On the other hand, Golgi cells are recognized by binding of the monoclonal antibody Rat-303 (Hockfield, 1987) and both enkephalin immunoreactive prod-

ucts (Schulman et al., 1981) and proenkephalin mRNA (Shivers et al., 1986). If indeed the uncharacterized cell is determined to be a Purkinje cell, it would mean that Purkinje cell, as well as granule cell, migration is affected by thyroid hormones.

Once the establishment of the hypothyroid state was verified biochemically, molecular studies were undertaken. The developmental regulation of apolipoprotein E (apo E) and transferrin (T_f) mRNA's produced by the cerebellum was considered.

The first molecular procedure involved the extraction of total RNA using the guanidinium thiocyanate method of Chirgwin et al. (1979). This protocol is widely used, because the yield and quality of extracted RNA is quite high and RNAase activity is negligible. Unfortunately, this method was ineffective in isolating RNA from the cerebellum. At the final stage of extraction, RNA is solubilized in water for separation from DNA by differential rates of hydration. However, some component(s) of the cerebellar RNA preparation prevented this. It was hypothesized that the solubility was affected by the high lipid content within the nervous tissue. Various detergents were added to the initial homogenization solution or to the final RNA pellet, but

to no avail, suggesting that lipids were not responsible for the lack of solubility. A small sample of the RNA pellet was electrophoresed on a SDS polyacrylamide gel and a large protein complex was observed. Evidently the guanidine hydrochloride and guanidinium thiocyanate were ineffective in dissociating some proteins from the RNA. Guanidinium extraction followed by centrifugation through a cesium chloride gradient (Sambrook et al., 1989) was also attempted without success. Finally, a phenol:chloroform method of RNA extraction was selected. This procedure has several drawbacks. First, phenol is a rather slow denaturant and, unlike guanidinium, allows for greater RNase action. Enzymatic degradation of RNA was minimized by homogenization of frozen tissue and initial extraction on ice. Second, phenol must be saturated for phase separation to occur. Saturation with buffer, rather than water, reduces the isolation of RNA into the aqueous phase (personal communication, Dr. Wojciech Kedzierski, University of Texas Southwestern Medical Center, Department of Obstetrics and Gynecology). Third, buffer saturated phenol results in decreased yields, but its pH is critical, since it is known that phenol at an acidic pH can trap poly A⁺ RNA (Wallace, 1987). Finally, unlike the guanidinium methods which result

in the isolation of total RNA from DNA, phenol:chloroform extracts both nucleic acids simultaneously. However, sodium acetate (pH 6.0) washes are successful at eliminating most, but not all, DNA. The best means of RNA extraction would incorporate both phenol:chloroform and guanidinium thiocyanate.

Following total RNA extraction, oligo (dT) affinity chromatography was used to isolate poly A⁺ RNA. To increase the yield and purity of poly A⁺ RNA isolation three factors were manipulated. First, the binding capacity of the oligo (dT) type used must be determined. One gram of oligo (dT) type 3 has a binding capacity of approximately the amount of poly A⁺ RNA found in about 1,000 A_{260nm} of total cellular RNA. The use of excess oligo (dT) does not increase mRNA yield. Second, when preparing the affinity column, the bed volume width to height ratio is important. To provide the most efficient flow and resistance, the bed height should be two to three times the bed width. Finally, poly A⁺ RNA binding is affected by salt concentration. Various salt concentrations were attempted before 0.2 M NaCl was selected. Lower salt concentrations resulted in decreased mRNA yields, while contaminating ribosomal RNA remained at higher salt concentrations.

Once mRNA had been isolated, a total protein profile was generated by *in vitro* translation to assess the overall developmental trend of *in vitro* translatable mRNA levels in control, vehicle (0.5 N NaOH titrated to pH 10.0) treated, and PTU treated tissue. In order to maintain a sufficient female breeding pool, male animals were selected for this study. Although cerebellum development appeared equivalent in both sexes, it was not known whether gender influenced the expression of specific cerebellar proteins. Recently, Litteria (1990) identified thirteen proteins in adult rats influenced by gender and/or gonadectomy, with five of these influenced by both. Since the cerebellum is not known to play a role in reproduction, the author suggested that gonadal steroids may have metabolic actions other than those associated with sexual activity. Therefore, even though none of these proteins has been identified as apo E or transferrin, the selection of male animals proved fortuitous.

It can clearly be seen that there were significant changes in the profiles during development and as a consequence of PTU treatment. Radioactive amino acid incorporation into specific proteins appeared accentuated early in the development of control cerebellar tissue. The data

indicated that the increase in *in vitro* protein synthesis, due to an increase in translatable mRNA's, was correlated with postnatal cerebellar maturation. As cerebellar neuronal and glial cell populations differentiated and established their appropriate patterns of connectivity, genes apparently were differentially expressed, thus changing the pattern of *in vitro* translated products. A potential correlate, oligodendrocyte differentiation is associated with the onset of myelination and activation of genes coding for myelin associated proteins, particularly myelin basic protein. The synthesis of these proteins is maximal between PN days 10 and 20 (Almazan et al., 1985). At PN day 20, cerebellar differentiation is largely complete. Afterwards, the total protein profile as well as ³⁵S-met incorporation into specific proteins appeared reduced. This altered protein profile may not necessarily be due to a decreased amount of cerebellar mRNA at the later developmental stages, but due to secondary mRNA effects. For example, one explanation for this phenomenon is that later in development the mRNA becomes altered (e.g. methylation, secondary structure), thus increasing the difficulty of *in vitro* translation in the reticulocyte system. When considering the translation of mRNA *in vitro*, two important assumptions must be borne in

mind. First, it is assumed that the translational efficiency of all mRNAs is equal. In reality, this is highly unlikely. Second, in order to analyze radioactive amino acid incorporation into the proteins synthesized, it is assumed that all proteins contain approximately the same numbers of methionine moieties. With the exception of either methionine rich or methionine depleted (e.g. histones) proteins, this is probably an accurate assumption. Therefore, TCA precipitation of a translation mixture aliquot followed by liquid scintillation counting can be used as a means of quantitating and comparing *in vitro* protein syntheses. These data are required to assure equal loading of incorporated counts into translated proteins during electrophoresis to allow for developmental and treatment comparisons.

Since the vehicle treated protein profile appeared similar to the control profile, it was assumed that subcutaneous injection of NaOH had no effect on cerebellar translatable mRNAs. When using *in vitro* translation, the amounts of specific proteins synthesized by the reticulocyte lysate are directly proportional to their respective mRNA contents within the cerebellum. The subcutaneously administered sodium hydroxide would have had to be transported from the plasma and cross the blood brain barrier in order to

affect cerebellar mRNA content. In actuality, since the 0.5 N NaOH was titrated to pH 10.0 with HCl, the PTU was administered in an alkaline saline solution. A solution of pH 10.0 has a pOH of 4.0, and is 1×10^{-4} N NaOH, not 0.5 N NaOH. Therefore, most of the solution is NaCl and it seems unlikely that this vehicle would alter the mRNA concentration, and thereby alter protein synthesis *in vitro*. However, the stress associated with repeated injections might alter related hormonal systems which might have secondary effects. While it appeared that the vehicle did not affect the overall protein profile, subtle undetectable changes in specific proteins may have occurred. Therefore, it was inappropriate that subsequent comparisons were conducted with control (untreated) animals.

The protein profile generated from PTU 1 treated tissue gave the first indication that thyroxine synthesis might have been initiated after PTU treatment ceased at PN day 10. In addition to an overall apparent increase in ^{35}S -met incorporation at PN days 20, 30 and 60, previously undetected proteins appeared. It was expected that the gene products regulated by thyroid hormones would be diminished in the hypothyroid state compared to controls, not enhanced. However, it was discovered that thyroid hormone was present

at PN day 20 in PTU 1 treated animals, and by PN day 30 T_3 levels were comparable to control values, yet PTU 1 protein profile appeared different. The increased *in vitro* translation observed in PTU 1 tissue at PN days 30 and 60 might have been due to the effect of thyroid hormone on differential gene expression, recovery from the delayed cerebellar developmental state, or an overall effect of increased metabolism. The early effects of PTU treatment are less clear. However, it was demonstrated that PTU treatment, and its resultant effect on thyroid hormone concentrations, did not equally affect all mRNA's synthesized within the cerebellum. The presence and intensity of other numerous protein bands in the profile appeared unaffected either during the time course of PTU treatment or after the initiation of thyroid hormone synthesis.

The protein profile of PTU 2 and PTU 3 treated tissue gave an improved indication of the affect of thyroid hormone deprivation on translatable cerebellar mRNA. Before analyzing this protein profile, it must be noted that the RNA from control animals was extracted nine months prior to the extraction from PTU 2 and PTU 3 treated animals. Aliquots were stored at -80°C and were not thawed and refrozen more than four times. The integrity of the control mRNA appeared

to be maintained, since the control protein profile generated concurrently with the PTU 2 and PTU 3 mRNA was similar to previously generated control profiles in the types and extent of mRNA's translated. Due to time constraints, an attempt was made to translate total RNA, thereby avoiding the affinity chromatography required to isolate poly A⁺ RNA. Whether the mRNAs represented too small a proportion of the total available RNA or the ribosomal RNA components were inhibitory is unknown. Therefore, poly A⁺ RNA was isolated and translated as before. It was noted that the translational efficiency of both PTU 2 and PTU 3 mRNA was enhanced (greater incorporation of ³⁵S-met). Previous translations resulted in an average incorporation of 2.5×10^4 cpm/ μ l, while PTU 2 and PTU 3 translations averaged 4.8×10^4 cpm/ μ l, when using equivalent mRNA concentrations. The enhanced incorporation might be due to two factors. First, newly extracted mRNA which had never been frozen was utilized. Second, ³⁵S-met from New England Nuclear (NEN), which contains a Tricine buffering system, rather than that from ICN was used. While either factor could account for this effect, both factors together may be involved in the two-fold increase in incorporation. This clearly demonstrates the need for standardization of protein loading. Since all

protein profiles contained 1×10^5 cpm per lane, comparison to control and all other PTU treatments was possible. Although PTU 2 treated animals contained decreased concentrations of free T_3 , cerebellar translated products from isolated mRNA did not appear to be altered in either the number of proteins translated or the extent of ^{35}S -met incorporation. In contrast to the overall apparent reduction in the protein profile at PN day 20, ^{35}S -met incorporation was greater in certain proteins at PN days 30 and 60. Although T_3 levels were significantly reduced in PTU 2 animals, T_3 was not completely absent. Perhaps the low concentration of T_3 was sufficient to induce synthesis of specific mRNA's from genes regulated by T_3 . The best indication of thyroid hormone's role in cerebellar protein synthesis was demonstrated in PTU 3 tissue. Throughout development these animals lacked detectable T_3 levels. The most striking effect was observed in the one remaining animal at PN day 30. Of the approximately fifty protein bands observed, several proteins in both the lower (below 20 kDa) and upper (above 85 kDa) molecular mass range were apparently absent from the profile and many of the remaining proteins appeared reduced in intensity. While this might have been due to the lysate system, it is rather unlikely since all other RNA prepara-

tion produced satisfactory profiles. Visual analysis of the densitometric scan of the entire profile indicated that the overall number of PN day 20 proteins in PTU 2 and PTU 3 treated tissue appeared reduced, compared to those of controls, but not to those of PTU 2 at PN days 30 and 60. Therefore, it seems that thyroid hormone status affected translatable cerebellar mRNA levels.

The amount of immunoprecipitated apo E appeared to change in all PTU treatment groups. Like hepatically synthesized apo E, cerebellar apo E translation appeared to increase as development proceeded in control tissue. In PTU 1 treated tissue, apo E levels appeared diminished during PTU treatment and apparently increased with serum free T_3 levels. Whether this apparent increase was the result of specific T_3 induction of the apo E gene or due to an overall metabolic effect is unknown. The most striking results were obtained from PTU 2 and PTU 3 apo E immunoprecipitation. Unlike hepatically synthesized apo E which increased in the hypothyroid state (Davidson et al., 1988), cerebellar apo E did not seem to be affected, relative to control values, by thyroid hormone deprivation. While one is eager to draw the conclusion that the cerebellar apo E gene is not regulated by thyroid hormone, there are several other plausible expla-

nations for this phenomenon. The total protein profile of PTU 2 and PTU 3 treated tissues appeared reduced as compared to controls. Because the level of apo E appeared unaltered by these PTU treatments, its representation as a proportion of total protein would be increased. Therefore, cerebellar apo E synthesis might indeed be regulated in a fashion similar to that of hepatically synthesized apo E and increase in the hypothyroid state.

Hypothyroidism is associated with severe hyperlipidemia and hypercholesterolemia. In this hyperlipemic state, serum apo E levels increase due to a two to three fold increase in hepatic synthesis. Apo E synthesized within the cerebellum, and possibly restricted by the blood brain barrier, would therefore not be expected to be a part of the compensatory mechanism of dealing with the altered lipid state. Conversely, endogenous cerebellar apo E synthesis does not preclude transport across the blood brain barrier. If apo E is not restricted to general circulation, hepatically synthesized apo E from the serum could cross the blood brain barrier, maintain a steady state apo E concentration and inhibit increased cerebellar apo E synthesis.

Although only one apo E gene is known to exist, the cell populations within the cerebellum and liver expressing

the gene are decidedly different. Previous research has focused on hepatic synthesis in adult animals, thereby avoiding any developmental effects of thyroid hormone. Within the model system used in this project, thyroid hormone deprivation was correlated with a delayed developmental state and alterations in the cell populations represented within the cerebellum. In previous reports, apo E was detected immunocytochemically within astrocytes (Boyles et al., 1985). In addition, the number of astrocytes and the glia to neuron ratio were increased in the hypothyroid state. Therefore, control and hypothyroid cerebellar tissues consist of different ratios of cell types whose synthetic abilities are bound to be different and would be reflected in the mRNA types and levels. Since hypothyroidism also results in a delayed developmental state, it is inaccurate to compare mRNA's from control and hypothyroid tissue of equivalent postnatal age. A more accurate comparison might be made between PN day 10 control and PN day 20 hypothyroid tissues.

While the expression and regulation of apo E within the cerebellum provides an interesting contrast to hepatic synthesis, the results concerning expression and regulation of transferrin were less compelling. First, and foremost, it

was difficult to discern the transferrin band from the nonspecifically precipitated reticulocyte proteins. To reduce this nonspecific binding, longer preincubation periods with Pansorbin should be attempted prior to the addition of the antibodies or the inclusion of excess unlabelled T_r. Transferrin appeared to be expressed in such low quantities that it is not readily detectible through immunoprecipitation. Before conducting further experiments, the specificity and titer of the transferrin antibody should be tested by immunoprecipitation of the purified transferrin used as a molecular weight standard.

Another means of detecting transferrin utilizes direct staining of the polyacrylamide gel. Protein within gels are generally stained with Coomassie blue. The two bound iron atoms of transferrin may be detected by interaction with the chromogenic ligand 3-(2-pyridyl)-5,6-bis(2-(5-furylsulfonic acid))-1,2,4-triazine, disodium salt, more commonly known as Ferene S (Chung, 1985). This method allows for detection of iron proteins at iron levels as low as 100 ng per band. More recently, Kuo et al. (1988) reported the detection of as little as 5 ng of protein-bound iron per band. This reaction is based on the ability of iron to catalyze the oxidation of diaminobenzoate by hydrogen peroxide. The only

disadvantage in this method is that the transferrin was synthesized *in vitro*. This assay is out of the range of sensitivity for *in vitro* translation which generates fg to pg quantities of *in vitro* products. In addition, while some translation systems include the iron carrier hemin, this does not guarantee the incorporation of iron into transferrin.

Data collected from the densitometric scans of the transferrin immunoprecipitated profiles allow only one conclusion to be drawn at this time. If indeed the 76 kDa band analyzed is actually transferrin, its cerebellar regulation would appear similar to hepatic regulation. Both proteins dramatically decline in the hypothyroid state.

The alterations observed in *in vitro* protein synthesis need to be correlated with fluctuations in mRNA levels. This requires cDNA probes specific for the mRNA of interest. Chloramphenicol amplification of the plasmid containing apo E cDNA was attempted without success. The polymerase chain reaction technology provides the most direct means of cDNA amplification and isolation from host vectors. Even with the use of specially constructed oligonucleotide primers, PCR amplification proved difficult. The best results were obtained when the cDNA template was preheated and amplified

in the presence of 4.0% DMSO. Unfortunately the presence of DMSO upon subsequent reamplification inhibited amplification. Recently, Sarkar et al. (1991) reported the use of formamide to improve the specificity of PCR amplification. Perhaps formamide would not inhibit as much as DMSO upon reamplification. The amplification of the transferrin cDNA proved straightforward.

These cDNA products were then used to analyze the changes in mRNA content throughout development and as a result of PTU treatment. Apo E mRNA levels appeared to decline as development proceeded. This is contrary to the increased *in vitro* translation observed in control tissue. Much of the poly A⁺ RNA at PN days 1 and 10 may be translationally inactive and not capable of generating proteins in an *in vitro* system. Alternatively, as development proceeds, the mRNA may become altered and more difficult to translate. Transferrin mRNA levels in control tissue appeared to parallel the pattern of *in vitro* translation observed, maximal synthesis at PN day 20 followed by slight declines. Both apo E and transferrin mRNA levels in PTU 1 treated tissue suggested that transcription of these genes may be affected by thyroid hormones. Before any conclusion can be drawn about levels of mRNA's it will first be neces-

sary to verify equal loading of RNA. The phenol/chloroform method of RNA extraction used does not completely eliminate contaminating DNA and this will affect the amount of RNA in each sample. Various means of determining equal loading may be used. First, an oligonucleotide probe for the 18S rRNA subunit may be used. Because oligonucleotide hybridization must occur in the absence of formamide the probe cannot be included with other cDNA probes. The ubiquitously expressed protein cyclophilin may also be used to determine equal loading (Travis et al., 1989). The use of cyclophilin has two advantages. First, the cDNA probe may be included with other probes, thus avoiding the need for stripping and reblotting under special hybridization conditions. Second, and more importantly, whereas the 18S rRNA oligo can only be used to determine loading of total RNA in gels, a cyclophilin probe may be used to determine loading of mRNA in gels.

Conclusions

1. PTU treatment is associated with gross morphological alterations in growth and development.
2. Cerebellar cortical stratification and cellular morphology are altered by prenatal, as well as postnatal PTU administration.
3. Apolipoprotein E mRNA levels within the cerebellum appear substantially greater than that of transferrin.
4. In control tissue, both apolipoprotein E and transferrin mRNA levels appear to increase as development occurs.
5. Cerebellar apolipoprotein E mRNA levels do not seem to be affected by PTU treatment.
6. Apolipoprotein mRNA levels do not appear to follow the same developmental trend as apolipoprotein E *in vitro* synthesized levels in control tissue.
7. Cerebellar transferrin mRNA levels appear affected by PTU treatment, and show substantial declines.
8. Both apolipoprotein E and transferrin mRNA quantities appear increased by the presence of thyroid hormone in the circulation, probably due to developmental recovery.

LIST OF REFERENCES

- Aizenman, Y.; de Vellis, J. (1987) Brain neurons develop in serum and glial free environment. *Brain Res.* 406:32-42.
- Almazan, G.; Honegger, P.; Matthieu, J. (1985) Triiodothyronine stimulation of oligodendroglial differentiation and myelination. *Dev. Neurosci.* 7:45-54.
- Altman, J. (1972) Postnatal development of the cerebellar cortex in the rat. III. Maturation of the granular layer. *J. Comp. Neurol.* 145:465-512.
- Angevine, J.B.; Sidman, R.L. (1961) Autoradiographic study of cell migration during histogenesis of cerebral cortex in the mouse. *Nature (Lond.)* 192:766-768.
- Apostolopoulos, J.J.; Howlett, G.J.; Fidge, N. (1987) Effects of dietary cholesterol and hypothyroidism on rat apolipoprotein mRNA metabolism. *J. Lipid Res.* 28:642-648.
- Aviv, H.; Leder, P. (1972) Purification of biologically active globin messenger RNA by chromatography on oligothymidylic acid-cellulose. *Proc. Natl. Acad. Sci. USA* 69:1408-1412.
- Balázs, R.; Kovács, S.; Teichgraber, P.; Cocks, W.A.; Eayrs, J.T. (1968) Biochemical effects of thyroid deficiency on the developing brain. *J. Neurochem.* 15:1335-1349.
- Balázs, R.; Brooksbank, B.W.L.; Davison, A.N.; Eayrs, J.T.; Wilson, D.A. (1969) The effect of neonatal thyroidectomy on myelination in the rat brain. *Brain Res.* 15:219-232.
- Bass, N.H.; Young, E. (1973) Effects of hypothyroidism on the differentiation of neurons and glia in developing rat cerebrum. *J. Neurol. Sci.* 18:155-173.
- Beach, R.L.; Popiela, H.; Festoff, B.W. (1983) The identification of neurotrophic factor as a transferrin. *FEBS Lett.* 156:151-156.
- Bittner, M.; Kupferer, P.; Morris, C.F. (1980) Electrophoretic transfer of proteins and nucleic acids from slab gels to diazobenzylxymethyl cellulose and nitrocellulose sheets. *Anal. Biochem.* 102:459-471.

- Bloch, B.; Popovici, T.; Levin, M.J.; Tuil, D.; Kahn, A. (1985) Transferrin gene expression visualized in oligodendrocytes of the rat brain by using *in situ* hybridization and immunohistochemistry. *Proc. Natl. Acad. Sci. USA* 82: 6706-6710.
- Boyles, J.K.; Pitas, R.E.; Wislon, E.; Mahley, R.W.; Taylor, J.M. (1985) Apolipoprotein E associated with astrocytic glia of the central nervous system and with nonmyelinating glia of the peripheral nervous system. *J. Clin. Invest.* 76: 1501-1513.
- Cavaliere, R.R.; Pitt-Rivers, R. (1981) The effects of drugs on the distribution and metabolism of thyroid hormone. *Pharmacol. Rev.* 33:55-80.
- Ceda, G.P.; Hoffman, A.R.; Silverberg, S.D.; Wilson, D.M.; Rosenfeld, R.G. (1985) Regulation of growth hormone from cultured human pituitary adenomas by somatomedins and insulin. *J. Clin. Endocrinol. Metab.* 60:1204-1209.
- Chirgwin, J.M.; Przybyla, A.E.; MacDonald, R.J.; Rutter, W.J. (1979) Isolation of biologically active ribonucleic acid from sources enriched in ribonuclease. *Biochemistry* 18:5294.
- Chomczynski, P.; Sacchi, N. (1987) Single-step method of RNA isolation by acid guanidinium thiocyanate-phenol-chloroform extraction. *Anal. Biochem.* 162:156-159.
- Chung, M. C-M. (1985) A specific stain for iron-binding proteins in polyacrylamide gels: application to transferrin and lactotransferrin. *Anal. Biochem.* 148:498-502.
- Clos, J.; Legrand, J. (1973) Effects of thyroid deficiency on the different cell populations of the cerebellum in the young rat. *Brain Res.* 63:450-455.
- Connor, J.R.; Fine, R.E. (1986) The distribution of transferrin immunoreactivity in the rat central nervous system. *Brain Res.* 368:319-328.
- Connor, J.R.; Fine, R.E. (1987) Development of transferrin-positive oligodendrocytes in the rat central nervous system. *J. Neurosci. Res.* 17:51-59.
- Cooper, O.S. (1984) Antithyroid drugs. *New Engl. J. Med.* 311:1353-1362.

Craft, C.M.; Whitmore, D.H.; Donoso, L.A. (1990) Differential expression of mRNA and protein encoding retinal and pineal S-antigen during the light/dark cycle. *J. Neurochem.* 55:1461-1473.

D'Angilo, S.A. (1967) Pituitary-thyroid interrelations in maternal, fetal and neonatal guinea pigs. *Endocrinology* 81: 132-138.

Davidson, N.O.; Carlos, R.C.; Drewek, M.J.; Parmer, T.G. (1988) Apolipoprotein gene expression in the rat is regulated in a tissue-specific manner by thyroid hormone. *J. Lipid Res.* 29:1511-1522.

deJong, G.; van Dijk, J.P.; van Eijk, H.G. (1990) The biology of transferrin. *Clin. Chim. Acta* 190:1-46.

diFiore, M.S.H. (1989) Atlas of Normal Histology. V.P. Eroschenko (Ed.) page 83. Lea & Febiger: Philadelphia.

Dory, L.; Roheim, P.S. (1981) Rat plasma lipoproteins and apolipoproteins in experimental hypothyroidism. *J. Lipid Res.* 22:287-296.

Dziegielewska, K.M.; Saunders, N.R.; Soreq, H. (1985) Messenger ribonucleic acid (mRNA) from developing rat cerebellum directs *in vitro* synthesis of plasma proteins. *Devel. Brain Res.* 23:259-267.

Elshourbagy, N.A.; Liao, W.S.; Mahley, R.W.; Taylor, J.M. (1985) Apolipoprotein E mRNA is abundant in the brain and adrenals, as well as in the liver, and is present in other peripheral tissues of rats and marmosets. *Proc. Natl. Acad. Sci. USA* 82:203-207.

Feinberg, A.P.; Vogelstein, B. (1983) A technique for radiolabeling DNA restriction endonuclease fragments to high specific activity. *Anal. Biochem.* 132:6-13.

Fletcher, J.; Huehns, E.R. (1968) Function of transferrin. *Nature (Lond.)* 218:1211-1214.

Francis, G.L.; Rennert, O.M. (1980) Thyroid hormone synthesis in the rat. *Metabolism* 29:415-420.

Giometto, B.; Bozza, F.; Argentiero, V.; Gallo, P.; Pagni, S.; Piccinno, M.G.; Tavolato, B. (1990) Transferrin receptors in rat central nervous system. *J. Neurol. Sci.* 98:81-90.

- Goubin, G.; Goldman, D.S.; Luce, J.; Neiman, P.E.; Cooper, G.M. (1983) Molecular cloning and nucleotide sequence of a transforming gene detected by transfection of chicken B-cell lymphoma DNA. *Nature (Lond.)* 302:114-119.
- Griffin, J.E.; Ojeda, S.R. (1988) *Textbook of Endocrine Physiology*. Oxford University Press: New York.
- Gray, H. (1977) *Anatomy, Descriptive and Surgical*. Bounty Books: New York.
- Gudernatsch, J.F. (1914) Feeding experiments on tadpoles. III. A further contribution to the knowledge of organs of internal secretion. *Am. J. Anat.* 15:431-481.
- Gullo, D.; Sinha, A.K.; Woods, R.; Pervin, K.; Ekins, R.P. (1987) Triiodothyronine binding in adult rat brain: compartmentation of receptor populations in purified neuronal and glial nuclei. *Endocrinology* 120:325-331.
- Hamburg, M. (1968) An analysis of the action of thyroid hormone on development based on *in vivo* and *in vitro* studies. *Gen. Comp. Endocr.* 10:198-213.
- Himwich, H.E. (1973) Early Studies of the Developing Brain. In: W. Himwich (Ed.) "*Biochemistry of the Developing Brain*" pp. 1-48. Marcel Dekker, Inc.: New York.
- Hockfield, S. (1987) A Mab to a unique cerebellar neuron generated by immunosuppression and rapid immunization. *Science* 237:67-70.
- House, E.L.; Pansky, B.; Siegel, A. (1979) *A Systemic Approach to Neuroscience*. McGraw-Hill Book Co.: New York.
- Huggenvick, J.I.; Idzerda, R.L.; Haywood, L.; Lee, D.C.; McKnight, G.S.; Griswold, M.D. (1987) Transferrin messenger ribonucleic acid: molecular cloning and hormonal regulation in rat sertoli cells. *Endocrinology* 120:332-340.
- Jacobson, M. (1978) *Developmental Neurobiology*. Plenum Press: New York.
- Jande, S.S.; Maler, L.; Lawson, D.E.M. (1981) Immunohistochemical mapping of vitamin D-dependent calcium-binding protein in brain. *Nature (Lond.)* 294:765-767.

Kahn, A.; Levin, M.J.; Zakin, M.M.; Bloch, B. (1987) The Transferrin Gene *In: G. Guroff (Ed.) "Oncogenes, Genes, and Growth Factors"* pp.277-309. John Wiley and Sons: New York.

Kandel, E.R.; Schwartz, J.H. (1985) *Principles of Neural Science*. Elsevier: New York.

Kawaoui, A.; Tsuneda, M. (1986) Effects of thyroidectomy and administration of propylthiouracil (PTU) or thyrotropin (TSH) to pregnant rats on the functional development of the fetal thyroid gland. *Endocrinol. Japon.* 33:835-841.

Kessler, S.W. (1981) Use of protein A-bearing Staphylococci for the immunoprecipitation of antigens from cells. *In: J.J. Langone & H.V. Vunakis (Eds.) "Methods in Enzymology Vol. 73: Immunochemical Techniques"* pp. 442-459. Academic Press: New York.

Kornguth, S.E.; Scott, G. (1972) The role of climbing fibers in the formation of Purkinje cell dendrites. *J. Comp. Neurol.* 146:61-82.

Kuo, C-F.; Fridovich, I. (1988) A stain for iron-containing proteins sensitive to nanogram levels of iron. *Anal. Biochem.* 170:183-185.

Laemmli, U.K. (1970) Cleavage of structural proteins during the assembly of the head of bacteriophage T4. *Nature (Lond.)* 227:680-685.

Larsen, P.R. (1976) Radioimmunoassay of thyroxine, triiodothyronine and thyrotropin in human serum. *In: N.R. Rose and H. Friedman (Eds.) "Manual of Clinical Immunology"* pp. 222-230. American Society for Microbiology: Washington, D.C.

Lau, C.; Slotkin, T.A. (1982) Maturation of sympathetic neurotransmission in the rat heart. VIII. Slowed development of noradrenergic synapses resulting from hypothyroidism. *J. Pharmacol. Exp. Ther.* 220:629-636.

Lauder, J.M. (1977) Effects of Thyroid State on Development of Rat Cerebellar Cortex. *In: G.D. Graves (Ed.) "Thyroid Hormones and Brain Development"* pp. 235-254. Raven Press: New York.

Legrand, J. (1967) Analyse de l'action morphogenetique des hormones thyroïdiennes sur le cervelet du jeune rat. *Arch. Anat. Miscosc. Morph. Exp.* 56:205-244.

- Legrand, J. (1979) Morphogenetic actions of thyroid hormones. *Trends Neurosci.* 2:234-236.
- Legrand, J. (1986) Thyroid Hormone Effects on Growth and Development. In: G. Hennemann (Ed.) "Thyroid Hormone Metabolism" pp. 503-534. Marcel Dekker, Inc.: New York.
- Lehrach, H.; Diamond, D.; Wozney, J.M.; Boedtke, H. (1977) RNA molecular weight determinations by gel electrophoresis under denaturing conditions, a critical reexamination. *Biochemistry* 16:4743-4751.
- Levin, M.J.; Tuil, D.; Uzan, G.; Dreyfus, J.; Kahn, A. (1984) Expression of the transferrin gene during development of non-hepatic tissues. *Biochem. Biophys. Res. Commun.* 122:212-217.
- Lin, C.; Xu, Y.; Wu, J.; Chan, L. (1986) Immunoreactive apolipoprotein E is a widely distributed cellular protein. *J. Clin. Invest.* 78:947-958.
- Lindsay, R.H.; Kelly, K.; Hill, J.B. (1978) Oxidation products of the antithyroid drug 6-n-propyl-2-thiouracil, synthesis, properties and preliminary identification in thyroid extracts. *Ala. J. Med. Sci.* 15:29-41.
- Litteria, M. (1990) Gender and gonadectomy influences specific proteins in the cerebellar cortex of the adult rat: a two-dimensional gel electrophoretic analysis. *Brain Res.* 529:120-125.
- Lund, R.D. (1978) *Development and Plasticity of the Brain.* Oxford University Press: Oxford.
- Mahley, R.W.; Innerarity, T.L.; Rall, R.C.; Weisgraber, K.H. (1984) Plasma lipoproteins: Apolipoprotein structure and function. *J. Lipid Res.* 25:1277-1294.
- Mandel, M. and Higa, A. (1970) Calcium-dependent bacteriophage DNA infection. *J. Mol. Biol.* 53:159-162.
- McEwen, B.S. (1981) Neural gonadal steroid actions. *Science* 211:1303-1311.
- McLean, J.W.; Fukazawa, C.; Taylor, J.M. (1983) Rat apolipoprotein E mRNA. *J. Biol. Chem.* 258:8993-9000.

Millhouse, O.E. The Golgi methods. (1981) In: L. Heimer & M.J. Robards (Eds.) "Neuroanatomical Tract-Tracing Methods" pp. 311-344. Plenum Press: New York.

Mills, N.C.; Gyves, M.T.; Ilan, J. (1985) Comparisons of human placental lactogen mRNA levels from placenta of diabetics and normal term. *Mol. Cell. Endo.* 39:61-69.

Morgan, E.H. (1969) Factors affecting the synthesis of transferrin by rat tissue slices. *J. Biol. Chem.* 244: 4193-4199.

Morgan, E.H. (1981) Transferrin, Biochemistry, Physiology and Clinical Significance. *Mol. Aspects Med.* 4:1-123.

Morgan, E.H. Synthesis and Secretion of Transferrin. (1983) In: H. Glaumann, T. Peters Jr., and C. Redman (Eds.) "Plasma Protein Secretion by the Liver" pp. 331-355. Academic Press: New York.

Morreale de Escobar, G.; Escobar del Rey, F. (1967) Extra-thyroid effects of some antithyroid drugs and their metabolic consequences. *Recent Prog. Horm. Res.* 23:87-137.

Moura, E.G.; Pazos-Moura, C.C.; Dorris, M.L.; Taurog, A. (1990) Lack of effect of propylthiouracil and methylmercaptoimidazole on thyroglobulin biosynthesis. *Proc. Soc. Exp. Biol. Med.* 194:48-53.

Nagasaka, A.; Hikada, H. (1976) Effect of antithyroid agents 6-propyl-2-thiouracil and 1-methyl-2-mercaptoimidazole on human thyroid iodine peroxidase. *J. Clin. Endocrinol. Metab.* 43:152-158.

Nicholson, J.L.; Altman, J. (1972a) The effects of early hypo- and hyperthyroidism on the development of rat cerebellar cortex I. Cell proliferation and differentiation. *Brain Res.* 44:13-23.

Nicholson, J.L.; Altman, J. (1972b) The effects of early hypo- and hyperthyroidism on the development of the rat cerebellar cortex II. Synaptogenesis in the molecular layer. *Brain Res.* 44:25-36.

Nunez, J. (1984) Effects of thyroid hormone during brain differentiation. *Mol. Cell. Endo.* 37:125-132.

- Oh, T.H.; Markelonis, G.J.; Royal, G.M.; Bregman, B.S. (1986) Immunocytochemical distribution of transferrin and its receptors in the developing chicken nervous system. *Dev. Brain Res.* 30:207-220.
- Oppenheimer, J.H.; Samuels, H.H. (1983) *Molecular Basis of Thyroid Hormone Action.* Academic Press: New York.
- Palay, S.L.; Chan-Palay, V. (1968) *Cerebellar Cortex, Cytology and Organisation.* Springer: Berlin.
- Panduro, A.; Shalaby, F.; Shafritz, D.A. (1987) Changing patterns of transcriptional and posttranscriptional control of liver specific gene expression during rat development. *Genes Dev.* 1:1172-1182.
- Panduro, A.; Lin-Lee, Y.C.; Chan, L.; Shafritz, D.A. (1990) Transcriptional and posttranslational regulation of Apolipoprotein E, A-I, and A-II gene expression in normal rat liver and during several pathophysiologic states. *Biochemistry* 29:8430-8435.
- Pansky, B.; Allen, D.J.; Budd, G.C. (1988) Review of Neuroscience pp.252-253. Macmillan Publ. Co.: New York.
- Paul, J.; Gilmour, R.S. (1968) Organ-specific restriction of transcription in mammalian chromatin. *J. Mol. Biol.* 34:317-330.
- Pelham, H.R.; Jackson, R.J. (1976) An efficient mRNA-dependent translation system from reticulocyte lysates. *Eur. J. Biochem.* 67:247-256.
- Pitts, F.N.; Quick, C. (1967) Brain succinate semialdehyde dehydrogenase II. Changes in the developing rat brain. *J. Neurochem.* 14:561-570.
- Polychronakos, C.; Guyda, H.J.; Patel, B.; Posner, B.I. (1986) Increase in the number of type II insulin-like growth factor receptors during propylthiouracil-induced hyperplasia in the rat thyroid. *Endocrinology* 119:1204-1209.
- Rakic, P. (1971) Neuron-glia relationship during granule cell migration in developing cerebellar cortex. A Golgi and electron microscopic study in Maccus Rhesus. *J. Comp. Neurol.* 141:283-312.

Ramón y Cajal, S. (1911) Histologie du système nerveux de l'homme et des vertébrés. Maloine: Paris.

Ratliff, C.R.; Gilliland, P.F.; Hall, F.F. (1972) Serum propylthiouracil: determination by a direct colorimetric procedure. Clin. Chem. 18:1373-1375.

Rosseel, M.T.; Lefebvre, R.A. (1990) High-performance liquid chromatographic determination of propylthiouracil in plasma. J. Chromatogr. 507:247-251.

Rutgers, M.; Pigmans, I.; Bonthuis, F.; Docter, R.; Visser, T.J. (1989) Effects of propylthiouracil on the biliary clearance of thyroxine (T_4) in rats. Endocrinology 125:2175-2186.

Rutgers, M.; Heusdens, F.A.; Bonthuis, F.; Rooda, S.E.; Visser, T.J. (1990) Identification of 3,3'-diiodothyroacetic acid sulfate: a major metabolite of 3,3',5-triiodothyronine in propylthiouracil-treated rats. Endocrinology 127:1617-1624.

Saiki, R.K.; Gelfand, D.H.; Stoffel, S.; Scharf, S.J.; Higuchi, R.; Horn, G.T.; Mullis, K.B.; Erlich, H.A. (1988) Primer-directed enzymatic amplification of DNA with a thermostable DNA polymerase. Science 239:487-491.

Sambrook, J.; Fritsch, E.F.; Maniatis, T. (1989) Molecular Cloning: A Laboratory Manual. Cold Spring Harbor Press: New York.

Sarkar, G.; Kapelner, S.; Sommer, S.S. (1991) Formamide can dramatically improve the specificity of PCR. Nucleic Acids Res. 18:7465.

Savu, L.; Vranckx, R.; Maya, M.; Gripois, D.; Blouquit, M.; Nunez, E.A. (1989) Thyroxine-binding globulin and thyroxine-binding prealbumin in hypothyroid and hyperthyroid developing rats. Biochim. Biophys. Acta 992:379-384.

Schaeffer, E.; Boissier, F.; Py, M.; Cohen, G.N.; Zakin, M.M. (1989) Cell type-specific expression of the human transferrin gene. J. Biol. Chem. 264:7153-7160.

Schulman, J.A.; Finger, T.E.; Brecha, N.C.; Karten, H.J. (1981) Enkephalin immunoreactivity in Golgi cells and mossy fibers of mammalian, avian, amphibian and teleost cerebellum. Neuroscience 6:2407-2416.

Shepherd, G.M. (1979) *The Synaptic Organization of the Brain*. Oxford University Press: New York.

Shivers, B.D.; Harlan, R.E.; Romano, G.J.; Howells, R.D.; Pfaff, D.W. (1986) Cellular localization of proenkephalin mRNA in rat brain: Gene expression in the caudate-putamen and cerebellar cortex. *Proc. Natl. Acad. Sci. USA* 83:6221-6225.

Sidman, R.L. (1975) Cell Interaction in Mammalian Brain Development. In: D.B. Tower (Ed.) "Nervous System: The Basic Neurosciences" pp. 605-609. Raven Press, Publ.: New York.

Slemmon, J.R.; Danho, W.; Hempstead, J.L.; Morgan, J.I. (1985) Cerebellin: A quantifiable marker for Purkinje cell maturation. *Proc. Natl. Acad. Sci. USA* 82:7145-7148.

Staels, B.; vanTol, A.; Chan, L.; Will, H.; Verhoeven, G.; Auwerx, J. (1990) Alterations in thyroid status modulate apolipoprotein, hepatic triglyceride lipase, and low density lipoprotein receptors in rats. *Endocrinology* 127:1144-1152.

Szentágothai, J.; Rajkovits, K. (1959) Ueber den Ursprung der Kletterfasern des Kleinhirns. *Z. Anat. Entwicklungsgesch.* 121:130-141.

Taurog, A. (1976) The mechanism of action of the thioureyllene antithyroid drugs. *Endocrinology* 98:1031-1046.

Toran-Allerand, C.D. (1984) The genesis of sexual differentiation of the central nervous system. In: G.J. DeVries, J.P.C. DeBruin, H.B.M. Vylings, and M.A. Corner (Eds.) "Progress in Brain Research Vol. 61: Sex Differences in the Brain." pp. 63-98. Elsevier: Amsterdam.

Travis, G.H.; Brennan, M.B.; Danielson, P.E., Kozak, C.A.; Sutcliffe, J.G. (1989) Identification of photoreceptor-specific mRNA encoded by the gene responsible for retinal degeneration slow (rds). *Nature (Lond.)* 338:70-73.

Uphouse, L.; Mason, G.; Bondy, S. (1982) Comments concerning the use of dimethylsulfoxide as a solvent for studies of chlordecone neurotoxicity. *Neurotoxicology* 3:149-154.

Valdermarsson, S. (1983) Plasma lipoprotein alterations in thyroid dysfunction. *Acta Endocrinol.* 103:255.

Wallace, D.M. (1987) Large- and small-scale phenol extractions. *Methods in Enzymology* Vol 152 pp. 33-41. Academic Press: New York.

Walters, S.N.; Morell, P. (1981) Effects of altered thyroid states on myelinogenesis. *J. Neurochem.* 36:1792-1801.

Westermarck, K.; Karlsson, F.A.; Westermarck, B. (1983) Epidermal growth factor modulates thyroid growth and function in culture. *Endocrinology* 112:1680.

Willis, W.D.; Grossman, R.G. (1973) *Medical Neurobiology*. The C.V. Mosby Co.: St Louis.

Wood, D.F.; Franklyn, J.A.; Docherty, K.; Ramsden, D.B.; Sheppard, M.C. (1987) The effect of thyroid hormones on growth hormone gene expression *in vivo* in rats. *J. Endocrinol.* 112:459-463.

Zar, J.H. (1984) *Biostatistical Analysis*. Prentice-Hall, Inc.: Englewood Cliffs, N.J..

Zeman, W.; Innes, J. (1963) *Craigie's Neuroanatomy of the Rat*. Academic Press, Inc.: New York.

Ziai, M.R.; Sangamewaran, L.; Hempstead, J.L.; Danho, W.; Morgan, J.I. (1988) An immunochemical analysis of the distribution of a brain-specific polypeptide, PEP-19. *J. Neurochem.* 51:1771-1776.

Appendix A

The Effects of Hypothyroidism on Body Weight (mean in g \pm s.d.)				
Age	Control	PTU 1	PTU 2	PTU 3
10	17.479 \pm 0.962 N = 28	11.987 \pm 1.534 N = 39		
20	28.215 \pm 3.326 N = 41	23.618 \pm 4.344 N = 34	28.560 \pm 2.405 N = 20	24.125 \pm 1.813 N = 16
30	63.585 \pm 6.421 N = 34	31.135 \pm 7.473 N = 43	32.433 \pm 2.035 N = 15	21.4 N = 1
60	188.536 \pm 12.342 N = 33	167.146 \pm 12.781 N = 39	82.245 \pm 19.59 N = 11	

Appendix B

The Effects of Hypothyroidism on Brain Weight (mean in g \pm s.d.)				
Age	Control	PTU 1	PTU 2	PTU 3
10	0.911 \pm 0.047 N = 28	0.677 \pm 0.055 N = 39		
20	1.272 \pm 0.060 N = 41	1.043 \pm 0.140 N = 34	1.204 \pm 0.038 N = 20	1.038 \pm 0.062 N = 16
30	1.475 \pm 0.064 N = 34	1.201 \pm 0.171 N = 43	1.235 \pm 0.031 N = 15	0.950 N = 1
60	1.698 \pm 0.052 N = 33	1.622 \pm 0.055 N = 39	1.390 \pm 0.125 N = 11	

Appendix C

The Effects of Hypothyroidism on Cerebellum Weight (mean in mg \pm s.d.)				
Age	Control	PTU 1	PTU 2	PTU 3
10	82.1 \pm 9.9 N = 28	54.6 \pm 7.5 N = 39		
20	158.3 \pm 18.4 N = 41	115.7 \pm 29.1 N = 34	153.0 \pm 6.1 N = 20	119.4 \pm 15.8 N = 16
30	201.8 \pm 15.9 N = 34	161.9 \pm 3.8 N = 43	165.0 \pm 11.0 N = 15	110.0 N = 1
60	260.3 \pm 10.7 N = 33	253.5 \pm 11.2 N = 39	207.0 \pm 25.0 N = 11	

Appendix D

The Effects of Hypothyroidism on Brain: Body Weight Ratio (mean in mg/g \pm s.d.)				
Age	Control	PTU 1	PTU 2	PTU 3
10	52.2 \pm 2.5 N = 28	57.2 \pm 6.7 N = 39		
20	45.6 \pm 5.4 N = 41	44.7 \pm 4.1 N = 34	42.3 \pm 2.4 N = 20	43.2 \pm 10.2 N = 16
30	23.4 \pm 2.0 N = 34	39.6 \pm 5.7 N = 43	38.2 \pm 2.0 N = 15	44.4 N = 1
60	9.0 \pm 0.5 N = 33	9.7 \pm 0.6 N = 39	17.5 \pm 2.5 N = 11	

Appendix E

The Effects of Hypothyroidism on Cerebellum:Brain Weight Ratio (mean in mg/g \pm s.d.)				
Age	Control	PTU 1	PTU 2	PTU 3
10	90.0 \pm 7.9 N = 28	80.7 \pm 9.6 N = 39		
20	124.3 \pm 12.1 N = 41	109.6 \pm 14.1 N = 34	127.1 \pm 4.0 N = 20	114.8 \pm 10.8 N = 16
30	136.6 \pm 6.2 N = 34	132.8 \pm 16.2 N = 43	133.5 \pm 7.9 N = 15	115.8 N = 1
60	153.3 \pm 5.3 N = 33	156.3 \pm 5.0 N = 39	148.6 \pm 7.0 N = 11	

Appendix F

The Effects of Hypothyroidism on Cerebellar External Granule Layer Thickness (mean in $\mu\text{m} \pm \text{sem}$)				
Age	Control	PTU 1	PTU 2	PTU 3
1	31.121 \pm 0.69 N = 137	20.613 \pm 0.60 N = 98		
10	27.302 \pm 0.74 N = 143	25.069 \pm 0.65 N = 124		
20	Not Present	20.690 \pm 0.75 N = 99	9.181 \pm 0.34 N = 100	23.871 \pm 0.63 N = 100

Appendix G

The Effects of Hypothyroidism on Cerebellar Molecular Layer Thickness (mean in $\mu\text{m} \pm \text{sem}$)				
Age	Control	PTU 1	PTU 2	PTU 3
20	176.7 \pm 2.9 N = 117	126.8 \pm 1.7 N = 118	126.8 \pm 2.9 N = 100	110.6 \pm 3.1 N = 100
30	189.1 \pm 4.4 N = 144	189.8 \pm 4.0 N = 129	179.1 \pm 4.3 N = 100	163.0 \pm 3.4 N = 100
60	247.6 \pm 5.4 N = 141	232.3 \pm 7.3 N = 158	246.7 \pm 6.4 N = 100	

Appendix H

The Effects of Hypothyroidism on Cerebellar Internal Granule Layer Thickness (mean in $\mu\text{m} \pm \text{sem}$)				
Age	Control	PTU 1	PTU 2	PTU 3
20	136.3 \pm 2.6 N = 127	128.8 \pm 1.9 N = 129	130.5 \pm 6.3 N = 100	187.8 \pm 6.3 N = 100
30	189.0 \pm 7.9 N = 149	153.7 \pm 4.1 N = 143	177.8 \pm 8.2 N = 100	171.2 \pm 5.8 N = 100
60	215.5 \pm 9.9 N = 150	188.5 \pm 6.2 N = 192	195.8 \pm 9.4 N = 100	

Appendix I

The Effects of Hypothyroidism on Total Cerebellar Cortical Depth (mean in $\mu\text{m} \pm \text{sem}$)				
Age	Control	PTU 1	PTU 2	PTU 3
10	250.5 \pm 5.8 N = 153	258.5 \pm 9.1 N = 153		
20	383.0 \pm 8.3 N = 113	355.7 \pm 7.2 N = 137	380.5 \pm 7.2 N = 100	284.7 \pm 5.6 N = 100
30	423.4 \pm 8.0 N = 148	402.9 \pm 11.0 N = 84	466.7 \pm 12.8 N = 100	395.4 \pm 7.6 N = 100
60	511.5 \pm 11.6 N = 143	482.2 \pm 14.7 N = 118	481.4 \pm 10.6 N = 100	

Appendix J

The Effects of Hypothyroidism on Purkinje Cell Somal Area (mean in $\mu\text{m} \pm \text{sem}$)				
Age	Control	PTU 1	PTU 2	PTU 3
20	159.3 \pm 4.5 N = 70	238.7 \pm 7.6 N = 70	236.2 \pm 8.8 N = 50	206.1 \pm 5.5 N = 50
30	148.9 \pm 6.3 N = 70	219.1 \pm 9.4 N = 70	186.0 \pm 5.1 N = 50	Purkinje cell not detectable
60	141.3 \pm 12.4 N = 70	248.0 \pm 7.9 N = 70	157.5 \pm 5.4 N = 50	

Appendix K

The Effects of Hypothyroidism on Purkinje Cell Somal Form PE (mean ± sem)				
Age	Control	PTU 1	PTU 2	PTU 3
20	0.811 ± 0.010 N = 70	0.668 ± 0.014 N = 70	0.800 ± 0.011 N = 50	0.753 ± 0.013 N = 50
30	0.816 ± 0.009 N = 70	0.736 ± 0.012 N = 70	0.872 ± 0.007 N = 50	Purkinje cell not detectable
60	0.860 ± 0.007 N = 70	0.776 ± 0.012 N = 70	0.823 ± 0.012 N = 50	

Appendix L

Form PE is calculated by the Zeiss Video-Plan as follows:

$$\text{Form PE} = \frac{4 \pi (\text{Area})}{(\text{Circumference})^2} \qquad \begin{array}{l} \text{Area} = \pi r^2 \\ \text{Circumference} = 2 \pi r \end{array}$$

$$= \frac{4 \pi (\pi r^2)}{(2 \pi r)^2}$$

$$= \frac{4 \pi^2 r^2}{4 \pi^2 r^2}$$

$$= 1.0$$

For a perfect circle, the Form PE = 1.0. As objects deviate from a spherical nature the Form PE decreases.